Doctorate Dissertation

博士論文

Cosmological consequences of quantum processes in strong gravity

(強重力場における量子的過程の宇宙論的帰結)

A Dissertation Submitted for Degree of Doctor of Philosophy
December 2018

平成30年12月博士（理学）申請

Department of Physics, Graduate School of Science,
The University of Tokyo

東京大学大学院理学系研究科

物理学専攻

Naritaka Oshita

大下 翔誉

Abstract

In the modern cosmology, there are several problems and interesting predictions involving strong gravity such as the initial cosmological singularity problem, problem of initial conditions for cosmic inflation, consistency of the generalized second law of thermodynamics, black hole information loss paradox, and metastability of the Higgs vacuum. It is one of the priorities of modern cosmology to provide plausible cosmological scenarios which can be resolutions to these problems or are consistent with some theoretical or experimental predictions. In this dissertation, we approach these problems and provide some plausible scenarios regarding the beginning and fate of the Universe by taking into account quantum effects in strong gravity.

Cosmic inflation is a standard scenario describing the early universe, which solves several fine-tuning problems, and is consistent with the observational data of Cosmic Microwave Background radiation. However, it has been expected that in order for inflation to start, homogeneity of the Universe is necessary to some extent. The problem of initial conditions for inflation is to assert how inflation began at the early stage of the Universe without assuming homogeneity of space from the outset. Our scenario implies that the quantum tunneling effect of the initial inhomogeneous space could lead to the birth of baby universes that accommodate inflating domains. This can be one of the possible scenarios to solve the problem of initial conditions for inflation. We also investigate the thermodynamical aspect of inflation, especially, the consistency of the generalized second law of thermodynamics during inflation.

After the end of inflation, the Universe is thermalized since the energy of inflation is converted to thermal radiation and the large scale structure eventually forms. In the present Universe, black holes, originating from gravitational collapses of matter, are ubiquitous. The evaporation process of black holes is still controversial due to the black hole information loss paradox. In particular, the firewall argument in the paradox perhaps requires a drastic modification of the picture of the multiverse and eternal inflation. We then provide a reasonable reason for rejecting the firewall argument by focusing on the gravitational decoherence inside a black hole.

Regarding the future of the Universe, a number of interesting scenarios have been proposed so far. For example, the metastability of the Higgs vacuum may lead to a catastrophic scenario of the Universe. This is because the metastability implies that the Higgs vacuum we live in until now might be metastable and the Universe could be filled by vacuum bubbles including large and negative vacuum energy because of the first order phase transition of the Higgs vacuum. Furthermore, it has been proposed that "impurities" in the Universe such as black holes would be catalysts for the vacuum decays of the Higgs field. We then investigate horizonless compact

objects as the catalysts for the vacuum decays.

We also discuss another interesting scenario regarding the fate of the Universe, and this may give us a deeper insight into the beginning of the Universe as well. The original initial singularity problem is an implication from the general relativity, which states that as long as a plausible energy condition (strong energy condition) is satisfied, the initial singularity is unavoidable at the finite past of the Universe. However, our scenario tells us that the initial singularity or the real beginning of the Universe are no longer necessary and the Universe can be eternal to past. Evaporating black holes in the far future of the Universe emit high-temperature Hawking radiation. In our scenario, the energy of Hawking radiation around the mini black hole is converted to vacuum energy due to the symmetry restoration of a related quantum field, and then the symmetry restored region eventually start to inflate after the quantum tunneling process. This implies that our Universe may have been created from a black hole in the previous generation of the Universe, and in this sense, the Universe can be eternal to past.

Acknowledgments

First and foremost I would like to thank my advisor Jun'ichi Yokoyama. It has been an honor to be his Ph.D. student. I have learned a lot from his insightful comments and guidance throughout my Ph.D. I appreciate all his contributions of time, ideas, and funding to make my Ph.D. experience productive and stimulating.

I thank Kazuhiro Yamamoto, Satoshi Iso, Teruaki Suyama, Rumi Tatsukawa, Daichi Tsuna, Masaki Yamada, Masahide Yamaguchi, Sen Zhang, and Qingwen Wang for helpful discussions. I have learned a lot from the discussions with them. I also greatly appreciate all members of Research Center for the Early Universe (RESCEU) and the University of Tokyo Theoretical Astrophysics for many useful discussions. A special thanks is also extended to the administrative staff of RESCEU, Sayuri Nagano, Chiyo Ueda, and Mieko Minamisawa, for providing comfortable research environments.

I am grateful to Alexander Vilenkin for insightful discussions and hospitality at the Tufts University during a part of my Ph.D. course. I also gratefully acknowledge Niayesh Afshordi for fruitful discussions and collaborations and for kind hospitality at the Perimeter Institute for theoretical physics.

A large portion of my work is supported by the Japan Society for the Promotion of Science (JSPS) and Advanced Learning Graduate Course for Photon Science (ALPS).

Finally, I would like to express my sincere gratitude to my family for continuous support in every way.

Contents

Chapter 1

Introduction

Cosmology is a science to understand the whole history of the Universe and the origin of matter existing in the Universe. However, the cosmology was more philosophical before 1915 since a tool to discuss the dynamics of spacetime, the general relativity (GR), had not been discovered yet. The GR is still the standard gravitation theory after more than a century has passed since its discovery. It gives us the dynamical picture of spacetime, that is, the Universe may expand or contract depending on the details of matter filling the Universe. Of course, not only the theoretical contribution from the GR but the observational contributions were also necessary to make cosmology an exact science. In 1920s Lemaître and Hubble discovered the isotropic redshift of galaxies, which implies that the Universe is almost uniformly expanding, and in 1965 Penzias and Wilson discovered the Cosmic Microwave Background radiation (CMB) with temperature ~ 3 K. Combining both discoveries, it seems natural to conclude that the Universe was small and extremely high temperature stuff at its early stage, and then it expanded and gradually became cold and isotropic. Furthermore, the development of particle physics and the study of big bang nucleosynthesis also contributed to the understanding of the origin of matter in the Universe.

Despite these radical developments of cosmology, there were fine-tuning problems in cosmology: why our universe is flat, why monopoles or other exotic relics have never been observed, and why the universe has its uniform temperature over the observable region although the Universe seemingly would not have any causality in the past. To solve these fine-tuning problems, in 1981 Sato [1] and Guth [2] proposed the "inflationary scenario", which is regarded as a successful paradigm in the modern cosmology since the idea does not only solve the fine-tuning problems, but its theoretical prediction also fits the CMB observational data [3, 4] in a good accuracy.

Soon after the proposal of cosmic inflation, Vilenkin proposed [5] that the inflationary universe could be born from "nothing". The quantum cosmology, a study of the creation of the

Universe in quantum mechanical manner, has started at this time. However, it is found that inflating space is not past-complete [6–9] and the Universe would suffer from the "initial singularity", at which the GR is broken, which is called the initial singularity problem.

It has been numerically and analytically investigated what kind of initial conditions are necessary to start inflation and it is found that the initial condition of inflation should have some power of homogeneous mode [10–22]. If we assume some homogeneity from the outset, the horizon problem and nearly isotropic CMB might be no longer needed to be explained by the inflationary paradigm. Therefore, this leads to another cosmological issue, that is, how natural it might be to have proper conditions that satisfy conditions for inflation. This is called the problem of initial conditions for inflation.

After the end of inflation, the vacuum energy is converted to the energy of thermal particles and those are diluted by cosmic expansion. Therefore, gravitational field in the present Universe is weaker than that during inflation, but still there exist (locally) strong gravity regions originating from gravitational collapses of matter which are called black holes. Black holes are very mysterious objects not only in the context of cosmology or astrophysics, but also in the context of thermodynamics [23–26], quantum field theory [27, 28], and (quantum) information theory [29–31]. Bekenstein pointed out [23] that a black hole possesses its "gravitational entropy" that is proportional to the area of black hole horizon. Hawking predicted thermal radiation emitted from a black hole by quantum mechanical processes [27], which is called Hawking radiation and its temperature is proportional to the inverse of black hole mass. Therefore, it has been believed that all black holes in the Universe eventually evaporate and the final stage of the Universe might be filled by thermal radiation*). On the other hand, the recent prediction of the Higgs metastability also gives another catastrophic scenario of the Universe, where an anti-de Sitter (AdS) vacuum bubble is nucleated by the first order phase transition of the Higgs field and expands to fill the whole Universe eventually.

In this dissertation, cosmological consequences of quantum effects under strong gravity (e.g., expanding universe, black holes, negative vacuum energy regions due to the Higgs metastability) are discussed throughout the history of the Universe (see Fig. 1.1). This dissertation is organized as follows. Chapter 2 is dedicated to the brief review of relevant topics; the initial singularity problem, problem of initial conditions for inflation, Hawking-Moss instanton, the generalized second law of thermodynamics, black hole information loss paradox, and Higgs metastability.

In Chapter 3, we discuss how inflation could began out of a highly inhomogeneous space.

*)Interestingly, this scenario was already discussed in the context of classical thermodynamics by Kelvin in 1852. The scenario called "thermal death" states that the universe would eventually evolve to a state whose entropy is maximized (the second law of thermodynamics) and there is no thermodynamic free energy.

The problem of initial conditions for inflation has been discussed by performing numerical simulations to follow the dynamics of an inhomogeneous space [10–16, 18, 20–22], but we here discuss the possibility that an inflationary universe was born out of such an inhomogeneous space by quantum tunneling process. We show that the quantum tunneling process of inhomogeneous space forms a wormhole-like configuration. As the space beyond the wormhole throat expands exponentially, being filled with false vacuum energy, this is interpreted as creation of an inflationary universe. This mechanism leads to the multiple-creation of inflationary universes beyond the wormhole throats, and therefore, this gives the picture of the multiverse.

Chapter 4 is dedicated to discussions regarding the consistency of the generalized second law of thermodynamics (GSL). In the first half of the chapter, we show that the stochastic inflation approach is consistent with the GSL. In the second half of the Chapter it is shown that the GSL would be broken in the Hawking-Moss instanton solution [32]. The former and latter parts are based on the author's paper [33] and [34], respectively.

In Chapter 5 a reasonable reason for rejecting the firewall argument is presented. The firewall [31] is an extremely energetic boundary at a black hole horizon argued by Almheiri, Marolf, Polchinski, Sully (AMPS) in 2012. AMPS pointed out that the unitarity, the low energy effective field theory (GR plus quantum field theory), and the equivalence principle of GR are mutually inconsistent, provided that the retrieval of information from an old black hole is assumed. To solve the inconsistency pointed out by them, they argue the existence of firewall at the horizon by which an infalling observer burns up there. AMPS also point out the possibility that firewalls exist even at cosmological horizons, such as those in de Sitter universe, as a natural extension of the argument. If their argument is correct and the firewall exists even at the cosmological horizon of the Universe, there would be neither the interior regions of black holes and nor exterior of the cosmological horizons, and the picture of the multiverse [35, 36] and eternal inflation [7, 37] would be rejected. In this sense, the firewall argument is really critical even in cosmology. In our proposal, the decoherence plays an essential role, and it is concluded that the firewall is not necessary and quantum field theory and GR are consistent, provided that the black hole mass is much larger than the Planck mass of roughly 2.17×10^{-8} kg. This section is based on [38].

Chapter 6 and 7 are dedicated to the discussions of the future of the Universe. For example, the Higgs metastability has been discussed in the context of cosmology since it could lead to a catastrophic scenario of the Universe where the whole Universe could be filled by AdS vacuum bubbles. In Chapter 6, we investigate a possibility that horizonless compact objects (e.g., monopoles [39], Q-balls [40–49], boson stars [50–64], and so on) promote the first order phase transition of the Higgs vacuum. We found that if its compactness is small enough and

satisfy a certain condition, an AdS vacuum bubble could be nucleated within the cosmological time. This section is based on [65]. Chapter 7 is dedicated to another possible scenario of the birth of other universes out of evaporating black holes. Hawking temperature is proportional to the inverse of a black hole mass, and therefore, there exists highly energetic radiation around the evaporating mini black holes. We will discuss a possibility that the next inflation, whose energy originates from the thermal energy of Hawking radiation, starts around an evaporating black hole in the future of our Universe. This section is based on [66].

Finally, we conclude the thesis with a summary of the results in Chapter 8.

We take the natural unit, $c = \hbar = k_B = 1$, and $G = M_{\rm Pl}^{-2} = \ell_{\rm Pl}^2 = t_{\rm Pl}^2$ throughout the thesis.

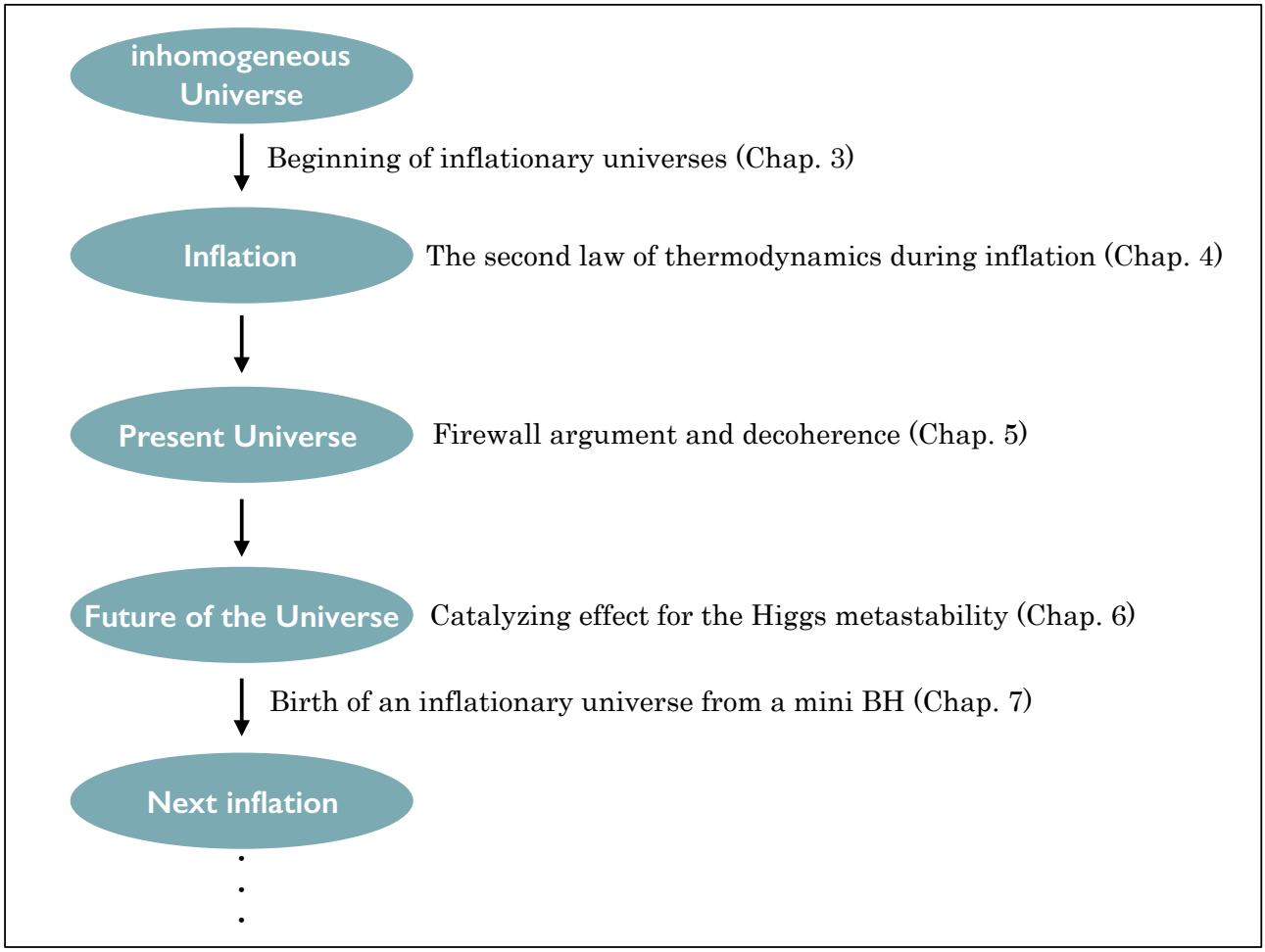

Figure 1.1: Flow chart showing the organization of thesis.

Chapter 2

A series of problems in cosmology

2.1 Problems in the inflationary scenario

The inflationary scenario is the current paradigm in modern cosmology. The exponential expansion of space at the early period of the Universe solves a number of fine-tuning problems. The observation of CMB shows [3, 4] that the Universe is unnaturally isotropic and flat. Without inflation, therefore, finely tuned initial conditions and acausal initial condition correlations are required. However, the inflationary scenario still has problems, i.e., the initial singularity problem [6–8,67] and the problem of initial conditions for inflation*), and the purpose of this section is reviewing those problems.

2.1.1 Brief review of inflation

Exponential expansion of the Universe is described by a de Sitter spacetime and its metric has the form

$$ds^2 = -dt^2 + e^{2\sqrt{\Lambda/3}t} d\mathbf{x}^2, \tag{2.1}$$

where Λ is a cosmological constant included in the Einstein-Hilbert action:

$$S_{\rm G} = \frac{1}{16\pi G} \int \sqrt{-g} d^4x \left(R - 2\Lambda\right). \tag{2.2}$$

However, inflation should end with a grateful exit after a sufficient number of e-folds (longer than 60 e-folds) to be consistent with the observed Universe. Therefore, the cosmological constant, Λ, should be dynamical rather than constant, and a dynamical cosmological constant can be modeled by a scalar field (inflaton), ϕ, with a non-trivial potential energy term $V(\phi)$:

$$S = S_{\rm G} + S_{\rm M} = \int \sqrt{-g} d^4x \left(\frac{R}{16\pi G} - \frac{1}{2}\partial_\mu\phi\partial^\mu\phi - V(\phi)\right). \tag{2.3}$$

*) See, e.g. [68] for a review of problem of initial conditions for inflation.

Once properly setting the shape of the potential and choosing the initial distribution of the scalar field, the Universe exponentially expands. Inflation must eventually ends, and the universe must be thermalized by the decay of inflaton to other particles.

The first idea of inflation model is the "old inflation" [1,2], which requires two local minima of the effective potential at $\phi = \phi_F$ (false vacuum) and $\phi = \phi_T$ (true vacuum) with $V(\phi_F) > V(\phi_T)$. The old inflation is the inflationary model where an inflaton initially stays in a false vacuum state for a long time and a local part of inflating space experiences the first order phase transition (quantum tunneling) from the false vacuum state to the true vacuum one. This gives a "bubble" configuration that is the spherical region filled by the true vacuum and surrounded by the false vacuum. The boundary of vacuum bubble (bubble wall) consists of the kinetic term of scalar field and the energy of potential barrier. In this model, however, it is difficult to thermalized the Universe after the nucleations of vacuum bubbles. Then another inflation model, the "slow-roll inflation", was proposed [69, 70]. It gives a density and curvature perturbations in good agreement with present observational data of CMB. In the slow-roll inflation, a plateau in the effective potential is required and the Universe experiences inflation during the inflaton slowly rolls on the plateau. After falling into a minimum of the potential, the inflaton decays into other particles and the Universe is thermalized.

This cosmological model gives us the picture of "multiverse", meaning that the Universe we have been observing is not a unique universe, but other uncountable universes also exist outside our observable patch. For instance, Sato's group [35, 71] proposed the multi-production of inflationary universes soon after his proposal of inflation. According to this picture, a spatial foliation of the entire spacetime may consist of both thermalized region and inflating region, and it is natural to ask if inflation eternally last somewhere or not. Aryal and Vilenkin have shown [72] that inflation is eternal to future by using the analysis of the "fractal dimension". However, it has been proved that inflation is not eternal to past in the simplest model where the inflating space is described by an exact de Sitter spacetime [6]. The essential reason why inflation with de Sitter spacetime is not past-eternal is that the de Sitter solution involves a contracting phase before the expanding phase. During the exponential contraction of the Universe, thermalized regions can fill the entire universe, which prevents the universe experience inflation. A more rigorous proof of the past-incompleteness of inflation is discussed in [7, 9].

2.1.2 Problem of initial conditions for cosmological inflation

In order for inflation to begin, homogeneity of the initial space is necessary to some extent. Otherwise, highly inhomogeneous initial conditions could lead to gravitational collapse rather than inflation. However, if we assume homogeneity from the outset, the horizon problem and

the nearly isotropic CMB are no longer needed to be explained by the inflationary paradigm. Therefore, inflation should arise without finely tuned initial conditions.

In [73], the authors argue that homogeneity on super-Hubble scales must be necessary as an initial condition by assuming the Einstein equations, the null energy condition, and the trivial topology of the Universe. Moreover, it is argued [74] that a probability for having such a homogeneous background to start inflation is extremely small [†)]. However, it has been pointed out [68] that the argument of [74] just gives a lower bound on the probability of inflation since the homogeneity over the Hubble scale is just a sufficient condition, not a necessary one, to start inflation. On the other hand, others argue [10–16, 18] that even if inhomogeneous modes dominate the initial energy density, the Universe likely to eventually enter the period of inflation as long as there is some power in the quasi-homogeneous mode (super-Hubble scale) in the case of large field inflation which has a local attractor. This is because such a quasi-homogeneous mode slowly rolls, inhomogeneities are redshifted and it will eventually dominate the Universe to begin inflation. This argument is also confirmed by numerical calculations in three dimensions [20–22], but when there is less power in quasi-homogeneous mode, it was found that the Universe does not inflate.

From the above discussions, one finds that the homogeneity over the Hubble scale is just a sufficient condition for inflation, and in order for inflation to start somewhere, only some power of quasi-homogeneous mode is necessary. An important problem is how natural it might be to have a sufficient power of quasi-homogeneous mode from the outset. In this sense, the problem of initial conditions for inflation is still an open question. In Chapter 3 we will provide a plausible resolution to this by taking into account a quantum effect on a highly inhomogeneous initial condition, where there is no homogeneous mode.

2.1.3 Initial singularity problem

Even if the initial conditions problem for inflation was not problematic and inflationary phase may be realized without fine-tuning on the initial conditions, there is a critical problem, called "initial singularity problem", in the inflationary paradigm. Before discussing the initial singularity problem, a brief review of the singularity theorem should be presented. The singularity theorem proven by Hawking and Penrose implies that there is a defect in the Big Bang universe, providing that the strong energy condition holds [75]. For instance, going back in time in a uniform and isotropic universe holding the strong energy condition, one inevitably hits the singularity where the scale factor becomes zero and its energy density and curvature diverge.

[†)] The authors' approach is based on defining a prior probability distribution for the inhomogeneity of an initial condition ,where they assume specific, yet quite general and well-grounded, conditions on the distribution.

This is very easy to see by starting with the Friedman equation:

$$\frac{\ddot{a}}{a} = -\frac{4\pi G}{3}\left(\rho + 3p\right), \tag{2.4}$$

where $a(t)$ is the scale factor, and ρ and p are energy density and pressure of medium in the Universe, respectively. Assuming the strong energy condition, $\rho+p \geq 0$ and $\rho+3p \geq 0$, the scale factor should be zero at the finite past. The singularity theorem shows that the assumption of the strong energy condition leads to the past-incompleteness of the Universe in general. Let us start with the Raychaudhri equation

$$\dot{\theta} = -\frac{1}{3}\theta^2 - \sigma_{\mu\nu}\sigma^{\mu\nu} - R_{\mu\nu}u^\mu u^\nu, \tag{2.5}$$

where θ is the change rate of the area of geodesics family denoted as δA, that is, $\theta \equiv (d\delta A/d\tau)/\delta A$. $\sigma_{\mu\nu}$ is a spatial tensor and $\sigma_{\mu\nu}\sigma^{\mu\nu}$ is a non-negative quantity. Using the Einstein equation, (2.5) can be rewritten as

$$\dot{\theta} + \frac{1}{3}\theta^2 = -\sigma_{\mu\nu}\sigma^{\mu\nu} - 8\pi G\left(T_{\mu\nu} - \frac{1}{2}g_{\mu\nu}T\right)u^\mu u^\nu. \tag{2.6}$$

The strong energy condition is given by

$$\left(T_{\mu\nu} - \frac{1}{2}g_{\mu\nu}T\right)u^\mu u^\nu \geq 0. \tag{2.7}$$

From (2.6) and (2.7), one can read

$$\dot{\theta} + \frac{1}{3}\theta^2 \leq 0, \tag{2.8}$$

which gives a relation

$$1/\theta(t) \leq 1/\theta_0 + t/3, \tag{2.9}$$

where $\theta_0 \equiv \theta(t=0)$. In the case of an expanding universe, the sign of θ is positive, and therefore, there is a point where $\theta \to -\infty$ (focus of geodesic) in the range of $t \leq 3/|\theta_0|$. This is the initial singularity problem that states that an expanding universe has the initial singularity at the finite past unavoidably, providing that the strong energy condition holds.

Since the strong energy condition is violated for inflation, Vilenkin questioned if the inflationary phase is eternal to past and if one can avoid the initial singularity problem in such a way. However, it was shown that the rapid expansion of the Universe cannot be the initial condition of the Universe and the initial singularity is unavoidable even in the inflationary model. Let us look into the case of a homogeneous and isotropic universe and we can easily prove that null geodesic is past-incomplete in such a case.

The metric takes the form of

$$ds^2 = -dt^2 + a^2(t)d\mathbf{x}^2, \tag{2.10}$$

where we assume $H(t) \equiv (da/dt)/a$ has the lower bound $H(t) \geq H_{min} > 0$. Introducing an affine parameter, λ, on the null geodesic, a wave-vector, k^μ, is given by $k^\mu \propto dx^\mu/d\lambda$. Since the frequency, $\omega \equiv k^0$, is proportional to the inverse of the scale factor, $\omega \propto a^{-1}(t)$, one finds $a^{-1}(t) \propto \omega \propto dx^0/d\lambda$, which reduces to

$$d\lambda \propto e^{Ht} dt. \tag{2.11}$$

We can normalize the affine parameter as $d\lambda = [a(t)/a(t_f)]dt$ so that $d\lambda/dt = 1$ when $t = t_f$, where t_f is a reference time. Let us introduce an averaged Hubble parameter, $H_{\rm av} \equiv (\lambda(t_f) - \lambda(t_i))^{-1} \int_{\lambda(t_i)}^{\lambda(t_f)} H(\lambda) d\lambda$, where $t_i (< t_f)$ is a chosen initial time. Using (2.11), one finds that the averaged Hubble parameter, $H_{\rm av}$, has an upper bound,

$$H_{\rm av} = \frac{1}{\lambda(t_f) - \lambda(t_i)} \int_{a(t_i)}^{a(t_f)} \frac{da}{a(t_f)} < \frac{1}{\lambda(t_f) - \lambda(t_i)} \tag{2.12}$$

since $a(t_f) > a(t_i)$. The inequality of (2.12) and the imposed assumption $H(t) \geq H_{min}$, it is found that the null geodesic cannot be extended to the past infinity:

$$\lambda(t_f) - \lambda(t_i) < 1/H_{\rm av}(t_i) < 1/H_{\rm min} \tag{2.13}$$

Therefore, even in the inflationary model that breaks the strong energy condition, the initial singularity is still unavoidable. This suggests that physics other than inflation is necessary to describe the past boundary of the inflating region of spacetime. In Chapter 7, we propose a possible scenario where inflation can begin by a quantum tunneling process without initial singularity.

2.2 Consistency of the second law of thermodynamics in strong gravity

2.2.1 GSL and black holes

The thermodynamics in strong gravity system is very mysterious. In particular, when the system involves gravitational horizons, "gravitational entropy" attributed to those horizons has been expected to exist. This idea is pioneered by Bekenstein [23–25] and his gedanken experiment [23] to introduce the gravitational entropy, called Bekenstein entropy, is as follows: Let an observer drop a package which has entropy into a black hole. In this case, the entropy of the world outside the black hole decreases whereas the black hole has only "three hairs" (mass, angular momentum, and charge) after the hole has settled down to equilibrium. The observer cannot exclude the possibility that the interior entropy decreases in the process. In this sense, the second law of thermodynamics is no longer a plausible conjecture under strong gravity.

Bekenstein points out that the second law of thermodynamics should be modified and he proposed this conjecture called "the generalized second law of thermodynamics" (GSL): Common entropy (exterior entropy) plus black-hole entropy never decrease[‡)]. Here black-hole entropy, S_B, has the form

$$S_B \equiv \eta \ell_{\rm Pl}^{-2} A, \tag{2.14}$$

where A is the horizon area of the black hole and η is a constant number of order unity. The introduction of a black-hole entropy may play an important role in the aforementioned gedanken experiment. The choice of the horizon area of a black hole as a measure of its entropy is motivated by the result of Hawking that the horizon area of black hole never decreases [77].

Let us illustrate a physical example he raised in his original paper [23] to see the validity of the GSL. Suppose a narrow beam of thermal radiation of temperature T falls into a black hole of mass M. Since this picture is based on geometrical optics, the characteristic wavelengths of the beam should be much shorter than the size of the black hole $\sim GM$:

$$T^{-1} \ll GM. \tag{2.15}$$

Introducing the energy of the beam, E, the entropy of the beam is given by

$$S_R \sim E/T, \tag{2.16}$$

and therefore, once the beam falls into the hole, the exterior entropy decreases by S_R.

On the other hand, the area of the black hole increases by ΔA (> 0) since its mass increases by the energy of the beam E. ΔA is therefore has the form

$$\Delta A = \Delta(16\pi G^2 M^2) \simeq 32\pi G^2 M \Delta M = 32\pi G^2 M E. \tag{2.17}$$

One can read the difference of a black-hole entropy as

$$\Delta S_B \simeq 32\eta\pi GME. \tag{2.18}$$

From (2.15), (2.16), and (2.18), we find the GSL is satisfied in this case:

$$|S_R| \ll \Delta S_B. \tag{2.19}$$

2.2.2 Stochastic inflation

It is known that the quantum fluctuation of inflaton ϕ in an expanding space with its positive vacuum energy density, governed by the effective potential $V(\phi)$, behaves like a stochastic fluctuation. This picture implies that the dynamics of a de Sitter universe is stochastic, and therefore,

[‡)] It was initially formulated for black holes by Bekenstein [25] and was extent to de Sitter universes by Davies [76].

its Bekenstein entropy is also stochastically fluctuates. Since this behavior of the entropy is important in the GSL, we will here review the stochastic approach based on [78].

We take the conformal metric of a de Sitter spacetime as

$$ds^2 = -dt^2 + e^{2Ht}d\mathbf{x}^2 = \frac{1}{(H\eta)^2}\left(-d\eta^2 + d\mathbf{x}^2\right), \tag{2.20}$$

where $d\eta \equiv dt/e^{Ht}$. Let us consider a quantum scalar field ϕ in a de Sitter spacetime

$$\phi(\mathbf{x},t) = \int \frac{d^3k}{(2\pi)^{3/2}}\left(\hat{a}_{\mathbf{k}}\phi_{\mathbf{k}}(t)e^{-i\mathbf{k}\cdot\mathbf{x}} + \hat{a}^{\dagger}_{\mathbf{k}}\phi^{*}_{\mathbf{k}}(t)e^{i\mathbf{k}\cdot\mathbf{x}}\right), \tag{2.21}$$

where $\hat{a}_{\mathbf{k}}$ ($\hat{a}^{\dagger}_{\mathbf{k}}$) is an annihilation (creation) operator of a wavenumber $\mathbf{k}$ and $\phi_{\mathbf{k}}(t)$ is a mode function which follows the field equation with some interaction potential $V(\phi)$

$$\ddot{\phi}_{\mathbf{k}} + 3H\dot{\phi}_{\mathbf{k}} + \frac{\mathbf{k}^2}{a^2(t)}\phi_{\mathbf{k}} + V'(\phi) = 0, \tag{2.22}$$

where a dot denotes the derivative with respect to t. The field equation is a linear second derivative equation and therefore two boundary conditions are necessary to obtain its solution. Imposing boundary conditions corresponds to choosing a vacuum state of the quantum field ϕ and the choice of

$$\lim_{\eta\to-\infty}(-H\eta)^{-1}\phi_{\mathbf{k}} = \frac{e^{-ik\eta}}{\sqrt{2k}} \tag{2.23}$$

is equivalent to taking the Bunch-Davies (BD) vacuum. In the case of the BD vacuum, the mode function $\phi_{\mathbf{k}}(t)$ with $k^2/a^2(t) \gg V'(\phi)$ has the form

$$\phi_{\mathbf{k}}(t) \simeq -\sqrt{\frac{\pi}{4}}H^{3/2}(-\eta)H^{(1)}_{3/2}(-k\eta) = -\frac{H}{\sqrt{2k}}\left(\eta - \frac{i}{k}\right)e^{-ik\eta}, \tag{2.24}$$

where $H^{(1)}_{3/2}(x)$ is the Hankel function of the first class. This asymptotically approaches the Minkowski vacuum in the limit $\eta \to -\infty$.

In the stochastic approach, long-wavelength modes, $k < \epsilon a(t)H$, are spatially coarse-grained over a constant physical 3D volume of $1/(\epsilon H)^3$, and is replaced by the coarse-grained field $\bar{\phi}(\mathbf{k},t)$:

$$\phi = \bar{\phi}(\mathbf{x},t) + \int \frac{d^3k}{(2\pi)^{3/2}}\theta(k - \epsilon a(t)H)\left(\hat{a}_{\mathbf{k}}\phi_{\mathbf{k}}(t)e^{-i\mathbf{k}\cdot\mathbf{x}} + \hat{a}^{\dagger}_{\mathbf{k}}\phi^{*}_{\mathbf{k}}(t)e^{i\mathbf{k}\cdot\mathbf{x}}\right), \tag{2.25}$$

where $\epsilon \ll 1$ is a constant and $\theta(x)$ is the Heaviside step function. From the equation of motion of the scalar field for $\bar{\phi}$ with the assumption of $\dddot{\bar{\phi}} \ll 3H\ddot{\bar{\phi}}$ (slow-roll condition) and of $V'(\bar{\phi}) \gg \mathbf{k}^2/a^2(t)\bar{\phi}$ (homogeneity condition), we obtain the Langevin equation:

$$\dot{\bar{\phi}}(\mathbf{x},t) = -\frac{1}{3H}V'(\bar{\phi}) + f(\mathbf{x},t), \tag{2.26}$$

where $f(\mathbf{x}, t)$ is given by

$$f(\mathbf{x}, t) \equiv \epsilon a(t) H^2 \int \frac{d^3k}{(2\pi)^{3/2}} \delta(k - \epsilon a(t) H) \left(\hat{a}_{\mathbf{k}} \phi_{\mathbf{k}}(t) e^{-i\mathbf{k}\cdot\mathbf{x}} + \hat{a}^{\dagger}_{\mathbf{k}} \phi^{*}_{\mathbf{k}}(t) e^{i\mathbf{k}\cdot\mathbf{x}} \right). \tag{2.27}$$

The Langevin equation (2.26) implies that the coarse-grained field $\bar{\phi}$ is a stochastic quantity and $f(\mathbf{x}, t)$ is a stochastic noise whose correlation function has the form

$$\langle f(\mathbf{x}_1, t_1) f(\mathbf{x}_2, t_2) \rangle = \frac{H^3}{4\pi^2} \delta(t_1 - t_2) j_0(\epsilon a(t) H |\mathbf{x}_1 - \mathbf{x}_2|), \tag{2.28}$$

$$\text{with } j_0(x) \equiv \frac{\sin x}{x}. \tag{2.29}$$

This correlation properties implies that the stochastic noise is a white noise and there is less correlation between two distant de Sitter patches.

Therefore, in the stochastic approach, we obtain a picture that a macroscopic mode is kicked by small quantum fluctuations and the behavior of the energy density of a de Sitter patch is also stochastic. Since the Bekenstein entropy of the de Sitter patch is proportional to its horizon area that is determined by the energy density, the Bekenstein entropy could stochastically decrease. In Chapter 4, we will discuss the detail of this problem.

2.2.3 Hawking-Moss instanton

The stochastic inflation approach provides the thermodynamical aspect of quantum field on de Sitter spacetime. Hawking and Moss discussed a thermal tunneling from a de Sitter universe with its lower energy density to another one with larger energy density [32]. This transition is known as the Hawking-Moss bounce solution [32, 79, 80], which also leads to the decrement of Bekenstein entropy. We here review the derivation of the Hawking-Moss bounce solution. in Section 4.2, the decrease of the Bekenstein entropy by the Hawking-Moss transition is discussed.

Assuming that the bounce solution has O(4) symmetry, the Euclidean metric can be characterized by one parameter ξ and its function $\rho(\xi)$,

$$ds^2 = d\xi^2 + \rho(\xi)^2 d\Omega^2_{\mathrm{III}}, \tag{2.30}$$

where $d\Omega_{\mathrm{III}}$ represents the line element of the unit three-sphere. The Euclidean action of the Einstein gravity and a canonical scalar field ϕ with a potential $V(\phi)$ is then written as follows.

$$I_{\mathrm{E}} = 2\pi^2 \int d\xi \left[\rho^3 \left(\frac{1}{2} \dot{\phi}^2 + V(\phi) \right) + \frac{3}{8\pi G} \left(\rho^2 \ddot{\rho} + \rho \dot{\rho}^2 - \rho \right) \right] \tag{2.31}$$

where an over-dot represents differentiation with respect to ξ. From (2.31), the field equations

read,

$$\ddot{\phi} + \frac{3\dot{\rho}}{\rho}\dot{\phi} = \frac{dV}{d\phi}, \tag{2.32}$$

$$\dot{\rho}^2 = 1 + \frac{8\pi G}{3}\rho^2\left(\frac{1}{2}\dot{\phi}^2 - V\right). \tag{2.33}$$

The Hawking-Moss solution corresponds to a static scalar field configuration with $\dot{\phi} = \ddot{\phi} = 0$ which is realized at potential extrema with $dV/d\phi = 0$. Hence (2.33) reads

$$\dot{\rho}^2 = 1 - \frac{8\pi G}{3}\rho^2 V \tag{2.34}$$

and its solution is given as

$$\rho(\xi) = H_{\rm s}^{-1}\sin\left(H_{\rm s}\xi\right), \tag{2.35}$$

$$H_{\rm s}^2 \equiv \frac{8\pi G}{3}V(\phi_{\rm s}), \tag{2.36}$$

where $\phi_{\rm s}$ is a field value at a potential extremum. Substituting the solution (2.35) into the action (2.31), we find

$$I_{\rm E}(\phi_{\rm s}) = -\frac{3}{8G^2V(\phi_{\rm s})}. \tag{2.37}$$

Hawking and Moss [32] originally considered the transition from a false vacuum state $\phi_{\rm s} = \phi_{\rm fv}$ to the local potential maximum $\phi_{\rm s} = \phi_{\rm top}$ and identified the transition rate as

$$\begin{aligned}\Gamma_{\rm fv\to top} &= Ae^{-B_{\rm HM}} = A\exp\left[-I_{\rm E}(\phi_{\rm top}) + I_{\rm E}(\phi_{\rm fv})\right] \\ &= A\exp\left[\frac{3}{8G^2}\left(\frac{1}{V(\phi_{\rm top})} - \frac{1}{V(\phi_{\rm fv})}\right)\right],\end{aligned} \tag{2.38}$$

where the prefactor A may be estimated as $A \sim H^4(\phi_{\rm fv})$ on dimensional grounds.

In [79], Weinberg proposed a thermal interpretation assuming

$$\frac{\Delta V}{V(\phi_{\rm fv})} \equiv \frac{V(\phi_{\rm top}) - V(\phi_{\rm fv})}{V(\phi_{\rm fv})} \ll 1, \tag{2.39}$$

when $B_{\rm HM}$ is given by

$$B_{\rm HM} \simeq \frac{\Delta E}{T_{\rm H}} \tag{2.40}$$

$$\text{with } \Delta E = \frac{4\pi}{3}H^{-3}(\phi_{\rm fv})\Delta V \text{ and } T_{\rm H} = \frac{H(\phi_{\rm fv})}{2\pi}.$$

Here ΔE is the potential energy increment in the horizon $H^{-1}(\phi_{\rm fv})(\simeq H^{-1}(\phi_{\rm top}))$, and $T_{\rm H}$ is the Hawking temperature of de Sitter space. He argues that the gravitational effect is negligible because the geometry does not change practically before and after the transition thanks to the

assumption $\Delta V/V \ll 1$. As a result the formula based on (2.40) is identical to the case a horizon-sized domain receives thermal fluctuation at the Hawking temperature. However, this argument is failed since the Hamiltonian constraint leads to zero bulk-energy of the de Sitter patch[§)] [34]. In Section 4.2 it is shown that the exponential suppression of the Hawking-Moss transition is due to the decrease of Bekenstein entropy. The consistency between the GSL and the Hawking-Moss transition is also discussed there.

2.3 Hawking radiation and the black hole information loss paradox

2.3.1 Hawking radiation

Here we review the particle creation around a black hole proposed by Hawking [27]. For simplicity, in this section we work on a massless scalar field ϕ.

Particle interpretation and particle production

Let us suppose that we have a curved spacetime with a "stationary" metric $g_{\mu\nu}$, that is, $g_{\mu\nu}$ has a time-like Killing vector ξ^μ leaving invariant the metric $\delta_{\xi^\lambda} g_{\mu\nu} = 0$, where δ_{ξ^λ} is the infinitesimal transformation generated by ξ^λ. The action of the massless scalar field ϕ on the curved spacetime has the form

$$I = \int \sqrt{-g} d^4x \left[-\frac{1}{2} g^{\mu\nu} \nabla_\mu \phi \nabla_\nu \phi \right] \tag{2.41}$$

and the field equation is given by the Klein-Gordon (KG) equation:

$$\Box \phi \equiv g^{\mu\nu} \nabla_\mu \nabla_\nu \phi = 0. \tag{2.42}$$

Let us define the creation and annihilation operators, $a^\dagger_{\mathbf{k}}$ and $a_{\mathbf{k}}$, respectively. Then the quantization of ϕ is performed as

$$\phi(t, \mathbf{x}) = \int d^3k \left[a_{\mathbf{k}} u_{\mathbf{k}}(t, \mathbf{x}) + a^\dagger_{\mathbf{k}} u^*_{\mathbf{k}}(t, \mathbf{x}) \right], \tag{2.43}$$

where $u_{\mathbf{k}}(t, \mathbf{x})$ and $u^*_{\mathbf{k}}(t, \mathbf{x})$ are positive and negative frequency solutions of KG equation with respect to the Killing time t. Using the normalized positive and negative frequency modes

$$u_{\mathbf{k}}(t, \mathbf{k}) = \frac{1}{(2\pi)^{3/2}\sqrt{2\omega}} e^{-i\omega t + i\mathbf{k}\cdot\mathbf{x}}, \tag{2.44}$$

[§)] Of course the vacuum energy density takes non-zero positive value, but the energy of gravity is negative so that it offsets the vacuum energy density. Therefore, the "total" bulk energy of the de Sitter patch is zero providing that the system is stationary.

where $\omega \equiv |\mathbf{k}|$, the canonical quantization requires the following equal time commutation relations

$$[\phi(t,\mathbf{x}),\pi(t,\mathbf{x}')] = i\delta^3(\mathbf{x}-\mathbf{x}'), \qquad [\phi(t,\mathbf{x}),\phi(t,\mathbf{x}')] = [\pi(t,\mathbf{x}),\pi(t,\mathbf{x}')] = 0, \tag{2.45}$$

where $\pi(t,\mathbf{x})$ is the conjugate momentum of ϕ. These relations reduce to

$$[a_{\mathbf{k}}, a^\dagger_{\mathbf{k}'}] = (u_{\mathbf{k}}, u_{\mathbf{k}'}) = \delta^3(\mathbf{k}-\mathbf{k}'), \tag{2.46}$$

$$[a_{\mathbf{k}}, a_{\mathbf{k}'}] = [a^\dagger_{\mathbf{k}}, a^\dagger_{\mathbf{k}'}] = 0, \tag{2.47}$$

where the KG product (u_1, u_2) is defined as

$$(u_1,u_2) \equiv -i\int_\Sigma d\Sigma n^\mu (u_1\partial_\mu u_2^* - f_2^*\partial_\mu u_1). \tag{2.48}$$

Here Σ is a Cauchy surface with $d\Sigma$ being the volume element and n^μ is a future directed normal vector on Σ. From the Gauss's theorem, one can show that the KG product does not depend on the choice of Cauchy surface.

If the spacetime is globally stationary and we define a space of positive frequency modes with respect to the Killing time as we did, there is no gravitational particle production. However, in a realistic situation, spacetime is not stationary due to gravitational collapse or the change of expansion rate of the Universe and so on. Although in the absence of global time-like Killing vector there is no unique notion of vacuum state (a particle interpretation is ill-defined), we can find a well-defined one for those spacetimes which possess asymptotic stationary regions in the past and future. In such a case, a gravitational particle production takes place.

In the following, we call the asymptotic stationary regions in the past and in the future the "in" and "out" regions, respectively. One can construct a space of positive frequency modes, $u^{in}_{\mathbf{k}}$, in the in-region and define the vacuum state $|in\rangle$. In addition, one can also construct another space of positive frequency modes, $u^{out}_{\mathbf{k}}$, with respect to the Killing time in the out-region. The difference between $u^{in}_{\mathbf{k}}$ and $u^{out}_{\mathbf{k}}$ makes the initial vacuum state $|in\rangle$ a excited state in the out-region.

Bogolubov transformations

We here explain how to calculate the number of produced particles of momentum $\mathbf{k}$

$$\langle in|\, N^{out}_{\mathbf{k}}\, |in\rangle \equiv \langle in|\, a^{out}_{\mathbf{k}} a^{\dagger\, out}_{\mathbf{k}}\, |in\rangle\,, \tag{2.49}$$

where $a^{\dagger\, out}_{\mathbf{k}}$ and $a^{out}_{\mathbf{k}}$ are the creation and annihilation operators associated with the out-modes. To calculate (2.49), we have to investigate the relation between the creation and annihilation operators in the in-region and those in the out-region.

Let us expand ϕ interns of the in-modes $u^{in}_{\mathbf{k}}$

$$\phi = \int d^3k \left[a^{in}_{\mathbf{k}} u^{in}_{\mathbf{k}} + a^{in\dagger}_{\mathbf{k}} u^{in*}_{\mathbf{k}} \right]. \tag{2.50}$$

On the other hand, we can perform the alternative expansion by choosing instead the out-modes $u^{out}_{\mathbf{k}}$

$$\phi = \int d^3k \left[a^{out}_{\mathbf{k}} u^{out}_{\mathbf{k}} + a^{out\dagger}_{\mathbf{k}} u^{out*}_{\mathbf{k}} \right]. \tag{2.51}$$

The both in-modes and out-modes satisfy the following orthonormal relations

$$(u_{\mathbf{k}}, u_{\mathbf{k}'}) = \delta^3(\mathbf{k} - \mathbf{k}'),\ (u^*_{\mathbf{k}}, u^*_{\mathbf{k}'}) = -\delta^3(\mathbf{k} - \mathbf{k}'),\ (u_{\mathbf{k}}, u^*_{\mathbf{k}'}) = 0, \tag{2.52}$$

where $u_{\mathbf{k}} = u^{in}_{\mathbf{k}}$ or $u^{out}_{\mathbf{k}}$. Both sets of modes are complete, and therefore, out-modes can be expanded by the set of in-modes as

$$u^{out}_{\mathbf{k}} = \int d^3k' (\alpha_{\mathbf{k}\mathbf{k}'} u^{in}_{\mathbf{k}'} + \beta_{\mathbf{k}\mathbf{k}'} u^{in*}_{\mathbf{k}'}). \tag{2.53}$$

These relations are called the Bogolubov transformations and $\alpha_{\mathbf{k}\mathbf{k}'}$, $\beta_{\mathbf{k}\mathbf{k}'}$ are called the Bogolubov coefficients. Using (2.52), one can obtain the Bogolubov coefficients

$$\alpha_{\mathbf{k}\mathbf{k}'} = (u^{out}_{\mathbf{k}}, u^{in}_{\mathbf{k}'}), \quad \beta_{\mathbf{k}\mathbf{k}'} = -(u^{out}_{\mathbf{k}}, u^{in*}_{\mathbf{k}'}), \tag{2.54}$$

and one can obtain the following relations

$$\int d^3\tilde{k} (\alpha_{\mathbf{k}\tilde{\mathbf{k}}} \alpha^*_{\mathbf{k}'\tilde{\mathbf{k}}} - \beta_{\mathbf{k}\tilde{\mathbf{k}}} \beta^*_{\mathbf{k}'\tilde{\mathbf{k}}}) = \delta^3(\mathbf{k} - \mathbf{k}'), \tag{2.55}$$

$$\int d^3\tilde{k} (\alpha_{\mathbf{k}\tilde{\mathbf{k}}} \beta^*_{\mathbf{k}'\tilde{\mathbf{k}}} - \beta_{\mathbf{k}\tilde{\mathbf{k}}} \alpha^*_{\mathbf{k}'\tilde{\mathbf{k}}}) = 0. \tag{2.56}$$

From the relations (2.53), one can obtain the inverted relations

$$u^{in}_{\mathbf{k}} = \int d^3k' (\alpha^*_{\mathbf{k}'\mathbf{k}} u^{out}_{\mathbf{k}'} - \beta_{\mathbf{k}'\mathbf{k}} u^{out*}_{\mathbf{k}'}), \tag{2.57}$$

and substituting this into the relations $a^{in}_{\mathbf{k}} = (\phi, u^{in}_{\mathbf{k}})$ and $a^{out}_{\mathbf{k}} = (\phi, u^{out}_{\mathbf{k}})$, one obtains the desired relations between the operators of in-region and those of out-region:

$$a^{in}_{\mathbf{k}} = \int d^3k' (\alpha_{\mathbf{k}'\mathbf{k}} a^{out}_{\mathbf{k}'} + \beta^*_{\mathbf{k}'\mathbf{k}} a^{out\dagger}_{\mathbf{k}'}), \tag{2.58}$$

$$a^{out}_{\mathbf{k}} = \int d^3k' (\alpha^*_{\mathbf{k}\mathbf{k}'} a^{in}_{\mathbf{k}'} - \beta^*_{\mathbf{k}\mathbf{k}'} a^{in\dagger}_{\mathbf{k}'}). \tag{2.59}$$

Substituting (2.58) and (2.59) into (2.49), finally we obtain

$$\langle in| N^{out}_{\mathbf{k}} |in\rangle = \int d^3k' |\beta_{\mathbf{k}\mathbf{k}'}|^2. \tag{2.60}$$

In the following, we calculate the in and out mode functions on a black hole spacetime.

Vaidya metric

Although the Schwarzschild metric is a well known metric to describe the spacetime around a black hole, this is not suitable for a black hole originating from a gravitational collapse since a realistic black hole does not possesses its past horizon beyond which there exists a white hole. Therefore, here we consider the Hawking effect on the Vaidya metric that describes the spacetime around the realistic black hole and it has the form

$$ds^2 = -\left(1 - \frac{2GM(v)}{r}\right) dv^2 + 2dvdr + r^2 d\Omega^2, \tag{2.61}$$

where v is the null coordinate (fig. 2.1). It is known that when the mass depends only on v, $M = M(v)$, this is an exact Einstein's solution with a stress-energy tensor of

$$T_{vv} = \frac{L(v)}{4\pi r^2} \tag{2.62}$$

$$\text{with } \frac{dM(v)}{dv} \equiv L(v). \tag{2.63}$$

$T_{vv} > 0$ gives a pure ingoing flux and if one assumes that the influx of radiation is turned on at some finite time v_i and turned off at a later time v_f, the Vaidya spacetime is decided by three regions: A Minkowski vacuum region ($v < v_i$), an intermediate region ($v_i < v < v_f$), and the Schwarzschild black hole region ($v > v_f$). In the following discussions, for simplicity, we will set $v_i = v_f = v_0$ that leads to

$$M(v) = M\theta(v - v_0), \tag{2.64}$$

$$L(v) = M\delta(v - v_0), \tag{2.65}$$

and the resulting metric is given by patching portions of Minkowski and Schwarzschild spacetimes along $v = v_0$ (see Fig. 2.1). The initial Minkowski spacetime has the metric of

$$ds^2 = -du_{in}dv + r_{\text{in}}^2 d\Omega^2 \tag{2.66}$$

while the final Schwarzschild metric is

$$ds^2 = -\left(1 - \frac{2GM}{r_{\text{out}}}\right) du_{\text{out}}dv + r_{\text{out}}^2 d\Omega^2, \tag{2.67}$$

where $u_{\text{in}} \equiv t_{\text{in}} - r_{\text{in}}$, $v_{\text{in}} \equiv t_{\text{in}} + r_{\text{in}}$, $u_{\text{out}} \equiv t_{\text{out}} - r^*_{\text{out}}$, and $v_{\text{out}} \equiv t_{\text{out}} + r^*_{\text{out}}$. The definition of the tortoise coordinate r^*_{out} is

$$r^*_{\text{out}} \equiv r_{\text{out}} + 2GM \log\left(\frac{r_{\text{out}}}{2GM} - 1\right). \tag{2.68}$$

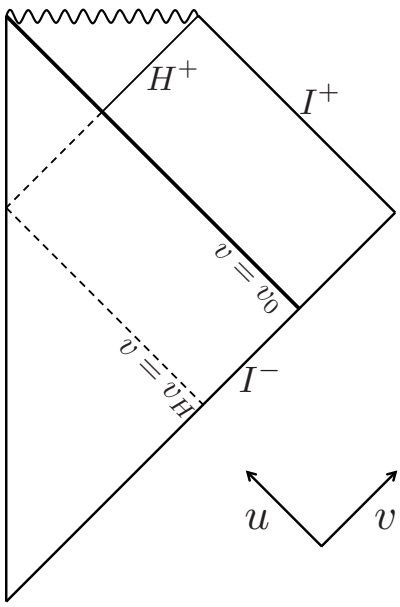

Figure 2.1: The Penrose diagram of a Vaidya metric. A thick solid line represents the trajectory of a collapsing shell.

Mode functions

We calculate mode functions of a massless scalar field on the simplified Vaidya metric. The mode functions follow the Klein-Gordon (KG) equation

$$\Box f = 0. \tag{2.69}$$

Since we here assume a spherically symmetric background, we can expand the mode function f as

$$f(x^\mu) = \sum_{l,m} \frac{f_l(t,r)}{r} Y_{lm}(\theta,\varphi), \tag{2.70}$$

where $Y_{l,m}$ is the spherical harmonics. In the Minkowski region on the Vaidya spacetime, the KG equation is

$$\left(-\frac{\partial^2}{\partial t^2} + \frac{\partial^2}{\partial r^2} - \frac{l(l+1)}{r^2}\right) f_l(t,r) = 0, \tag{2.71}$$

while in the Schwarzschild region, it has the form

$$\left(-\frac{\partial^2}{\partial t^2} + \frac{\partial^2}{\partial r^{*2}} - \left(1 - \frac{2GM}{r}\right)\left(\frac{l(l+1)}{r^2} + \frac{2GM}{r^3}\right)\right) f_l(t,r) = 0. \tag{2.72}$$

In the following we will look into the physics near horizon, $r^* \to -\infty$, where the angular potential disappears, and therefore, we shall neglect the potential. This approximation is better justified

for $l = 0$ and so that we will focus on the mode function of $l = 0$. We simply denotes $f_{l=0}$ as f in the following. The KG equations in (2.71) and (2.72) reduces to

$$\left(-\frac{\partial^2}{\partial t^2} + \frac{\partial^2}{\partial r^2}\right) f(t,r) = 0 \tag{2.73}$$

$$\text{and } \left(-\frac{\partial^2}{\partial t^2} + \frac{\partial^2}{\partial r^{*2}}\right) f(t,r) = 0, \tag{2.74}$$

respectively. Furthermore, since we are interested in positive frequency modes, we assume

$$f(t,r) = e^{-i\omega t} f(r). \tag{2.75}$$

The above equations are simplified as

$$\left(\frac{\partial^2}{\partial r^2} + \omega^2\right) f(t,r) = 0, \tag{2.76}$$

$$\text{and } \left(\frac{\partial^2}{\partial r^{*2}} + \omega^2\right) f(t,r) = 0, \tag{2.77}$$

respectively. The solutions of the wave equation in the initial Minkowski spacetime is given only by the outgoing modes, $e^{-i\omega u_{\rm in}}$, while in the final Schwarzschild region, the solution is given by the superposition of the ingoing modes, $e^{-i\omega v}$, and the outgoing modes, $e^{+i\omega u_{\rm out}}$. Therefore, the renormalized positive frequency modes at I^-, $u^{\rm in}_\omega$, are

$$u^{\rm in}_\omega = \frac{1}{4\pi\sqrt{\omega}} \frac{e^{-i\omega v}}{r}, \tag{2.78}$$

and on the other hand, the set of positive frequency modes at I^+, $u^{\rm out}_\omega$, are[¶)]

$$u^{\rm out}_\omega = \frac{1}{4\pi\sqrt{\omega}} \frac{e^{-i\omega u_{\rm out}}}{r}. \tag{2.79}$$

Taking into account the matching condition of the metrics along $v = v_0$, we can obtain the relation between $u_{\rm out}$ and $u_{\rm in}$. The condition is given by

$$r(v_0, u_{\rm in}) = r(v_0, u_{\rm out}), \tag{2.80}$$

where

$$r(v_0, u_{\rm in}) = \frac{v_0 - u_{\rm in}}{2} \tag{2.81}$$

[¶)] Taking these positive frequency modes is equivalent to choosing I^+ as an alternative Cauchy surface. However, this is not correct since I^+ is not a Cauchy surface but $H^+ \bigcup I^+$ is. Therefore, to construct the complete set of the mode functions, we have to add those modes that cross the future horizon H^+, $u^{\rm int}_\omega$. However, to calculate the particle production rate at I^+, the detail of $u^{\rm int}_\omega$ is insensitive to it. Therefore, we can neglect $u^{\rm int}_\omega$ in the following discussions.

and

$$r(v_0, u_{\rm out}) + 2GM \log\left(\frac{r(v_0, u_{\rm out})}{2GM} - 1\right) = \frac{v_0 - u_{\rm out}}{2}. \tag{2.82}$$

This gives the following relation

$$u_{\rm out}(u_{\rm in}) = u_{\rm in} - 4GM \log\left(\frac{|v_0 - 4GM - u_{\rm in}|}{4GM}\right). \tag{2.83}$$

Furthermore, we require the regularity of the mode functions at $r = 0$, which leads to the following form of $u_\omega^{\rm out}$

$$u_\omega^{\rm out} = \frac{1}{4\pi\sqrt{\omega}}\left(\frac{e^{-i\omega u_{\rm out}(u_{\rm in})}}{r} - \frac{e^{-i\omega u_{\rm out}(v)}}{r}\theta(v_H - v)\right), \tag{2.84}$$

where $v_H \equiv v_0 - 4GM$.

Let us investigate the behavior of $u_\omega^{\rm out}$ in the limits of $v \to -\infty (u_{\rm out} \to -\infty)$ and $v \to v_H - 0 (u_{\rm out} \to +\infty)$. Since we have $u_{\rm out}(v) \simeq v$ in the former limit, and therefore, the mode function $u_\omega^{\rm out}$ at I^- can be approximated as

$$u_\omega^{\rm out} \simeq -\frac{1}{4\pi\sqrt{\omega}}\frac{e^{-i\omega v}}{r} + \frac{1}{4\pi\sqrt{w}}\frac{e^{-i\omega u_{\rm out}(u_{\rm in})}}{r}, \tag{2.85}$$

which is still a positive frequency mode with respect to the inertial time at I^-. The dependence of the mode function on $u_{\rm in}$, i.e. the second term in (2.85), is actually irreverent to derive the particle creation around a black hole and its detail is shown later. On the other hand, in the latter limit, $v \to v_H - 0$, we have the following relation

$$u_{\rm out}(v) \simeq v_H - 4GM \log\left(\frac{v_H - v}{4GM}\right), \tag{2.86}$$

which gives the following form of the mode

$$u_\omega^{\rm out} \simeq -\frac{1}{4\pi\sqrt{\omega}}\frac{e^{-i\omega(v_H - 4GM\log\left(\frac{v_H - v}{4GM}\right))}}{r}\theta(v_H - v). \tag{2.87}$$

This mode function is a superposition of positive and negative frequency mode and leads to the particle creation around a black hole. Note that the critical time to take place the Hawking effect v_H is determined by the detail of the black hole formation, which significantly affects the form of mode functions.

Now we can calculate the Bogolubov coefficients $\beta_{\omega\omega'}$ by using (2.78) and (2.87). However, we should slightly modify the form of (2.87) since we are interested in the mean particle number produced at late time $u_{\rm out} \to \infty$. To properly evaluate the late time particle production, the out-modes, which are plane waves and are delocalized, should be replaced by the wave packets

localized at $u_{\rm out} \to \infty$. Introducing a parameter to specify the width of wave packets ϵ, a modified complete orthonormal set of out-modes at I_+ is given by

$$\tilde{u}^{\rm out}_{\omega_{jn}} = \frac{1}{\sqrt{\epsilon}} \int_{j\epsilon}^{(j+1)\epsilon} d\omega' e^{2\pi i \omega' n/\epsilon} u^{\rm out}_{\omega'}, \tag{2.88}$$

where j and n are positive integers. This wave packet type mode functions are localized at $u_{\rm out} = 2\pi n/\epsilon$ with width $2\pi/\epsilon$. Since we are interested in the wave packets localized at $u_{\rm out} \to \infty$, we have to calculate the Bogolubov coefficients with $n \to \infty$. From (2.54), the coefficients are

$$\beta_{\omega_{jn},\omega} = -(\tilde{u}^{\rm out}_{\omega_{jn}}, u^{\rm in*}_{\omega}) = i \int_{I_-} dv r^2 d\Omega (\tilde{u}^{\rm out}_{\omega_{jn}} \partial_v u^{\rm in}_{\omega} - u^{\rm in}_{\omega} \partial_v \tilde{u}^{\rm out}_{\omega_{jn}}) \tag{2.89}$$

Performing a partial integration, this reduces to

$$\beta_{\omega_{jn},\omega} = 2i \int_{I_-} dv r^2 d\Omega \tilde{u}^{\rm out}_{\omega_{jn}} \partial_v u^{\rm in}_{\omega}, \tag{2.90}$$

where we neglected the boundary term since the wave packets propagated backwards are localized around $v = v_H$ at I_- and the modes $\tilde{u}^{\rm out}_{\omega_{jn}}$ vanish at $v = \pm\infty$. It is easy to find the similar expressions for $\alpha_{\omega_{jn},\omega}$, and using (2.78) and (2.88), one finds the following relation at late time $n \to \infty$ (see Appendix A for the details of the derivation)

$$|\alpha_{\omega_{jn},\omega}| = e^{4\pi G M \omega_{jn}} |\beta_{\omega_{jn},\omega}|. \tag{2.91}$$

Since the modification of out-modes changes the relation (2.55) as

$$\int_0^\infty d\omega' (\alpha_{\omega_{jn},\omega'} \alpha^*_{\omega_{j'n'},\omega'} - \beta_{\omega_{jn},\omega'} \beta^*_{\omega_{j'n'},\omega'}) = \delta_{jj'} \delta_{nn'}, \tag{2.92}$$

we have

$$\int_0^\infty d\omega' (|\alpha_{\omega_{jn},\omega'}|^2 - |\beta_{\omega_{jn},\omega'}|^2) = 1. \tag{2.93}$$

From (2.91) and (2.93), we obtain the mean particle number produced at late time

$$\langle in \,|\, N_{\omega_{jn}} \,|\, in \rangle = \int_0^\infty d\omega' |\beta_{\omega_{jn},\omega'}|^2 = \frac{1}{e^{8\pi G M \omega_{jn}} - 1} = \frac{1}{e^{\omega_{jn}/T_H} - 1}, \tag{2.94}$$

where $T_H \equiv (8\pi G M)^{-1}$ is the Hawking temperature of the black hole.

2.3.2 Black hole information loss paradox

The Hawking effect by which a black hole radiates thermal radiation leads to an apparent breakdown of the unitarity of quantum mechanics. Here we will briefly review this problem so called the black hole information loss paradox pointed out by Hawking [29].

Evaporation of a black hole

In the previous subsection, we derived the Hawking effect by fixing the background spacetime. However, from the consideration of the law of energy conservation, a radiating black hole must lose its mass in time, and in this sense, the validity of fixing the background should be discussed. In the case of a non-rotating black hole, all physical scale is determined only by its mass M and the Gravitational constant G [‖)]. Therefore, a Hawking particle, whose energy expectation value is roughly its Hawking temperature $T_H \equiv (8\pi GM)^{-1}$, would be emitted at the rate of $t \sim GM$. Therefore, we can estimate the luminosity of the black hole as

$$\frac{dM}{dt} \sim \frac{-T_H}{GM} \sim -(G^2M^2)^{-1}, \tag{2.95}$$

and this gives its life time, $t_{\rm life}$, as

$$t_{\rm life} \sim G^2M^3. \tag{2.96}$$

To be consistent with the result of a more rigorous derivation (see e.g. [81]), we need a factor of about 10^5 in (2.96)

$$t_{\rm life} \simeq 10^5 G^2M^3 \simeq 4 \times 10^{75} \left(\frac{M}{M_\odot}\right)^3 [\text{sec}], \tag{2.97}$$

which means that a solar-mass black hole takes much time longer than the age of the Universe to evaporate[**)]. The argument of evaporation of a black hole is true, at least, until reaching the Planck mass. The possibility of leaving a "remnant" after the evaporation is also pointed out (see e.g. [82–85]), but it has been believed that the most natural possibility is that only Hawking radiation would be left after the evaporation.

Breakdown of the unitarity of quantum mechanics

In the quantum mechanics, the evolution of a physical system is described by a unitary operator, $\hat{U}$, that maps a quantum state $|in\rangle$ on a Cauchy surface Σ_i into a final quantum state $|f\rangle$ on a final Cauchy surface Σ_f. This implies that we can obtain the initial state out of the final state as

$$|in\rangle = \hat{U}^\dagger |f\rangle . \tag{2.98}$$

This argument is true, for example, in the full Minkowski spacetime. However, in the existence of an evaporating black hole, this becomes quite controversial as discussed below.

[‖)] Remember that we take the natural unit $\hbar = c = 1$.

[**)] Since the age of the Universe is about $\sim 10^{17}$ sec, the lower mass bound of a mini black hole that survives until now is $M \sim 10^{11}$ kg. It is known that such a mini black hole cannot form by a gravitational collapse, but it might be created at the early stage of the Universe.

Assuming the black hole evaporation leaves nothing else but Hawking radiation, the Penrose diagram describing the evaporation process is given by Fig. 2.2. Let us consider three quantum states: an initial quantum state $|in\rangle$ on Σ_i, an intermediate quantum state $|mid\rangle$ on Σ_m, and a final quantum state $|f\rangle$ on Σ_f, where Σ_i, Σ_m, and Σ_f are the Cauchy surfaces. Since Σ_m crosses the future horizon H^+, it can split into the interior and exterior regions as $\Sigma_m \equiv \Sigma_{int} \cup \Sigma_{ext}$ (see Fig. 2.2).

Roughly speaking, the reason why the information loss seemingly takes place by a black hole evaporation is that the final state $|f\rangle$ may be determined only by information on the exterior part of the intermediate Cauchy surface Σ_{ext} rather than that on the full Cauchy surface Σ_m. To be more specific, we consider a pure quantum state as the initial state

$$|in\rangle = \sum_i c_i^{in} |\psi_i\rangle \,. \tag{2.99}$$

Although the intermediate state is also a pure state due to the unitary evolution of $|in\rangle$,

$$|mid\rangle = \sum_{i,j} c_{i,j} |\psi_i\rangle_{int} \otimes |\psi_j\rangle_{ext} \,, \tag{2.100}$$

we can show that the evolution from Σ_m to Σ_f is non-unitary if all states on Σ_f is determined by Σ_{ext}. The density matrix of the intermediate state restricted to Σ_{ext}, $\hat{\rho}_{ext}$ is obtained by tracing over all the internal states:

$$\hat{\rho}_{ext} = \sum_k \langle\psi_k|_{int} |mid\rangle \langle mid|\psi_k\rangle_{int} = \sum_{k,j,j'} c_{k,j} c^*_{k,j'} |\psi_j\rangle_{ext} \langle\psi_{j'}|_{ext} \,. \tag{2.101}$$

The resulting density matrix on Σ_{ext}, (2.101), is obviously independent of the interior orthogonal basis $\left\{|\psi_j\rangle_{int}\right\}$ due to the tracing operation. Note that the above considerations still do not lead to the breakdown of the unitarity at a fundamental level since the total quantum state $|m\rangle$ is pure. The problematic situation indeed comes from that all information on Σ_f would be determined by that of Σ_{ext}, which is independent of the interior information as is seen in (2.101). The loss of the interior information generically leads to its non-unitary evolution and the quantum state becomes a mixed state after the black hole evaporation.

2.3.3 Black hole complementarity

Although the possibility of the loss of information by the black hole evaporation has been pointed out by Hawking, a number of scenarios to explain the retrieval of information from a black hole has been proposed. Here we will briefly review the "black hole complementarity" which is one of the most plausible proposal regarding the retrieval of black hole information by Susskind, Thorlacius, and Uglum [30].

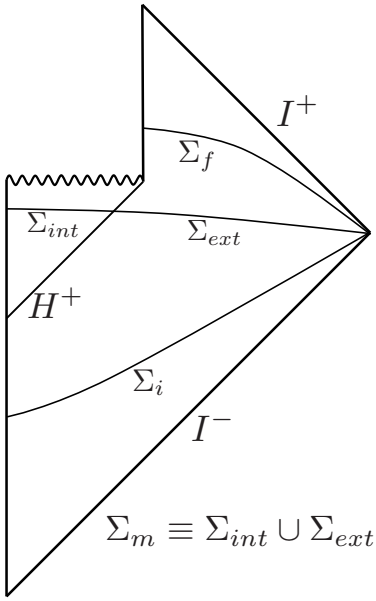

Figure 2.2: The Penrose diagram describing an evaporating black hole.

As is seen in (2.87), due to the infinite redshift at a black hole horizon, the Hawking radiation involves modes of transplanckian frequency whose energy can be arbitrarily large in the vicinity of the horizon. This picture is for a distant observer, and considering an infalling observer, he/she would not observe nothing special during infalling because of the equivalence principle. Therefore, it might be natural to expect that for the distant observer, there exists an "stretched horizon", which can absorb, thermalize, and reemit information, on the back hole horizon. Then, they argue that such a picture regarding the retrieval of black hole information by the stretched horizon is consistent with the following three plausible postulates:

*P*ostulate 1 (unitarity)— For a distant observer, the formation of a black hole and the evaporation process can be described within the framework of standard quantum theory. In particular, there exists a unitary S-matrix to describe a process from infalling matter to outgoing Hawking-like radiation.
*P*ostulate 2 (semi-classical Einstein equation)— Outside the stretched horizon of a massive black hole, around which gravitational curvature is weak and the quantum gravity regime is not necessary, physics can be described by a set of semi-classical field equations in a good approximation.
*P*ostulate 3 (thermodynamical picture)— For a distant observer, the number of microscopic states of a black hole of mass M is the exponential of its Bekenstein entropy $S(M)$.

This scenario seemingly contradicts with the expectation that a freely falling observer sees nothing special when crossing a large black hole horizon. Although the contradiction may arise only when attempting to correlate the results of experiment performed on both sides of horizon, the gedanken experiments by Susskind and Thorlacius implies that such an attempt is impossible because of a back reaction of the transplanckian modes on the stretched horizon [86]. In this sense, the argument of the black hole complementarity may be plausible.

2.3.4 Monogamy of entanglement

Before introducing the firewall argument, we briefly review a fundamental theorem in quantum information theory, the monogamy of entanglement. Let us consider three independent quantum systems, A, B, and C. The strong subadditivity relation of entropy is given by

$$S_{AB} + S_{BC} \geq S_B + S_{ABC}. \tag{2.102}$$

If A and B is fully entangled, we have

$$S_{AB} = 0 \quad \text{and} \quad S_{ABC} = S_C. \tag{2.103}$$

Then the strong subadditivity relation reduces to

$$I_{BC} = S_B + S_C - S_{BC} \leq 0. \tag{2.104}$$

Since I_{BC} is the mutual information of B and C and it is a non-zero quantity, (2.104) reduces to

$$I_{BC} = S_B + S_C - S_{BC} = 0, \tag{2.105}$$

which means that there is no correlation between B and C. Therefore, the quantum system B cannot fully entangle with both A and C simultaneously. This is the monogamy of entanglement that plays an essential role in the firewall argument.

2.3.5 Firewall argument

Let us summarize the three postulates in the black hole complementarity: (postulate 1) Hawking radiation is in a pure state, provided that an initial state is pure, (postulate 2) outside the region near the horizon of a massive black hole, physics can be described by an effective field theory of GR plus quantum field theory, and (postulate 3) a black hole is regarded as a quantum system with discrete energy levels whose number is the exponential of the Bekenstein entropy of the black hole.

In 2012, Almheiri, Marolf, Polchinski and Sully (AMPS) pointed out in Ref. [31] that postulate 1, postulate 2, and the equivalence principle of GR are mutually inconsistent for an *old black hole* [87–89] and AMPS's idea that we briefly review here is as follows. Let us consider an old black hole with early Hawking radiation A, late Hawking radiation B and infalling quanta behind the horizon C. A and B have to be fully entangled so that the final state of the black hole is a pure state (postulate 1). On the other hand, according to quantum field theory in curved spacetime, B and C, pair-created particles, are also fully entangled (postulate 2). That is, according to postulate 1 and 2, B should be fully entangled simultaneously with both A and C. This contradicts with the monogamy of entanglement, reviewed in the previous subsection, that forbids any quantum system being entangled with two independent systems fully and simultaneously. AMPS then proposed "*firewalls*", high-energy quanta at horizons energetic enough to break the entanglement of Hawking pairs, which would get rid of the inconsistency between postulate 1 and 2. However, the existence of firewalls implies that the free falling observer going across the horizon has a dramatic experience: the observer burns up at the horizon. That is, firewalls amounts to abandoning the equivalence principle.

AMPS also point out the possibility that firewalls exist even at cosmological horizons, such as those in de Sitter universe, as a natural extension of the argument. If the firewall argument is correct and the firewall exists even at the cosmological horizon of the Universe, there would be neither the interior regions of black holes and nor exterior of the cosmological horizons and the picture of the multiverse [35, 36] and eternal inflation [7, 37] would be rejected.

In Chapter 5, we discuss how we can resolve the inconsistency between postulate 1 and 2 without introducing the firewalls that violates the equivalence principle.

2.4 Higgs metastability and the fate of the Universe

2.4.1 Metastability of the Higgs vacuum

Phase transitions are involved in many physical models, and for example, boiling water is one of the most common experiences involving phase transitions in our daily life. This phenomenon is also important in cosmology since the vacuum bubble nucleations [90–92], quantum tunneling from a false vacuum state to a true vacuum state, can be regarded as the first order phase transition. Although such vacuum decay processes are important to discuss the early universe, a possibility of phase transitions in the future of the Universe has also been gathering a lot of attentions due to the metastability of the Higgs vacuum [93–116]. It has been considered that the Higgs metastability may lead to vacuum decay from our vacuum to another vacuum that exists at a large Higgs field value whose energy density is negative. Soon after the vacuum

decay, a nucleated bubble expands at nearly light-speed and the Universe would be filled by the negative vacuum. Therefore this metastability is regarded as a catastrophe at the final stage of the Universe.

The Higgs effective potential has been precisely determined by the two-loop calculation in the standard model (SM) [114–117] (see also [113] for an updated calculation up to three-loop). Since we are concerned with large Higgs field values, we can neglect the Higgs mass term and approximate the effective potential of the real neutral component h in the Higgs doublet $H = (0, v + h/\sqrt{2})$ as

$$V_H = \lambda(|H|^2 - v^2)^2 \simeq \frac{\lambda}{4}h^4, \tag{2.106}$$

where $v = 174$ GeV and the Higgs mass is given by $m_h = 2v/\sqrt{\lambda}$ at tree level. Including two renormalization group (RG) equations for the SM couplings and all the known one or two-loop corrections, the Higgs potential is improved and its coupling, λ, becomes negative around $10^9(10^{10})$ GeV for $m_h = 124(126)$ GeV and for the best-fit values of top mass and of strong couplings. The negativity of the coupling in the Higgs potential implies that the Higgs vacuum we live in is metastable and the vacuum decay induced by the metastability leads to a catastrophe of the Universe.

Recently, Bednyakov et al. [113] took into account renormalization group evolution up to three loops and strong-interaction corrections up to four loops, they concluded that the best theoretical fit to measured parameters still points to a metastable state. However, their result also shows that values of parameters are closer to an absolutely stable region than suggested by previous studies [114–117].

The metastability of the Universe has been hotly discussed in the context of cosmology to put tighter constrains on the parameters in the standard model or to discuss the fate of the Universe. For instance, Gregory et al. pointed out [118–121] that black holes would be catalysts for vacuum decays because of its strong gravity. If there were a super mini black hole (a primordial black hole) in the observable patch of the Universe, it could promote a vacuum decay of the Higgs vacuum around it, and the Universe would be entirely filled by the negative energy density. Therefore, in the far future of the Universe, all black holes become microscopic due to their Hawking radiation and may lead to the vacuum decays around them to fill the Universe with negative energy vacuum bubbles.

However, they did not take into account the thermal effect of black holes (i.e. Hawking radiation) and Yamada et al. [122] and Kohri et al. [123] pointed out that such a thermal effect would stabilize the Higgs potential and mini black holes might promote the vacuum decays less efficiently than expected. However, this argument highly depends on the details of the beyond SM or quantum gravity, and therefore, whether the thermal contributions from black holes are

significant for the Higgs metastability is still an open question.

2.4.2 Black holes as the catalysts for vacuum decays

In this subsection, a brief review of the vacuum decay around a black hole proposed by Hiscock [124] and by Gregory, Moss, Withers, and Burda [118–121] will be presented. If the Higgs potential develops a second minimum which has a negative energy density, the metastability of the Higgs potential would lead to vacuum decays. On the other hand, Hiscock pointed out [124] that black holes can be catalysts for vacuum decays because of their strong gravity. Burda et al. [119–121] then investigated the stability of Higgs (metastable) vacuum around black holes. They concluded that mini black holes could have promoted the vacuum decay of the Higgs sector within the cosmological time if mini black holes had existed in the Universe, provided that thermal effects of Hawking radiation is negligible.

Let us assume that bubbles nucleated due to the metastability of the Higgs potential can be modeled as thin wall bubbles and the interior and exterior metric has the form

$$ds_{\pm}^2 = -f_{\pm}(r_{\pm})dt_{\pm}^2 + f_{\pm}^{-1}(r_{\pm})dr_{\pm}^2 + r_{\pm}^2 d\Omega_2^2, \tag{2.107}$$

where indices of $+$ and $-$ represent the exterior and interior quantities, respectively, and a function$f_{\pm}(r)$ is given by

$$f_+ \equiv 1 - \frac{2GM_{\rm seed}}{r},\ f_- \equiv 1 - \frac{2GM_-}{r} + H^2 r^2. \tag{2.108}$$

Here $M_{\rm seed}$ is the mass of a seed black hole, M_- is the mass of the interior black hole, and $H \equiv \sqrt{(8\pi G/3)|\rho|}$ is a Hubble parameter of the energy density of the second minimum ρ (< 0). Since a thin wall bubble is assumed, one can use the Israel junction condition [125] instead of solving the Einstein equations:

$$\epsilon_- \sqrt{f_- + (dR/d\tau)^2} - \epsilon_+ \sqrt{f_+ + (dR/d\tau)^2} = 4\pi G\sigma R \ \text{ with } \ \epsilon_{\pm} \equiv \text{sign}[f_{\pm} dt_{\pm}/d\tau], \tag{2.109}$$

where σ is the energy density of the bubble wall, R is the radius of the wall, and τ is the proper time on the wall. This reduces to the following equation which has a similar form of the energy conservation law for a one-dimensional system:

$$\left(\frac{dR}{d\tau}\right)^2 + V(R) = 0, \tag{2.110}$$

$$\text{with } V(R) \equiv 1 - \frac{2GM_-}{R} + H^2R^2 - \left(\frac{2G\Delta M/R + (\Sigma^2 + H^2)R^2}{2\Sigma R}\right)^2, \tag{2.111}$$

where $\Sigma \equiv 4\pi G\sigma$ and $\Delta M \equiv M_{\rm seed} - M_-$. Since a vacuum bubble has zero velocity at the moment of nucleation, it is nucleated at position of $V = 0$. In general, the potential $V(R)$ gives

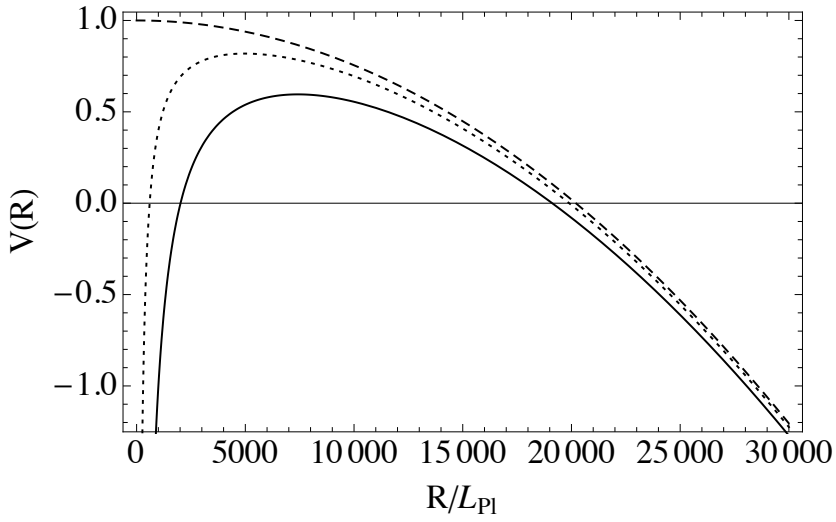

Figure 2.3: A plot of $V(R)$ with $H = 10^{-5}M_{\rm Pl}$ and $\Sigma = 10^{-4}M_{\rm Pl}$. We choose $M_{\rm seed} = M_- = 1000$ (solid line), 300 (dotted line), and 0 (dashed line).

two nucleation positions and one is a growing mode and the other is a decaying mode as seen in Fig. 2.3. If a black hole is not involved in a bubble nucleation ($M_{\rm seed} = M_- = 0$), the nucleation is described by the Coleman De-Luccia (CDL) instanton, which has its growing mode and there is no decaying mode (a dashed line in Fig. 2.3).

In general, the nucleation rate, Γ, is calculated by the path-integral method, and in the semi-classical approximation, it is given by the exponent of on-shell Euclidean action (a brief review of the Euclidean path integral method is presented in Appendix C):

$$\Gamma \simeq Ae^{-(I^f_{\rm E}-I^i_{\rm E})}. \tag{2.112}$$

The "on-shell Euclidean action" is a quantity one can obtain by substituting an Euclidean solution into its Euclidean action and $I^f_{\rm E}$ ($I^i_{\rm E}$) is the on-shell Euclidean action after (before) the tunneling. To obtain the Euclidean solution of the system after the bubble nucleation around a black hole of $M_{\rm seed}$, one should perform the Wick rotation, $\tau = -i\tilde{\tau}$, and the dynamics of the nucleated bubble becomes periodic [††)] since the energy conservation law of the bubble (2.110) reduces to

$$\left(\frac{dR}{d\tilde{\tau}}\right)^2 - V(R) = 0. \tag{2.113}$$

[††)]The periodic Euclidean solution links between a decaying mode and growing mode, and if one performs the analytic continuation at the point associated with the growing (decaying) mode, the solution describing the bubble nucleation of the growing (decaying) mode is obtained.

Let us calculate the initial on-shell Euclidean action $I^i_{\rm E}$ on the Euclidean space $\mathcal{M}$ which includes Killing horizons, i.e. black hole horizons and de Sitter horizons, by dividing $\mathcal{M}$ into $\mathcal{M}-\mathcal{B}$ and $\mathcal{B}$, where $\mathcal{B}$ is a small region around the Killing horizon areas:

$$\mathcal{B} \equiv \{x^\mu : |r - r_h| < \mathcal{O}(\epsilon)\} \tag{2.114}$$

with small ϵ. We can divide $I^i_{\rm E}$ into two parts

$$I^i_{\rm E} = I_{\mathcal{M}-\mathcal{B}} + I_{\mathcal{B}}, \tag{2.115}$$

where $I_{\mathcal{B}}$ is the Euclidean action on the horizons and $I_{\mathcal{M}-\mathcal{B}}$ is that of the other space. We can smooth out the singularities at the Killing horizons (conical singularities) by performing integral, then taking the limit of $\epsilon \to 0$. The system here we consider consists of gravitational field $g_{\mu\nu}$ and the Higgs field h, and therefore, the bulk part of the Euclidean action is

$$I_{\mathcal{M}-\mathcal{B}} = -\frac{1}{16\pi G}\int_{\mathcal{M}-\mathcal{B}} \mathcal{R} - \int_{\mathcal{M}-\mathcal{B}} \mathcal{L}_m(g,h) + \frac{1}{8\pi G}\int_{\partial\mathcal{B}} K. \tag{2.116}$$

Now we have a periodic Euclidean solution of period β_i and the evaluation of this on-shell reduces to

$$I_{\mathcal{M}-\mathcal{B}} = \frac{1}{16\pi G}\int_0^{\beta_i} d\tilde{\tau}\left[\int_{\Sigma_{\tilde{\tau}}}\left({}^{(3)}\partial_{\tilde{\tau}} g_{ij}\pi^{ij} + \partial_{\tilde{\tau}} h\pi - N\mathcal{H} - N^i\mathcal{H}_i\right) - \int_{\partial\mathcal{B}_{\tilde{\tau}}} NK\right], \tag{2.117}$$

where $\Sigma_{\tilde{\tau}}$ is a foliation of $\mathcal{M}-\mathcal{B}$ with a family of spatial hypersurfaces of Euclidean time with $0 < \tilde{\tau} < \beta_i$, $\mathcal{H}$ and $\mathcal{H}_i$ are the hamiltonian and momentum constraints, and K is the extrinsic curvature of $\partial\mathcal{B}_{\tilde{\tau}} \equiv \partial\mathcal{B} \cap \Sigma_{\tilde{\tau}}$. Since $\mathcal{M}-\mathcal{B}$ has a Killing vector $\partial_{\tilde{\tau}}$, $\partial_{\tilde{\tau}} h = {}^{(3)}\partial_{\tilde{\tau}} g_{ij} = 0$. Furthermore, since we evaluate the on-shell action, one has $\mathcal{H} = \mathcal{H}_i = 0$. Therefore, we have

$$I_{\mathcal{M}-\mathcal{B}} = -\frac{1}{16\pi G}\int_{\partial\mathcal{B}_{\tilde{\tau}}} NK \sim \mathcal{O}(\sqrt{\epsilon}), \tag{2.118}$$

where we used $N \sim \mathcal{O}(\sqrt{\epsilon})$ near the conical singularities. Finally, we find $I_{\mathcal{M}-\mathcal{B}} = 0$ in the limit of $\epsilon \to 0$. Therefore, the contribution from the conical singularities is

$$I^i_{\rm E} = I_{\mathcal{B}} = -\frac{1}{16\pi G}\int_{\mathcal{B}} \mathcal{R} + \frac{1}{8\pi G}\int_{\partial\mathcal{B}} K = -\frac{\mathcal{A}}{4G}, \tag{2.119}$$

which is known as the action of a gravitational instanton by Gibbons and Hawking [26, 126]. Gregory, Moss, and Withers [118] derived this in the existence of conical singularities. Now we have the action of the initial Euclidean space

$$I^i_{\rm E} = -\frac{\mathcal{A}}{4G} = -4\pi G M^2_{\rm seed}. \tag{2.120}$$

After the tunneling, we have the bubble wall in the Euclidean space, which has its period β_f, and therefore, we can not use the symmetry associated with the Killing vector $\partial_{\tilde{\tau}}$. The

contribution from the boundary term of the dynamical bubble wall should be taken into account, and the action after the tunneling reduces to (for the details of the derivation, see Appendix C)

$$I_{\rm E}^{f} = -4\pi G M_{-}^{2} - \frac{1}{2}\int_{\mathcal{W}} \sigma - \frac{1}{16\pi G}\int_{\mathcal{W}} (f'_{+}\dot{\tilde{\tau}}_{+} - f'_{-}\dot{\tilde{\tau}}_{-}). \tag{2.121}$$

From the action of the initial and final Euclidean space, (2.120) and (2.121), (2.112) reduces to

$$\Gamma \simeq A \exp\left[4\pi G(M_{-}^{2} - M_{\rm seed}^{2}) - \frac{1}{4G}\int d\tilde{\tau}\left[(2R - 6GM_{\rm seed})\dot{\tilde{t}}_{+} - (2R - 6GM_{-})\dot{\tilde{t}}_{-}\right]\right], \tag{2.122}$$

where $t_{\pm} \equiv -i\tilde{t}_{\pm}$. As is shown in [118] or in Section 6 of the thesis, this transition rate is higher than the transition rate calculated by the CDL instanton [92] that corresponds to a vacuum decay without any impurities such as black holes.

Chapter 3

Beginning of inflationary universes

Although the inflation is a successful paradigm which solves a number of puzzling problems and fits with observations of WMAP and Planck with high accuracies, in order for inflation to be counted as a real success, it should happen without any fine-tuned initial conditions. In this section, we present a simple model where inflation can start from a highly inhomogeneous field configuration by virtue of quantum effects.

3.1 Inhomogeneous initial conditions for inflation

3.1.1 Instantaneous percolation of vacuum bubbles and thermalized bubbles

Here as a minimalistic approach based on the classical Big Bang cosmology, we assume that the Universe started from the Big Bang singularity in a thermal state with a ultra high temperature well above the scale of the Grand Unified Theory (GUT), and that symmetry is restored at this moment. To model this situation, in the following, we introduce a scalar field χ and ϕ with a potential

$$V(\chi, \phi, T = 0) \equiv \frac{1}{2} g_1^2 \phi^2 \chi^2 - \frac{1}{4}\kappa\chi^4 + \frac{1}{2M_{\rm Pl}^2}\lambda\chi^6 + V_0, \tag{3.1}$$

where g_1, κ and λ are coupling constants and $V_0 \equiv (\kappa^3/(108\lambda^2))M_{\rm Pl}^4$. The field χ gives inhomogeneous configurations of the Universe and ϕ behaves as massless particles at $\chi = 0$ and is massive at the global minimum $\chi = \chi_0 \equiv \sqrt{\kappa/(3\lambda)}$. Taking into account the thermal correction for the potential, it can be approximated by*)

$$V(\chi, T) \simeq \frac{1}{2} g^2 T^2 \chi^2 - \frac{1}{4}\kappa\chi^4 + \frac{1}{2M_{\rm Pl}^2}\lambda\chi^6 + V_0, \tag{3.2}$$

*)The one-loop correction of the quartic term is included in the thermal mass of the first term. Thermal corrections for the third term are ignored since those are subdominant when $T/M_{\rm Pl} \lesssim \sqrt{\kappa/\lambda}$ and $T/M_{\rm Pl} \lesssim g/\sqrt{\lambda}$ and we are interested in the symmetry breaking phase.

where $g \equiv (g_1^2/3 - \kappa/2)/4$. One finds that the symmetry is restored when $T > T_c \equiv \kappa/(4g\sqrt{\lambda})$. For $T \ll T_c$, the potential has the global minimum at $\chi = \chi_0$ and a local minimum at $\chi = 0$ with the vacuum energy density $V = V_0$ (Fig. 3.1).

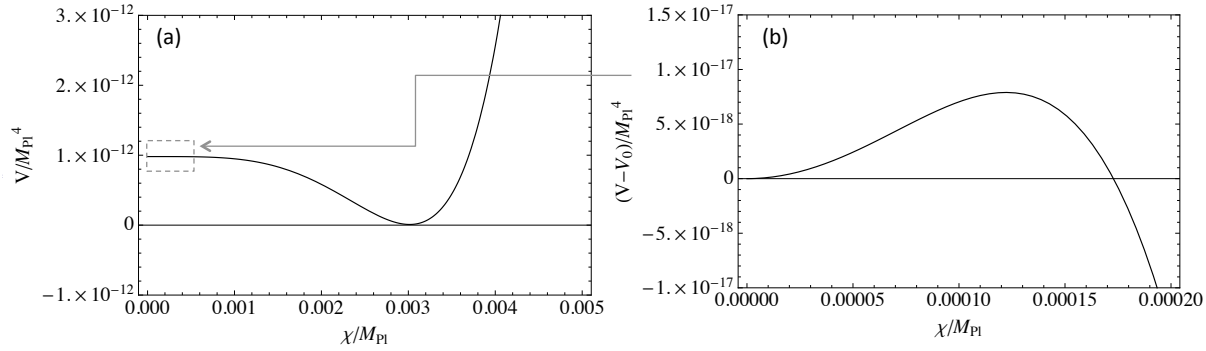

Figure 3.1: Plots of the effective potential with $g = 0.13$, $\kappa = 0.14$, and $\lambda = 5.2 \times 10^3$. (a) shows the global minimum at $\chi = \chi_0$ and (b) shows the local minimum at $\chi = 0$.

Since the radiation dominated Universe expands and its temperature eventually falls to the critical temperature, the symmetry is broken and the Universe becomes inhomogeneous. The size of inhomogeneity is determined by the percolation of vacuum bubbles. Each nucleated true-vacuum bubble grows at light speed until their walls collide each other. Those bubbles eventually coalesce one by one (percolation) and false vacuum domains will be trapped by the true vacuum regions. If the bubble nucleation is significantly enhanced by the thermal effect of primordial radiation, the percolation instantaneously occurs and small trapped false vacuum regions including the primordial radiation may be left. The trapped false vacuum regions may be stabilized by the thermal pressure of the interior radiation (hereinafter referred to as thermalized bubbles) as we discuss it below.

The epoch when true-vacuum bubbles start to percolate to form an infinite network (see Fig. 3.2) is referred to as the percolation time t_p, which can be estimated by the value of the volume fraction of false vacuum phase. Introducing the thermal nucleation rate of true-vacuum bubbles $P(t)$ and the scale factor $a(t)$, the volume fraction of the false vacuum phase $u(t)$ can be expressed as

$$u(t) \equiv \exp\left[-\frac{4\pi}{3}\int_{t_i}^{t} dt' P(t') a^3(t) \left(\int_{t'}^{t} \frac{dt''}{a(t'')}\right)^3\right], \tag{3.3}$$

where t_i is the time when the temperature reaches the critical temperature. From the percolation theory for same-size bubbles, the percolation time is determined by $u(t_p) \simeq 0.3$ [35].

Let us calculate the time evolution of $u(t)$ by fixing the parameters of the theory $g = 0.13$,

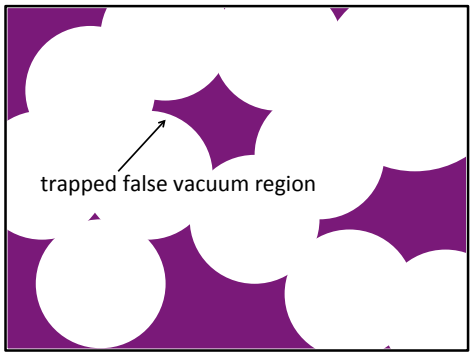

Figure 3.2: Schematic picture showing the percolation of vacuum bubbles.

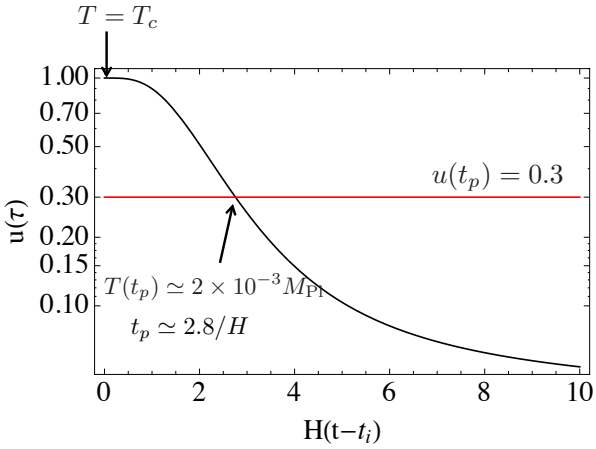

Figure 3.3: Plot of the function $u(t)$. The percolation of bubbles occurs at $t \simeq 2.8/H$.

$\kappa = 0.14$, and $\lambda = 5.2 \times 10^3$. In the symmetry breaking phase, the potential near $\chi = 0$ is determined only by the quadratic and quartic terms in (3.2), and the thermal tunneling rate P can be analytically calculated as [127]

$$P \simeq T^4 \left(\frac{S_3}{2\pi T}\right)^{3/2} \exp\left(-\frac{S_3}{T}\right), \tag{3.4}$$

$$S_3 = 6\pi \frac{g}{\kappa} T. \tag{3.5}$$

The exponent of the tunneling rate, S_3/T, for this potential is independent of the temperature. The temperature decreases in time as $T(t) \propto a^{-1}(t)$ during the radiation dominated era. Since the primordial Universe we here assume consists of the thermal radiation and vacuum energy,

the scale factor has the form

$$a(t) = \sinh^{1/2}(2Ht) \simeq (2Ht)^{1/2} \quad \text{for} \quad t \ll H^{-1}, \tag{3.6}$$

where $H^2 \equiv (8\pi G/3)V_0$. We can calculate $u(t)$ by substituting (3.5) and (3.6) into (3.3), and then it is found that the percolation starts when (see Fig. 3.3)

$$T(t_p) \sim 2 \times 10^{-3} M_{\rm Pl}. \tag{3.7}$$

The number density of bubbles n_B at $t = t_p$ is given by

$$n_B(t_p) = a^{-3}(t_p) \int_{t_i}^{t_p} dt' a^3(t') P(t') u(t'), \tag{3.8}$$

and the mean separation distance of bubbles d can be roughly estimated by

$$d \sim n_B^{-1/3} \sim 1.4 \times 10^4 \ell_{\rm Pl}. \tag{3.9}$$

From (3.7) and (3.9), the interior entropy can be roughly estimated as

$$S \simeq \left(\frac{8\pi^3}{135}\right) T^3 d^3 \sim 10^5. \tag{3.10}$$

This mean distance d may be comparable to the mean size of trapped false vacuum regions. On the other hand, the thickness of a bubble wall, w, can be estimated by

$$w \sim 1/\sqrt{V''}|_{\chi=\chi_0} = \left(\frac{2\kappa^2}{3\lambda}\right)^{-1/2} \simeq 6 \times 10^2 \ell_{\rm Pl}. \tag{3.11}$$

We found that $w \ll d$ is satisfied in our setup, and therefore we use the thin wall approximation in the following discussions. The tension of the thin wall σ can be estimated by

$$\sigma \simeq \int_0^{\chi_0} d\chi \sqrt{V} \sim \sqrt{V_0} \times \chi_0 \simeq 10^{-8} M_{\rm Pl}^3. \tag{3.12}$$

3.1.2 Lifetime of the thermalized bubble

Since the thermal radiation has a high-energy tail in its spectrum, the thermalized bubble is not an eternal object and has a finite lifetime, τ_f. In terms of the number of the ϕ-particle, N, trapped in the bubble with volume V, the lifetime can be estimated as

$$\tau_f = N\left(\frac{dN}{dt}\right)^{-1} \sim N\left(\frac{\delta N}{\delta t}\right)^{-1} \sim N\left(\frac{(V/2\pi^2)\int_{m_\phi}^{\infty} \nu^2 d\nu/(e^{\nu/T}-1)}{V^{1/3}}\right)^{-1} \simeq 2\zeta(3)\frac{T^2}{m_\phi^2} e^{m_\phi/T} V^{1/3}, \tag{3.13}$$

where the bubble crossing time δt is estimated by $V^{1/3}$ and $N/V = \zeta(3)T^3/\pi^2$. To derive the final expression in (3.13), we assumed that the mass of ϕ-particle at $\chi = \chi_0$, $m_\phi \equiv g_1\chi_0$, is much

larger than T. The entropy is conserved as long as the thermal radiation is trapped almost completely, and this picture is valid when the exterior mass of ϕ-particle is much larger than the interior thermal energy $\sim T$. When this condition is not satisfied, the thermalized bubble gravitationally collapses to form a black hole.

3.1.3 Conditions for the thermalized bubbles

Note that our proposal would not be affected by the details of the assumed model as long as the following conditions[†)] are satisfied:

1. The resulting configuration well after the spontaneous symmetry breaking ($T \ll T_c$) involves a bubble configuration whose interior is filled by a positive vacuum energy density ρ_- and thermal radiation of temperature T, and is also surrounded by a lower vacuum energy density $\rho_+ (< \rho_-)$.

2. The thin wall approximation is valid and it is almost spherical due to its surface tension.

3. This configuration is stabilized by the balance between a wall tension and the radiation pressure of interior radiation.

4. The interior thermal radiation is almost completely trapped by the wall, so that the total interior entropy can be regarded as a conserved quantity.

In our setup, ϕ-particle is massless in the bubble interior ($\chi = 0$) although the exterior mass of ϕ-particle is $m_\phi \equiv g_1 \chi_0$. Remember that we here set the value of the lower energy density, surrounding the bubble, to zero ($\rho_+ = 0$) since the true-vacuum bubbles surrounding a false vacuum region are supposed to have no bulk energy density.

3.2 Model of inhomogeneous space

In the following we model a part of the inhomogeneous space by a trapped false vacuum region in which thermal radiation is trapped. That is, $\chi = 0$ inside the bubble and the interior is filled by thermal radiation of ϕ whose temperature is $T < T_c$. In the exterior, $\chi = \chi_0$ and there is no vacuum energy there. We will also concentrate on the cases where the bubble has its thin wall ($w \ll R$) for simplicity. Hence we need to solve the Israel junction condition [125] to follow the dynamics of the bubble. Assuming that the interior radiation fills the bubble uniformly, the

[†)] When the third or fourth conditions are not satisfied, the bubble gravitationally collapses and a black hole forms. We discussed the creation of an inflationary universe from an evaporating black hole in [66], where the thermal energy due to Hawking radiation plays an important role.

interior geometry is described by the Friedmann-Lemaître-Robertson-Walker (FLRW) metric (the static form of the FLRW metric is presented in the Appendix B). For simplicity we consider a situation that the exterior radiation is diluted by the cosmic expansion and that the metric there can be approximated by the Schwarzschild solution, corresponding to the case the inhomogeneity over the horizon scale is the largest. We show that inflation is possible even from such a highly inhomogeneous initial condition.

The thin wall of false vacuum bubble can be characterized by its tension, σ. The Israel junction condition has the form

$$K^+_{ab} - K^-_{ab} = -8\pi G \left(S_{ab} - \frac{1}{2} h_{ab} \mathrm{Tr}[S_{ab}] \right), \tag{3.14}$$

where the K^+_{ab} (K^-_{ab}) is the exterior (interior) extrinsic curvature on the wall, h_{ab} is the induced metric there, S_{ab} is the energy momentum tensor (EMT) of the wall. (θ, θ)-component of the interior and exterior extrinsic curvature has the form [128]

$$K^\pm_{\theta\theta} = \frac{\epsilon_\pm}{R} \sqrt{\dot{R}^2 + f_\pm(R)}, \tag{3.15}$$

$$f_- \equiv 1 - (8\pi G/3)\rho R^2, \quad f_+ \equiv 1 - 2GM/R, \tag{3.16}$$

$$\text{with } \rho \equiv \rho_- + \frac{\pi^2}{30} T^4, \tag{3.17}$$

where a dot denotes the derivative with respective to the proper time on the wall and $\epsilon_\pm = \mathrm{sign}[f_\pm \dot{t}_\pm]$ is the sign of the extrinsic curvature, which is very important to determine the spacetime configuration as is discussed later. Here we assume that the lifetime of the thermalized bubble is longer than the related time scale. In this case, the entropy of the interior radiation, S, is constant and the following condition is satisfied [129]:

$$T^3 R^3 = \frac{135 S}{8\pi^3} \equiv C_0^3. \tag{3.18}$$

From (3.17) and (3.18), we have

$$\rho = \frac{3}{8\pi G} \left(H^2 + \frac{135^{4/3} S^{4/3}}{180\pi} \frac{G}{R^2} \right), \tag{3.19}$$

where $H^2 \equiv 8\pi G \rho_- / 3$. On the other hand, the EMT, S_{ab}, is

$$S_{ab} = \mathrm{diag}\left(\sigma, p, p\right), \tag{3.20}$$

where σ and p is the energy density and pressure of the wall and $p = -\sigma$ is assumed in the following. Then, the (θ, θ)-component of the junction condition reduces to

$$\epsilon_- \beta_- - \epsilon_+ \beta_+ = 4\pi G \sigma R, \tag{3.21}$$

$$\text{with } \beta_\pm \equiv \sqrt{\dot{R}^2 + f_\pm}. \tag{3.22}$$

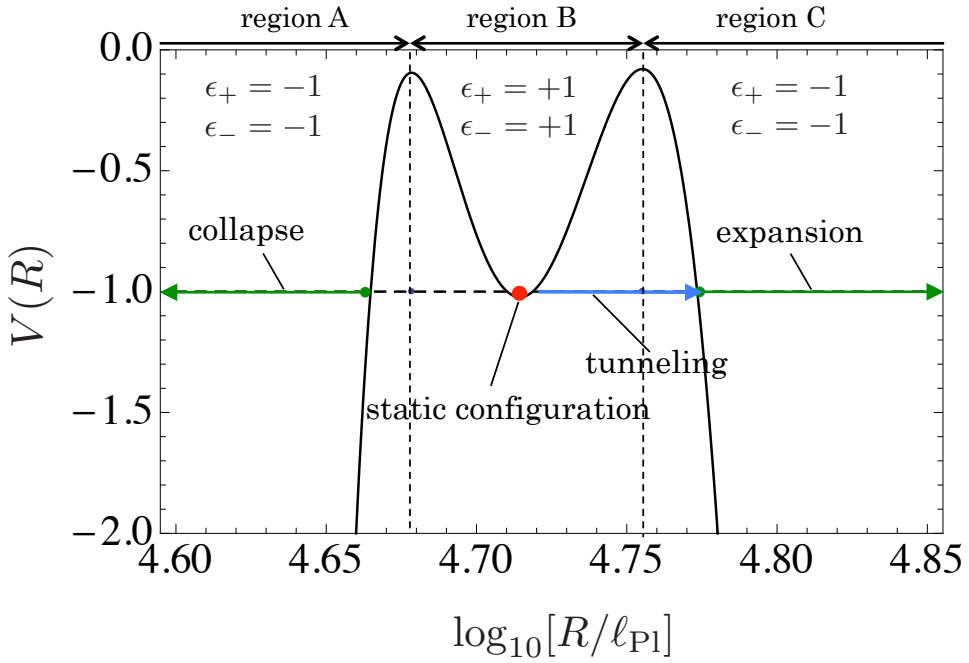

Figure 3.4: Plot of the effective potential governing the position of the wall. Choosing the static state as an initial condition, there is a possible quantum tunneling path (blue arrow).

After some calculations, (6.10) reduces to

$$\left(\frac{dR}{d\tau}\right)^2 + V(R) = -1, \tag{3.23}$$

$$V(R) \equiv -\frac{2GM}{R} - \left(\frac{2GM - \left(8\pi G\rho/3 + \Sigma^2\right) R^3}{2\Sigma R^2}\right)^2, \tag{3.24}$$

where $\Sigma \equiv 4\pi G\sigma$. One finds that an effective potential, $V(R)$, governs the position of the bubble wall. We plot the effective potentials by fixing parameters as $\Sigma = 10^{-8} M_{\rm Pl}$, $H = 2.8 \times 10^{-6} M_{\rm Pl}$, $S = 1.3 \times 10^6$ and $M = 2.26 \times 10^3 M_{\rm Pl}$ in Fig. 3.4. The corresponding temperature is found to be $T \simeq 1.7 \times 10^{-3} M_{\rm Pl}$ from the relation (3.18). Those values are consistent with the estimations in Subsection 3.1.1 up to the order of 10 or less. This potential has a stable region located at $R = 5.13 \times 10^4 \ell_{\rm Pl}$ (a red point in Fig. 3.4) because of the balance between the pressure of thermal radiation and the wall tension, and on the other hand, a larger (smaller) bubble expands (collapses) and inflation begins (a black hole forms) eventually (green arrows in Fig. 3.4). We choose parameters so that the four conditions are satisfied and find that the potential barrier separates the static state and the expansion phase. Here we can check if the third condition is satisfied at the static point. The equilibrium condition between the wall tension and interior

thermal radiation is given by

$$dE/dR = 0, \quad E \simeq \frac{4\pi}{3}\rho_- R^3 + 4\pi R^2\sigma + \frac{4\pi}{3}R^3\frac{\pi^2}{30}T^4. \tag{3.25}$$

Using this condition and (3.18), the equilibrium point is $R = 5.18 \times 10^4 \ell_{\rm Pl}$, which is almost consistent[‡)] with the result of the Israel junction condition.

3.3 Quantum effect on the initial inhomogeneous space

Here we consider quantum tunneling from the stable bubble to a larger bubble (a blue arrow in Fig. 3.4), whose spacetime configuration actually accommodates an inflationary domain as shown in the following. To determine the spacetime configuration of bubble-like regions, ϵ_+ (ϵ_-) plays an important role [130,131] since it is equivalent to the sign of spatial components of extrinsic curvature on the outer (inner) surface of the wall and the sign determines the orientation of the wall. From (6.10) we can obtain the form of $\epsilon_\pm$ as a function of R:

$$\epsilon_\pm(R) = \text{sign}\left(\frac{2GM}{R} - \left(8\pi G\rho/3 \pm \Sigma^2\right) R^2\right). \tag{3.26}$$

In Fig. 3.4, the sign of $\epsilon_\pm$ is shown, and the Regions-A, B, and C denote those with $(\epsilon_+, \epsilon_-) = (-,-)$, $(+,+)$, and $(-,-)$, respectively. One finds that a stable bubble is smaller than the de Sitter horizon, and therefore it never experiences inflation in a classical manner. However, once the bubble quantum mechanically tunnels to a larger one, both ϵ_+ and ϵ_- change from $+1$ to -1 and the bubble expands so that the false vacuum region experiences inflation eventually.

[‡)] The small deviation up to 1% comes from higher-order effects in GR.

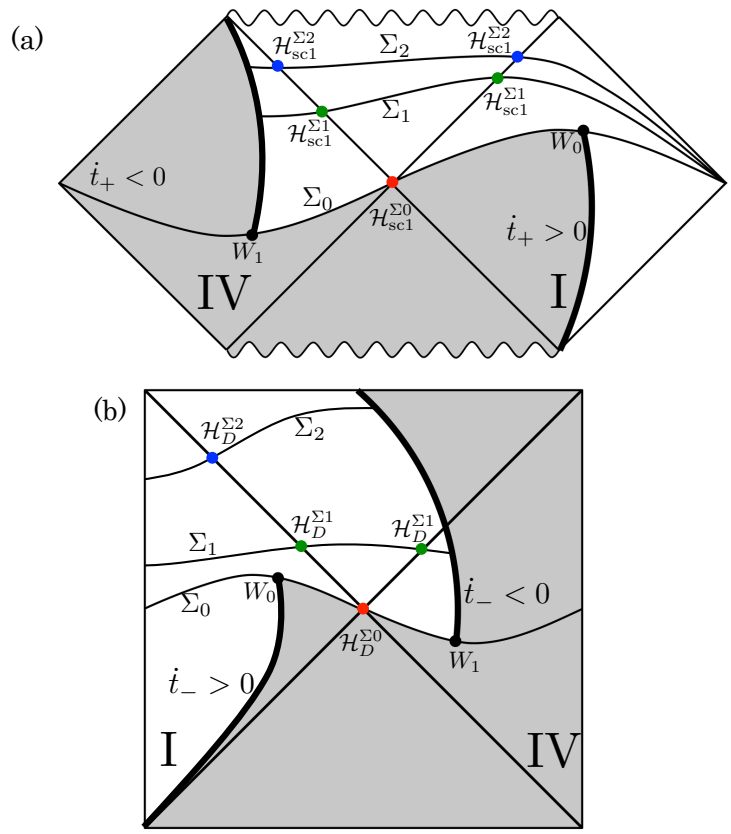

Figure 3.5: The trajectory of the bubble wall (a black thick lines) on (a) the Penrose diagram of the Schwarzschild spacetime (exterior) and on (b) the Penrose diagram of the de Sitter spacetime (interior). The tunneling occurs on a hypersurface Σ_0 (a bubble wall tunnels to W_1 from W_0) and Σ_0 evolves to Σ_1 and to Σ_2. Red, green, and blue points represent horizons on the hypersurface Σ_0, Σ_1, and Σ_2, respectively. One observes a black hole horizon, $\mathcal{H}^{\Sigma 0}_{\rm sc1}$, and a de Sitter horizon, $\mathcal{H}^{\Sigma 0}_{D}$, on Σ_0 soon after the tunneling (red points). The hypersurface Σ_1 accommodates two black hole horizons, $\mathcal{H}^{\Sigma 1}_{\rm sc1}$, and two de Sitter horizons, $\mathcal{H}^{\Sigma_1}_{D}$, (green points). The hypersurface Σ_2 accommodates two black hole horizons, $\mathcal{H}^{\Sigma 2}_{\rm sc1}$, and a de Sitter horizon $\mathcal{H}^{\Sigma 2}_{D}$ (blue points).

To be consistent with the change of $\epsilon_\pm$ [130, 131], the spacetime configuration drastically changes after the tunneling. The sign of both $\dot{t}_+$ and $\dot{t}_-$ are definitely positive (negative) in the Region-I (IV) of the Penrose diagrams describing the exterior (Fig. 3.5-(a)) and interior (Fig. 3.5-(b)) spacetime. Once the stable bubble tunnels to a larger bubble from Region-B to Region-C, the bubble wall tunnels to the Region-IV ($\dot{t}_\pm < 0$) from I ($\dot{t}_\pm > 0$) in the Penrose diagrams (Fig. 3.5), which leads to the appearance of an Einstein-Rosen (ER) bridge, beyond which a false vacuum region starts to inflate (Fig. 3.6).

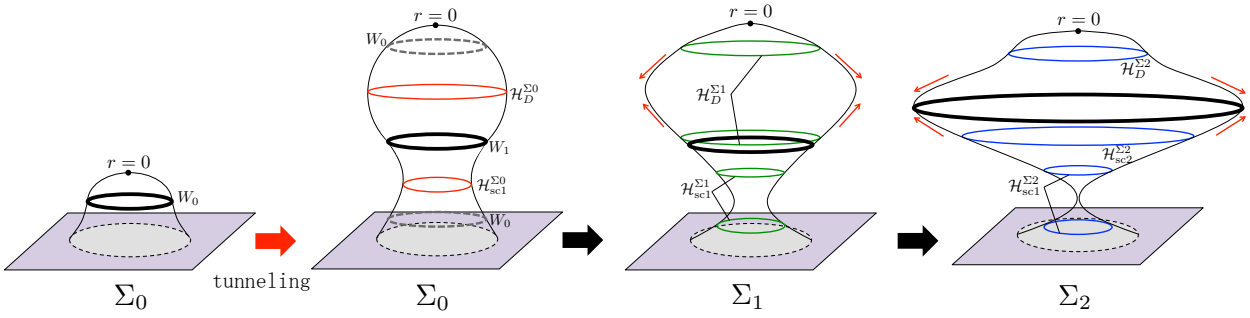

Figure 3.6: A schematic picture showing the time-evolution of the false vacuum bubble before and after the tunneling. Red, green, and blue lines correspond to the horizons shown in Fig. 3.5 with red, green, and blue points, respectively. The domain beyond the ER bridge starts to inflate (red arrows) and the bubble wall (a black thick line) expands after the tunneling.

Let us calculate the tunneling rate by calculating the on-shell Euclidean action[§)] $I_{\rm E}$ [118]:

$$I_{\rm E} \equiv B - \Delta S, \tag{3.27}$$

$$B \equiv \frac{1}{2G} \oint d\tilde{\tau} \left[(R - 3GM) \frac{d\tilde{t}_+}{d\tilde{\tau}} - \left(R - 2J\frac{G}{R} \right) \frac{d\tilde{t}_-}{d\tilde{\tau}} \right], \tag{3.28}$$

$$\Delta S \equiv \frac{\Delta A}{4G}, \tag{3.29}$$

where we introduced the Euclidean time, $\tau \equiv -i\tilde{\tau}$ and $t_\pm \equiv -i\tilde{t}_\pm$, and ΔA represents the change of horizon areas associated with the quantum tunneling. The change of Bekenstein entropy in the Euclidean on-shell action, ΔS, originates from the conical singularities on the Euclidean manifold before and after the tunneling[¶)]. A factor $B > 0$ depends on the dynamics of the wall[‖)] in the Euclidean picture, which suppresses the tunneling rate:

$$\Gamma \sim H e^{-I_{\rm E}} = H e^{-B+\Delta S}. \tag{3.30}$$

The quantum tunneling of the wall leads to the appearance of a black hole horizon and a de

[§)] For a brief review of the quantum tunneling in the framework of the Euclidean path integral method, see Appendix C.

[¶)] Although the space-like foliation Σ_0 after the quantum tunneling covers the space beyond the ER bridge, the black hole interior ($r < 2GM$) is not included in the foliation. Therefore, the Bekenstein entropy of black hole, which is associated with the interior information of black hole, is well defined.

[‖)] Since we are interested only in the tunneling process of wall and the energy of interior thermal radiation is subdominant for the larger bubble, in the calculation of factor B the Euclidean dynamics of thermal radiation is ignored. Furthermore, in our setup, the period of the Euclidean dynamics is shorter than the lifetime of bubble calculated in (3.13) although the exterior mass of ϕ-particle m_ϕ is comparable to the interior radiation temperature T. In this sense, the fourth condition in Subsection 3.1.3 is satisfied during the tunneling time scale.

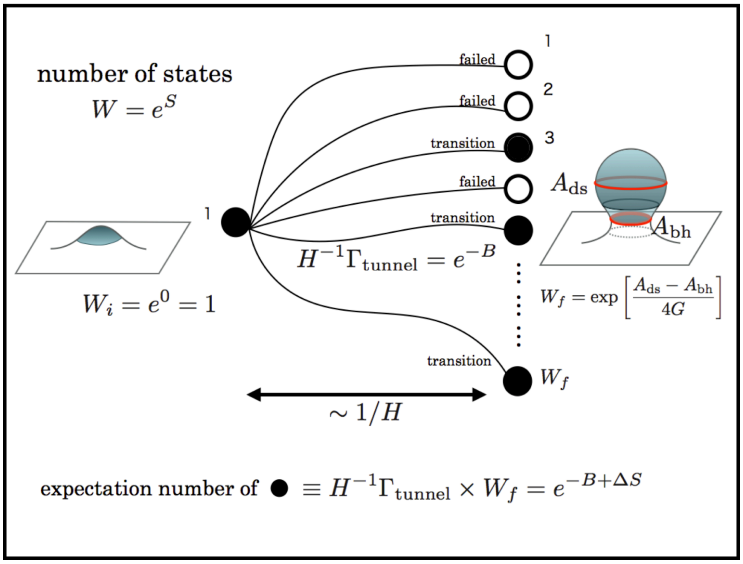

Figure 3.7: A schematic picture showing how a great number of microscopic degrees of freedom in the final state enhances the tunneling rate. Each path represents a quantum tunneling process from the initial state to one of the final states. Open and filled circles in the final state represent the failure and success of quantum tunneling. Since the expectation number of the filled circles is larger than unity ($\Delta S > B$), the quantum tunneling is exponentially enhanced.

Sitter horizon, whose area are denoted by $A_{\rm bh}$ and $A_{\rm ds}$, respectively. This gives the increment of the Bekenstein entropy, $\Delta S = (A_{\rm bh} + A_{\rm ds})/4G > 0$ and enhances the transition rate in (3.30). In the parameters we chose in Fig. 3.4, the factor B and the Bekenstein entropies are

$$B \simeq 3.0 \times 10^7, \frac{A_{\rm ds}}{4G} \simeq 4.0 \times 10^{11}, \frac{A_{\rm bh}}{4G} \simeq 6.4 \times 10^7, \tag{3.31}$$

which yields $\Delta S \gg B$, that is, the quantum tunneling rate is exponentially enhanced by the increment of Bekenstein entropy. One might wonder if the former case breaks the semi-classical approximation based on the Euclidean path integral method. We answer this question by taking into account the microscopic degrees of freedom on gravitational horizons [24]. Although the initial state has no microscopic degrees of freedom originating from horizons, the final state has a black hole horizon and a de Sitter horizon with areas, $A_{\rm bh}$ and $A_{\rm ds}$, respectively, after the tunneling. Then, the initial and final number of microscopic degrees of freedom, denoted by $W_{\rm i}$ and $W_{\rm f}$, respectively, can be estimated as $W_{\rm i} = e^{0/4G} = 1$ and $W_{\rm f} = e^{(A_{\rm bh}+A_{\rm ds})/4G}$. From $e^{\Delta S} = W_{\rm f}/W_{\rm i}$, we can interpret the quantum tunneling we have discussed so far as a transition from one initial state to one of a great number of final states, whose number is given by $W_{\rm f}$, and

the transition rate from one initial state to another microscopic final state is given by

$$\Gamma_{\rm micro} \sim He^{-B} \tag{3.32}$$

up to the ambiguity of the pre-factor. Since the final states whose number is $W_{\rm f}$ are not distinguishable among them, the original transition rate is derived as

$$\Gamma \sim W_{\rm f} \times \Gamma_{\rm micro} = He^{-B+\Delta S}. \tag{3.33}$$

Therefore, the reason why the tunneling rate is exponentially enhanced is that there are a great number of final states in the microscopic sense, and each tunneling rate, $\Gamma_{\rm micro}$, is exponentially suppressed, which means that our calculation is consistent with the semi-classical approximation (Fig. 3.7).

Intriguingly, the enhancement of a tunneling rate due to the Bekenstein entropy has been reported in a different problem: it has been proposed [132] that a collapsing shell might tunnel to a fuzzball configurations and the amplitude for the tunneling would be enhanced by the large Bekenstein entropy of the fuzzball states. This is another case in which the large Bekenstein entropy of a final state enhances the quantum tunneling rate.

3.4 Summary

We have presented a counter example against the claim that inflation requires a region which is sufficiently homogeneous beyond the Hubble scale as the initial condition so that the horizon problem cannot be solved in a strict sense. Our model starts with a bubble-like false vacuum region surrounded by thermally nucleated true-vacuum bubbles, whose size is well below the Hubble scale, and the region outside the bubble is taken to be a vacuum. Thus the initial configuration is highly inhomogeneous over the horizon scale. We can, however, realize inflation by virtue of quantum tunneling. It is also interesting to note that the Bekenstein entropy may play an important role in the beginning of inflationary universes since it may be involved in the creation rate of inflationary universes.

Chapter 4

The second law of thermodynamics during inflation

The analogy between a thermodynamical system and an inflationary universe has been pointed out in various contexts [26,32,78,79,133,134]. In the previous section, for example, it was shown that the Bekenstein entropy of inflating space plays an essential role in the quantum tunneling from an inhomogeneous space to an inflationary universe. In this chapter we investigate to what extent inflation is consistent with the thermodynamics or (non-equilibrium) statistical mechanics from the point of view of the second law of thermodynamics.

4.1 GSL and the stochastic inflation

4.1.1 Decrease in the Bekenstein entropy of a cosmological horizon

The second law of thermodynamics states that "*the entropy of an isolated system does not decrease*" and the Universe is an isolated system including all of the entropy in it. The picture of the Universe has been drastically changed and the landscape [135] is one of the most innovative pictures where the spacetime accommodates a great number of universes with the various vacuum energies and our Universe is just one of them. Although our Universe has already experienced inflation, other universes still inflate and some of them may change their vacuum energies by thermally fluctuating on a gently curved effective potential $V(\phi)$ [37, 136] (or by quantum tunneling a potential barrier [90–92]), where ϕ is the inflaton field (Fig. 4.1). Such a thermally fluctuating universe can be described by the stochastic inflation scheme [78, 137] and this universe seemingly violates the GSL [23–25] as is explained below. Let us consider a universe governed by the inflaton field ϕ which stochastically fluctuates on a gently curved region of effective potential in which $|V''| \ll H^2 \equiv (8\pi G/3)V$ is satisfied. Its total entropy, S, is given

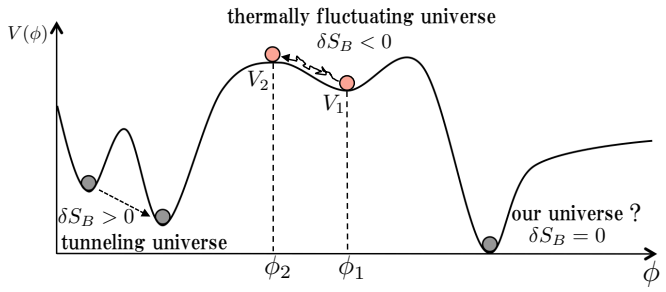

Figure 4.1: The schematic picture of the landscape in which some universes may be thermally excited ($\delta H > 0$) (red), tunnel to a more stable state ($\delta H < 0$) or stay in a lower energy vacuum ($\delta H = 0$) (gray). Our universe might be the latest case.

by the sum of the Bekenstein entropy, $S_{\rm B} \equiv A/4G$, and that of the inflaton field, $S_{\rm M}$, where $A \equiv 4\pi/H^2$ is an area of the cosmological horizon [26]. The former and latter originate from the gravitational and matter sectors of the total system respectively. The entropy production of the inflaton should be zero $\delta S_M = 0$ as long as it evolves in a unitary fashion, which means that the total entropy production δS is equivalent to the difference in the Bekenstein entropy

$$\delta S = \delta S_B = \delta\left(\frac{\pi}{GH^2}\right) = -\frac{2\pi\delta H}{GH^3}. \tag{4.1}$$

According to the stochastic inflation, the universe could be thermally excited from a lower energy density, $V_1 \equiv V(\phi_1) \equiv 3H_1^2/(8\pi G)$, to a higher energy density, $V_2 \equiv V(\phi_2) \equiv 3H_2^2/(8\pi G)$ (Fig. 4.1). In the case of $\delta H \equiv H_2 - H_1 > 0$, using (4.1), it is found that the total entropy production decreases and the decrement can be much larger than the unity. Taking the parameters as, for example, $H_1 \simeq H_2 = 10^{13}$GeV and $\delta H/H_1 = 10^{-3}$, the entropy production is $\delta S \sim -10^9$. This very large decrement of entropy implies the (seeming) violation of the GSL on a universe. Although Davies has proved that in the "classical" level, a cosmological horizon area never decreases ($\delta S_B \geq 0$) if a cosmological fluid is subject to condition $\rho + p \geq 0$ and the scale factor $a(t)$ diverges for $t \to \infty$ [138], we here take into account the stochastic fluctuation of inflaton that is "quantum-mechanically" driven [78, 137]. Then the question is whether there exist inflationary universes in which the GSL is violated by their quantum fluctuations.

4.1.2 Cosmological decoherence

The stochastic inflation scheme starts with splitting the quantum fluctuations into two components, the short-wavelength modes $\phi_>$ (sub-horizon modes) and long-wavelength modes $\phi_<$ (super-horizon modes). The former is regarded as mere white noises interacting with the latter

(see (2.28)). Here the inflaton field ϕ can be described as

$$\phi(x) = \phi_>(x) + \phi_<(x) \tag{4.2}$$

with

$$\phi_>(x) = \int_{k>\Lambda_{\rm cut}} \frac{d^3k}{(2\pi)^3}\phi(\mathbf{k},\eta)e^{i\mathbf{k}\cdot\mathbf{x}}, \tag{4.3}$$

$$\phi_<(x) = \int_{k<\Lambda_{\rm cut}} \frac{d^3k}{(2\pi)^3}\phi(\mathbf{k},\eta)e^{i\mathbf{k}\cdot\mathbf{x}}, \tag{4.4}$$

where Λ is a certain cutoff and η is the conformal time. In the FLRW metric

$$ds^2 = a^2(\eta)\left[-d\eta^2 + d\mathbf{x}^2\right], \tag{4.5}$$

we can set the cutoff $\Lambda_{\rm cut} = \epsilon H a(\eta)$, where $a(\eta)$ is a scale factor and ϵ is a small constant parameter [78]. Coarse-graining the sub-horizon modes which are inaccessible environment interacting with the super-horizon modes leads to the decoherence and entropy production [139–144], $S_M > 0$, which could offset the decrement of the Bekenstein entropy, $S_B + S_M > 0$, as is shown in the latter part of this section.

Let us consider a scalar field (inflaton) ϕ and an external scalar field (environment) φ which interacts with ϕ in a curved spacetime. The action, $S = S_\phi + S_\varphi + S_{\rm int}$, is modeled as [142, 145]

$$\begin{aligned} S_\phi &\equiv \int d^4x\sqrt{-g}\left[-\frac{1}{2}g^{\mu\nu}\partial_\mu\phi\partial_\nu\phi - \frac{1}{2}m^2\phi^2\right], \\ S_\varphi &\equiv \int d^4x\sqrt{-g}\left[-\frac{1}{2}g^{\mu\nu}\partial_\mu\varphi\partial_\nu\varphi - \frac{1}{2}\xi\mathcal{R}\varphi^2\right], \\ S_{\rm int} &\equiv -\lambda\int d^4x\sqrt{-g}\phi\varphi^2, \end{aligned} \tag{4.6}$$

where m is the mass of ϕ, λ is a coupling constant, ξ is the non-minimal coupling constant, and $\mathcal{R}$ is the Ricci scalar. Redefining the fields as $\chi \equiv a\phi$ and $\psi \equiv a\varphi$, S_ϕ, S_φ and $S_{\rm int}$ reduce to

$$\begin{aligned} S_\phi \equiv S_\chi &= \int d^4x\left[-\frac{1}{2}\eta^{\mu\nu}\partial_\mu\chi\partial_\nu\chi - \frac{1}{2}M_\chi^2 a^2\chi^2\right], \\ S_\varphi \equiv S_\psi &= \int d^4x\left[-\frac{1}{2}\eta^{\mu\nu}\partial_\mu\psi\partial_\nu\psi - \frac{1}{2}M_\psi^2 a^2\psi^2\right], \\ S_{\rm int} &= \int d^4x\frac{\lambda}{H\eta}\chi\psi^2, \end{aligned} \tag{4.7}$$

where $M_\chi^2 \equiv m^2 - a''/a^3$ and $M_\psi^2 \equiv \xi\mathcal{R} - a''/a^3$. Here we are interested in the case of de Sitter spacetime, and therefore the mass terms M_χ^2 and M_ψ^2 in (4.7) reduce to $M_\chi^2 = m^2 - 2H^2$ and $M_\psi^2 = (12\xi - 2)H^2$ respectively. We take ψ to be a conformally coupled field by taking $\xi = 1/6$ ($M_\psi = 0$). The conformally coupled field does not feel the cosmic expansion, and therefore the

field ψ is not squeezed while the field χ is getting squeezed after horizon exit. Therefore, we can regard the fields χ and ψ as a super-horizon and sub-horizon modes, respectively. In this sense, this model attempts to model an IR-UV split of a self-interacting single field.

Coarse-graining the environment field ψ, which leads to decoherence, corresponds to taking trace over ψ as

$$\begin{aligned}&\int \mathcal{D}\psi^+\mathcal{D}\psi^-\rho(\chi^+,\chi^-,\psi^+,\psi^-;\eta)\delta(\psi^+-\psi^-)\\&\equiv \rho_R(\chi^+,\chi^-;\eta),\end{aligned} \tag{4.8}$$

where $\rho(\chi^+,\chi^-,\psi^+,\psi^-;\eta)$ is the total density matrix and $\rho_R(\chi^+,\chi^-;\eta)$ is the reduced density matrix. Assuming the weak interaction between ϕ and ψ, the reduced density matrix can be factorized as

$$\rho_R(\chi^+,\chi^-;\eta)=\prod_{\mathbf{k}}\otimes\rho_R(\chi^+_{\mathbf{k}},\chi^-_{\mathbf{k}};\eta)+\mathcal{O}(\lambda^3), \tag{4.9}$$

and in the limit of $|k\eta|\ll 1$, its master equation is given by [142]

$$\begin{aligned}\frac{d}{d\eta}\rho_R(\chi^+_{\mathbf{k}},\chi^-_{\mathbf{k}};\eta)\simeq&-i\mathcal{L}^{(u)}_{\mathbf{k}}[\chi_{\mathbf{k}},\partial_{\chi_{\mathbf{k}}}]\ \rho_R(\chi^+_{\mathbf{k}},\chi^-_{\mathbf{k}};\eta)\\&-\frac{\lambda^2}{8\pi H^2\eta^2}|\chi^+_{\mathbf{k}}-\chi^-_{\mathbf{k}}|^2\rho_R(\chi^+_{\mathbf{k}},\chi^-_{\mathbf{k}};\eta),\end{aligned} \tag{4.10}$$

where $\mathcal{L}^{(u)}_{\mathbf{k}}$ is the unitary time-evolution operator for the field χ. The second term in (4.10) suppresses the non-diagonal terms and leads to decoherence. In the following, we will omit the suffix $\mathbf{k}$. Solving (4.10), one obtains

$$\begin{aligned}\rho_R(\chi^+,\chi^-;\eta)&\simeq\rho_0(\chi^+,\chi^-;\eta)e^{-\frac{D(\eta)}{2}|\chi^+-\chi^-|^2},\\D(\eta)&\equiv-\frac{\lambda^2}{12\pi H^2\eta}.\end{aligned} \tag{4.11}$$

where ρ_0 is the unitary density matrix and the effect of interaction is encoded in the exponential factor in (4.11), which suppresses the non-diagonal components of the reduced density matrix and leads to the decoherence.

4.1.3 Entropy production

For the calculation of an entropy production δS_M, a Wigner function that is a probability distribution function on phase space is useful. The definition of Wigner function is

$$\begin{aligned}w(\chi,\pi_\chi;\eta)\equiv&\frac{1}{\pi^2}\int dx_R dx_I\\&e^{2i\pi_{\chi R}x_R+2i\pi_{\chi I}x_I}\rho(\chi+x/2,\chi-x/2),\end{aligned} \tag{4.12}$$

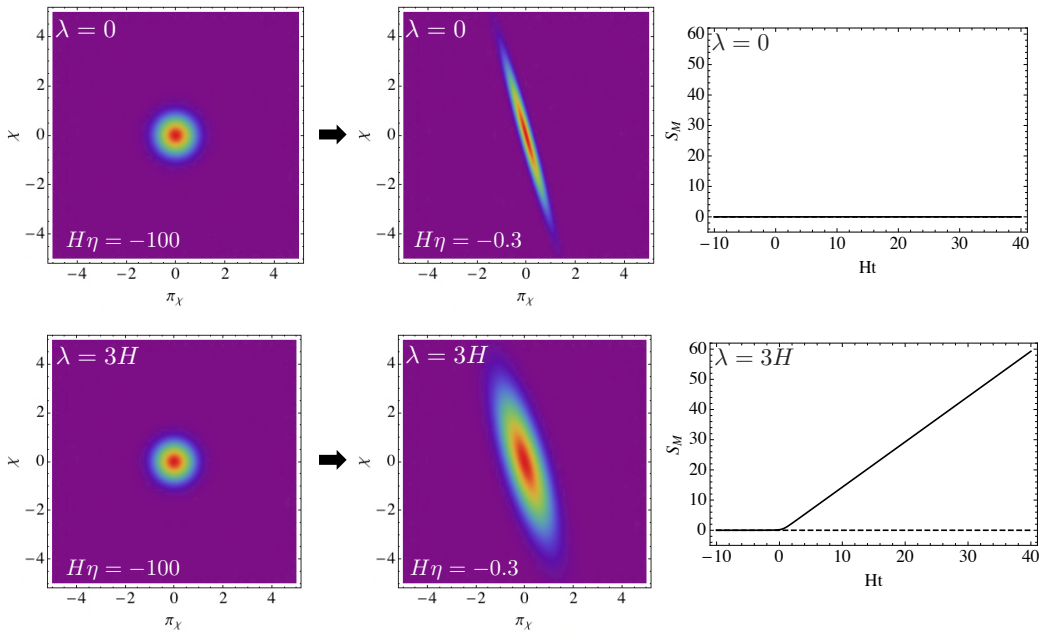

Figure 4.2: Plots of Wigner functions (left and middle) and the time evolutions of entropy (right) with $\lambda = 0$, $m = 0$, $k = H$ (top) and $\lambda = 3H$, $m = 0$, $k = H$ (bottom).

where π_χ is the conjugate momentum of χ and the suffixes R and I indicate a real and imaginary part, respectively. Taking the Bunch-Davies vacuum state, in which the mode function, $f_\chi(k,\eta)$, is given by

$$\begin{aligned} f_\chi(k,\eta) &= e^{-i3\pi/4 + i\nu\pi/2}\frac{\sqrt{-\pi\eta}}{2}H^{(1)}(\nu;-k\eta) \\ \text{with } \nu &\equiv \sqrt{\frac{9}{4}-\frac{m^2}{H^2}}, \end{aligned} \tag{4.13}$$

the unitary density matrix ρ_0 has the form [139, 142]

$$\begin{aligned} \rho_0(\chi^+,\chi^-;\eta) &= \sqrt{\frac{2\Omega_R}{\pi}} \\ &\times \exp\left(-\frac{\Omega_R}{2}(\chi^+-\chi^-)^2 - i\Omega_I(\chi^+-\chi^-)(\chi^++\chi^-) - \frac{\Omega_R}{2}(\chi^++\chi^-)^2\right), \end{aligned} \tag{4.14}$$

where Ω_R and Ω_I are the real and imaginary part of the function $\Omega(k,\eta) \equiv -i\left(f_\chi^{*\prime}/f_\chi^* - aH\right)$. From (4.11), (4.12) and (4.14), the Wigner function for the reduced density matrix ρ_R is obtained as

$$\begin{aligned} w_R(\chi,\pi_\chi;\eta) &= \frac{4}{\pi^2}\frac{\Omega_R}{\Omega_R+D} \\ &\times \exp\left(-2\frac{|\pi_\chi - 2\Omega_I\chi|^2}{\Omega_R+D} - 2\Omega_R|\chi|^2\right). \end{aligned} \tag{4.15}$$

As is shown in Fig. 4.2, one finds that the Wigner distribution is squeezed due to the cosmic expansion. In the case of $\lambda = 0$, the system is obviously in a pure state and the area of Wigner ellipse $A(\eta)$ remains constant, that is, the entropy production is zero $\delta S_M = 0$. On the other hand, when $\lambda > 0$ and $m \ll H$, smearing out the degrees of freedom of the environment ψ may affect the state of ϕ so that its number of states (entropy) monotonically grows. The number of states W is proportional to the area of Wigner ellipse, $A \equiv \pi\alpha\beta$. From (4.15), A is given by [142]

$$A = \frac{\pi}{2}\left(1 + \frac{D}{\Omega_R}\right)^{1/2}. \tag{4.16}$$

Defining $W \equiv (2/\pi)A$ so that the matter entropy is zero when the interaction is turned off ($\lambda = 0$), the entropy is given by

$$S_M \equiv \ln W = \frac{1}{2}\ln\left(1 + \frac{D}{\Omega_R}\right) = \frac{1}{2}\ln\left(1 + \frac{\tilde{\lambda}^2}{12\pi(-H\eta)\omega_R}\right), \tag{4.17}$$

where $\tilde{\lambda} \equiv \lambda/H$ and $\omega_R \equiv \Omega_R/H$. In the limit of $|k\eta| \ll 1$, we found the asymptotic behavior of ω_R as

$$\omega_R \propto (-H\eta)^{-1+2\nu} \text{ for } m < \frac{3}{2}H. \tag{4.18}$$

We now can estimate the entropy production rate due to decoherence, $\dot{S}_M \equiv dS_M/dt$, from (4.17) and (4.18). For the case of $m \ll H$, the entropy production rate $\dot{S}_M$ is

$$\dot{S}_M \simeq \nu H = \frac{3}{2}H + \mathcal{O}(m^2/H^2). \tag{4.19}$$

The previous works [139–141, 143, 144] in which other models are used to estimate the entropy production rate, δS_M, also predict that the rate is of the order of Hubble parameter $\delta\dot{S}_M \sim H$. This implies that the entropy is constantly produced with the cosmological time scale, $t \sim 1/H$, which is caused by the squeezing [139, 143, 144]. Squeezing can equivalently be rephrased as "particle creation" [139] with average particle number $n \sim e^{2r} = e^{(2\nu-1)Ht} \propto \omega_R^{-1}$ [143, 144]. Although the created particles are in a pure state in the case of $\lambda = 0$, once the interaction is turned on ($\lambda > 0$), particle correlation is leaked into the environment degrees of freedom which are inaccessible and the particles apparently lose their correlation, see, e.g., [140]. In this sense, we can say that the endless creation of less correlated thermal particles may constantly produce its entropy with time scale $\sim 1/H$.

4.1.4 GSL on inflationary universes

Now our concern is if the entropy production $\delta S_M \sim H\delta t$ could recover the GSL by offsetting the decrement of Bekenstein entropy $\delta S_B \sim -\delta H/(GH^3)$. In the first place, to observe a thermally

(stochastically) excited universe, the condition

$$\frac{H}{2\pi} \gg \frac{V'(\phi)}{3H^2} \tag{4.20}$$

should be satisfied. This is because, in the stochastic inflation scheme, the coarse-grained field ϕ follows the Langevin equation [78, 137, 146]

$$\frac{d\phi}{dN} = -\frac{V'(\phi)}{3H^2} + \frac{H}{2\pi}\xi(N), \tag{4.21}$$

where $N \equiv Ht$ and $\xi(N)$ is a white noise whose origin is a quantum fluctuation, from which one can read the condition (4.20) for a dominant thermal noise (the second term in (4.21)). Let us consider the situation where the field ϕ goes up a gentle slope of effective potential $V(\phi)$ by a step $\delta\phi \sim H/2\pi$ [136] within the cosmological time scale $\delta t \sim 1/H$. Replacing $V'(\phi)$ by $\delta V/\delta\phi$ and using the Friedmann equation $V = 3H^2/(8\pi G)$, the condition (4.20) reduces to $\delta\phi \gg \delta H/2GH^2$ and we obtain

$$1 \gg \frac{\delta H}{GH^3}. \tag{4.22}$$

Remembering $\delta S_M \sim H\delta t \sim 1$ and $\delta S_B \sim -\frac{\delta H}{GH^3}$ (see (4.1)), the inequality (4.22) reduces to the GSL:

$$\delta S_M + \delta S_B > 0. \tag{4.23}$$

Now we confirm that the decoherence, which is responsible for the entropy production $\dot{S}_M \sim H$, allows de Sitter universes whose vacuum energy densities thermally fluctuate to be excited without the violation of the GSL.

4.1.5 Summary and discussion

In summary, using a system which models an IR-UV split of a self-interacting single field as in Refs. [142,145], we have shown that the entropy production due to the cosmological decoherence, δS_M, could offset the decrease of the Bekenstein entropy, δS_B, during the thermal excitation of universe. This means taking decoherence into account is necessary to satisfy the GSL on thermal universes. The constant entropy production $\dot{S}_M \sim H$ originates from the squeezing due to the cosmic expansion, by which thermal particles are created and lose their quantum correlations (i.e. quantum entanglement) due to decoherence. That is, uncorrelated thermal particles would be produced with the cosmic time scale $\sim 1/H$, which is responsible for the entropy production $\dot{S}_M \sim H$. Moreover, in the context of the warm inflation [147, 148] (see also [149, 150]) in which the thermal equilibrium of external fields is maintained even during inflation, the entropy production may be enhanced compared to that we have calculated. In this sense, we have discussed if the GSL can be satisfied in a conservative setting. Davies has

shown that the GSL is satisfied in the classical level [76, 138]. On the other hand, we here have shown that the GSL is satisfied even in the case where the stochastic fluctuations of inflaton are taken into account. However, we have shown that [34] the cosmological horizon area may instantaneously decrease due to the Hawking-Moss transition [32], that is the quantum jump of a spatially homogeneous vacuum energy, and the GSL is broken. This is discussed in the next section.

4.2 GSL and the Hawking-Moss transition

4.2.1 Interpretation of the decrease in entropy

When the Hawking-Moss bounce was first discovered [32], it was interpreted as describing quantum tunneling from a de Sitter universe as a whole to another de Sitter space with a larger (effective) cosmological constant. Since a transition to a state with larger energy density is counterintuitive, many people perceived it with surprise. Another counterintuitive aspect is that it depends only on the potential energy densities before and after the transition independent of the "distance" in the field space. On the other hand, the time scale of stochastic transition of a de Sitter patch discussed in Section 4.1 depends on the distance.

Since the Hawking-Moss transition is an instantaneous quantum tunneling process from the bottom to the top of the potential, the low entropy production of the cosmological decoherence cannot overwhelm the instantaneous decrement of Bekenstein entropy. Therefore, once taking into account such a quantum process, the GSL is broken. However, it is no surprise that there exists a process in which the GSL is broken since the celebrated Jarzynski equality [151], whose simplified form is

$$\langle e^{\Delta S} \rangle = 1, \tag{4.24}$$

implies that in the context of non-equilibrium statistical mechanics, the second law of thermodynamics is only "statistically" valid at the microscopic level. Here ΔS is the increment of entropy in a certain process and $\langle \cdot \rangle$ denotes an ensemble average over all possible processes. The equality (4.24) means that a small fraction of them must be accompanied by the decrease in entropy. In addition, it is found that the probability for a process of $\Delta S < 0$ is suppressed by $e^{\Delta S}$ in a situation where the fluctuation theorem [152, 153] can be applied. Note, however, that these theorems, the Jarzynski equality and fluctuation theorem, are valid in classical theory, and therefore it is not obvious if such a naive extension of these arguments to the Hawking-Moss instanton is really allowed. Nevertheless, we obtain an interesting result that the transition rate of the Hawking-Moss tunneling is suppressed by the exponent of the decrement of Bekenstein entropy $e^{\delta S_B}$.

4.2.2 Transition rate of the Hawking-Moss tunneling

In the following, we show that the Hawking-Moss transition is exponentially suppressed and its exponent is given only by the decrement of the entropy, as the bulk energy of the scalar field is fully canceled out by the negative gravitational energy due to the Hamiltonian constraint. It is therefore concluded that only the gravitational entropy affects the Hawking-Moss transition, and that it does not break the conservation of energy.

In order to prove the above statement, it is essential to describe the (Euclidean) de Sitter space with a static metric $(\mathcal{M}, g_{\mu\nu})$. Here, we start with a more general Arnowitt-Deser-Misner (ADM) decomposition [154]

$$ds^2 = -N^2 dt^2 + h_{ij}(dx^i + N^i dt)(dx^j + N^j dt) \tag{4.25}$$

where N is the lapse function, N^i is the shift vector, and h_{ij} is the spatial metric. The Latin indices run from 1 to 3. Applying the Wick rotation $t = -i\tilde{t}$ to introduce the Euclidean time $\tilde{t}$, (4.25) reads

$$d\tilde{s}^2 = N^2 d\tilde{t}^2 + h_{ij}(dx^i + \tilde{N}^i d\tilde{t})(dx^j + \tilde{N}^j d\tilde{t}) \tag{4.26}$$

with $\tilde{N}^i \equiv -iN^i$. Here and hereafter we put a tilde on quantities in the Euclidean space which is multiplied by some power of i upon Wick rotation. Correspondence to the unrotated Lorentzian counterpart is also shown below. For example, the extrinsic curvature of the $\tilde{t}$ =const. three-space $\Sigma_{\tilde{t}}$ is expressed as

$$\tilde{K}_{ij} = \frac{1}{2N}\left(\frac{\partial h_{ij}}{\partial \tilde{t}} - D_i \tilde{N}_j - D_j \tilde{N}_i\right) = -iK_{ij}, \tag{4.27}$$

where D_i denotes covariant derivative with respect to h_{ij}.

The Euclidean Einstein action $I_{\rm E}^{(\rm G)}$ is expressed as

$$\begin{aligned} I_{\rm E}^{(\rm G)} &= -\frac{1}{16\pi G}\int_{\mathcal{M}} d^3x d\tilde{t}\sqrt{\tilde{g}}\tilde{R} \\ &= \int d\tilde{t}\left[\int_{\Sigma_{\tilde{t}}} d^3x\left(\tilde{\pi}^{ij}\partial_{\tilde{t}}h_{ij} + N\tilde{\mathcal{H}}^{(\rm G)} - \tilde{N}^i\tilde{\mathcal{H}}_i^{(\rm G)}\right) - \int_{\rm S} d^2x\sqrt{\sigma}\left(\frac{n^i\partial_i N}{8\pi G} - \frac{2}{\sqrt{h}}n_i\tilde{N}_j\tilde{\pi}^{ij}\right)\right]. \end{aligned} \tag{4.28}$$

Here $\tilde{\pi}^{ij}$ is the Euclidean momentum conjugate to h_{ij}, σ_{ij} is an induced metric on the boundary surface S with $\sigma \equiv \det\sigma_{ij}$, and n^i is the unit normal vector on the boundary surface S where we assume $\partial_i\tilde{N}_j$ vanishes. $\tilde{\mathcal{H}}^{(\rm G)}$ and $\tilde{\mathcal{H}}_i^{(\rm G)}$ are the gravitational Hamiltonian and the momentum for the dynamics of the foliation $\Sigma_{\tilde{t}}$. They are given by

$$\begin{aligned} &\tilde{\mathcal{H}}^{(\rm G)} = \frac{\sqrt{h}}{16\pi G}\left(-{}^{(3)}R - \tilde{K}_{ij}\tilde{K}^{ij} + \tilde{K}^2\right), \quad \tilde{\mathcal{H}}_i^{(\rm G)} = -2h_{ij}D_k\tilde{\pi}^{jk}, \\ &\tilde{\pi}^{ij} = \frac{\sqrt{h}}{16\pi G}\left(\tilde{K}^{ij} - h^{ij}\tilde{K}\right) = -i\pi^{ij}, \end{aligned} \tag{4.29}$$

where ${}^{(3)}R$ denotes the three-curvature on the hypersurface $\Sigma_{\tilde{t}}$ and $\tilde{K}$ represents the trace of the extrinsic curvature $h^{ij}\tilde{K}_{ij}$.

The matter Euclidean action, on the other hand, is expressed as

$$\begin{aligned} I_{\rm E}^{(\rm M)} &= \int d^3x d\tilde{t}\sqrt{\tilde{g}}\left[\frac{1}{2}\tilde{g}^{\mu\nu}\partial_\mu\phi\partial_\nu\phi + V(\phi)\right] \\ &= \int d\tilde{t}\int_{\Sigma_{\tilde{t}}} d^3x\left(\tilde{\mathcal{P}}_\phi\partial_{\tilde{t}}\phi + N\tilde{\mathcal{H}}^{(\rm M)} - \tilde{N}^i\tilde{\mathcal{H}}_i^{(\rm M)}\right) \end{aligned} \tag{4.30}$$

where

$$\tilde{\mathcal{P}}_\phi = \sqrt{h}\left[\frac{1}{N}\partial_{\tilde{t}}\phi - \frac{\tilde{N}^i}{N}\partial_i\phi\right] \tag{4.31}$$

is the momentum conjugate to ϕ, and

$$\begin{aligned} \tilde{\mathcal{H}}^{(\rm M)} &= \sqrt{h}\left[-\frac{1}{2}\left(\frac{1}{N}\partial_{\tilde{t}}\phi - \frac{\tilde{N}^i}{N}\partial_i\phi\right)^2 + \frac{1}{2}h^{ij}\partial_i\phi\partial_j\phi + V\right], \\ \tilde{\mathcal{H}}_i^{(\rm M)} &= \sqrt{h}\left[\frac{1}{N}\partial_{\tilde{t}}\phi\partial_i\phi - \frac{\tilde{N}^j}{N}\partial_j\phi\partial_i\phi\right] \end{aligned} \tag{4.32}$$

are the matter part of the Hamiltonian and momentum, respectively.

Classical Euclidean solutions are found by taking variation of the total Euclidean action $I_{\rm E}^{(\rm tot)} = I_{\rm E}^{(\rm G)} + I_{\rm E}^{(\rm M)}$. From variation with respect to N and $\tilde{N}^i$, we find the Hamiltonian and the momentum constraints,

$$\tilde{\mathcal{H}}^{(\rm tot)} \equiv \tilde{\mathcal{H}}^{(\rm G)} + \tilde{\mathcal{H}}^{(\rm M)} = 0, \quad \tilde{\mathcal{H}}_i^{(\rm tot)} \equiv \tilde{\mathcal{H}}_i^{(\rm G)} + \tilde{\mathcal{H}}_i^{(\rm M)} = 0. \tag{4.33}$$

Therefore for a static configuration with $\partial_{\tilde{t}}h_{ij} = 0$ and $\partial_{\tilde{t}}\phi = 0$, the total Euclidean action is simply given by the surface terms as

$$I_{\rm E\ static}^{(\rm tot)} = -\int_{\rm S} d\tilde{t}d^2x\sqrt{\sigma}\left(\frac{n^i\partial_i N}{8\pi G} - \frac{2}{\sqrt{h}}n_i\tilde{N}_j\tilde{\pi}^{ij}\right). \tag{4.34}$$

For the particular case of de Sitter space, the static metric is given by

$$\begin{aligned} d\tilde{s}^2 &= \tilde{g}_{\mu\nu}dx^\mu dx^\nu \\ &= \left(1 - H^2r^2\right)d\tilde{t}^2 + \frac{dr^2}{1 - H^2r^2} + r^2 d\Omega_{\rm II}^2, \end{aligned} \tag{4.35}$$

where H is the Hubble parameter, r denotes radial coordinate and $d\Omega_{\rm II}^2$ is the metric on the unit two sphere. In the following, we impose the periodic boundary condition on the Euclidean time $\tilde{t}$ with a period β.

Introducing a foliation $\Sigma_{\tilde{t}}$ in the spacetime fixed at constant Euclidean time $\tilde{t}$, which takes the value in the range $0 \leq \tilde{t} < \beta$, we can easily decompose the Euclidean de Sitter metric with

$$N = \sqrt{1 - H^2 r^2},\ \tilde{N}^i = 0, \tag{4.36}$$

$$\begin{aligned} h_{\mu\nu} =& g_{\mu\nu} - t_\mu t_\nu \\ =& \mathrm{diag}\left(0, (1 - H^2 r^2)^{-1},\ r^2,\ r^2 \sin^2\theta\right) \end{aligned} \tag{4.37}$$

$$t_\mu \equiv (\sqrt{1 - H^2 r^2}, 0, 0, 0), \tag{4.38}$$

where t_μ is the unit normal vector on the hypersurface $\Sigma_{\tilde{t}}$. This manifold generally has a conical singularity at $r = 1/H$ where $N = 0$. This implies that the curvature is divergent on the de Sitter horizon, although the horizon is not a physical singularity.

As we see below, the conical singularity can be avoided by a specific choice of β, namely the inverse Hawking temperature $\beta_{\mathrm{H}} \equiv 2\pi/H$. It should be noted, however, that the manifold still collapses to a single point on the horizon and, as shown below, this plays an important role in deriving the entropy term from the Euclidean action.

In the following, therefore, we regularize the collapsing part of the manifold by first restricting the integration to the region $\mathcal{M}_\epsilon \equiv \left\{x^\mu : r \leq \frac{1}{H} - \epsilon\right\}$ and then setting the regularization parameter ϵ to zero after the calculation of the Euclidean action (Fig. 4.3).

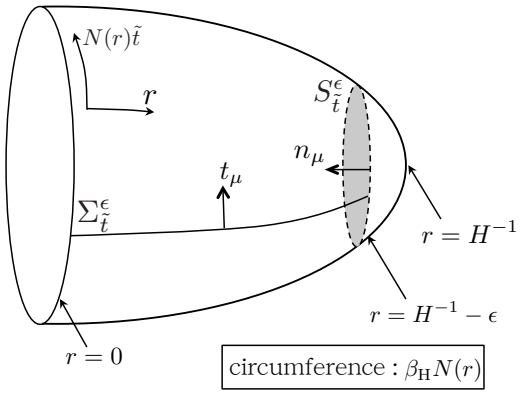

Figure 4.3: The manifold $\mathcal{M}$ including the horizon at $r = 1/H$ where $N = 0$. We can regularize the Euclidean action by introducing a hypothetical boundary at $r = H^{-1} - \epsilon$ denoted by $\mathrm{S} = S^\epsilon_{\tilde{t}}$ with the cut off parameter ϵ set to zero at the end of the calculation.

In this case the action (4.34) has only the first term, where the surface $S^\epsilon_{\tilde{t}}$ is located at $r = 1/H - \epsilon$ with its normal vector n_μ given by

$$n_\mu = (0, -1/\sqrt{1 - H^2 r^2}, 0, 0). \tag{4.39}$$

Note that, since this surface is not a real boundary of the theory, being introduced just for the sake of regularization, one should not apply the Gibbons-Hawking boundary terms [26, 126] here. The length of circumference of the manifold $\mathcal{M}$ is βN and the relation

$$\lim_{\epsilon\to 0} n^i \partial_i \left[\beta N\right] = \beta H = 2\pi \tag{4.40}$$

should be satisfied to ensure the absence of the conical singularity. This is the reason we must identify β with the inverse Hawking temperature β_H.

Hence, the nonvanishing term in (4.34) is calculated as

$$\lim_{\epsilon\to 0}\left[-\beta_H \int_{S^\epsilon_{\tilde{t}}} d^2x\sqrt{\sigma}\frac{n^i\partial_i N}{8\pi G}\right] = -\frac{A}{4G}, \tag{4.41}$$

where A is the area of the horizon given as

$$A \equiv \int_{S^\epsilon_{\tilde{t}}} d^2x\sqrt{\sigma}\bigg|_{\epsilon=0} = \frac{4\pi}{H^2}. \tag{4.42}$$

Thus, for the case $\phi = \phi_{\rm s}$ giving a static de Sitter space with potential energy density $V(\phi_{\rm s})$, the action of the Hawking-Moss instanton

$$I_{\rm E}^{(\rm tot)}(\phi_{\rm s}) = -\frac{A(\phi_{\rm s})}{4G} = \frac{\pi}{GH^2} = \frac{3}{8G^2V(\phi_{\rm s})} \tag{4.43}$$

is entirely given by the contribution of the de Sitter entropy [126]. This is primarily because in the static configuration the bulk term of the action vanishes due to the Hamiltonian constraint.

4.2.3 Discussion

From the above result, one can extend the thermal interpretation of the Hawking-Moss solution more rigorously to argue that $e^{-I_{\rm E}(\phi_s)}$ is indeed proportional to the thermodynamical probability of the state $\phi = \phi_s$, $e^{-F/T}$, where $F = E - TS$ is the free energy. Here, since $E = 0$, $e^{-F/T}$ simply reads $e^S = e^{\ln W(\phi_{\rm s})} = W(\phi_{\rm s})$. In other words, the probability is just proportional to the number of internal states $W(\phi_{\rm s})$ associated with the de Sitter space with the energy density $V(\phi_{\rm s})$. Thus the smallness of the transition rate (2.38) to a state with a higher potential energy density is not due to the largeness of the energy—in fact, the total energy is always zero—, but because of the smallness of the number of microscopic states there.

Again, it should be noted that the Hawking-Moss tunneling violates the GSL, as it is an instantaneous transition to a state with smaller entropy unlike the stochastic transition of de Sitter patch discussed in section 4.1. The difference between them comes from the duration time of transition: the stochastic transition is a mere microscopic process analogous to the Brownian

motion, while the Hawking-Moss transition is an instantaneous quantum tunneling process that is statistically rare. As is discussed in the first part of this section, this work also suggests that a study of the dynamics of a de Sitter universe may give an important perspective on the relation between the quantum field theory in curved spacetime and non-equilibrium statistical mechanics.

Chapter 5

Firewall argument and decoherence

5.1 Introduction — Firewall argument and cosmology

The firewall argument [31] was emerged in 2012 in the context of the black hole information loss paradox. Almheiri, Marolf, Polchinski, and Sully (AMPS) pointed out that the following three postulates cannot be consistent: (postulate 1) Hawking radiation is in a pure state, (postulate 2) the black hole information carried by the Hawking radiation is emitted near the horizon, with low energy effective theory (GR plus quantum field theory), and (postulate 3) the infalling observer experiences nothing special at the horizon due to the equivalence principle of GR. Then the AMPS argues the existence of a firewall at the horizon by which the infalling observer burns up. In other words, they give up the postulate 3, the equivalence principle. AMPS also point out the possibility that firewalls exist even at cosmological horizons, such as those in de Sitter universe. If the firewall argument is correct and the firewall exists even at the cosmological horizon of the Universe, there would be neither the interior regions of black holes and nor exterior of the cosmological horizons and the picture of the multiverse [35,36] and eternal inflation [7,37] would be rejected. In this sense, the firewall argument is really critical even in cosmology.

In this section a reason for rejecting the AMPS firewall concept is presented. We show that an infalling mode inside a black hole C is infinitely squeezed due to the gravitational effect of a black hole, which makes the infalling mode highly sensitive to decoherence*) and leads to the loss of its entanglement with the outgoing mode B (Fig. 5.1). This means that there would be no violation of monogamy of entanglement around a black hole and the black hole complementarity principle can be consistent with the equivalence principle.

The plan of this chapter is as follows. In Sec. 5.2 we introduce a quantum state around a

*) This mechanism is closely related to the quantum-to-classical transition of quantum fluctuations in a de Sitter spacetime that is discussed in Section 4.1.2 and has been well investigated in Refs. [139–141, 155–162].

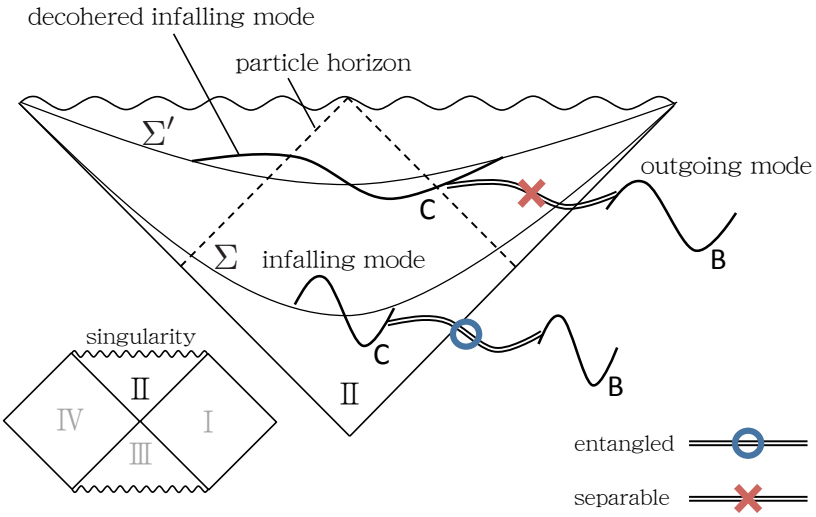

Figure 5.1: The infalling mode near the horizon, C on the hyper surface Σ, can hold coherence, whereas the infalling mode in the vicinity of the singularity, C on the hyper surface Σ', exits the particle horizon (dashed line) and loses causal contact as a whole, which leads to the decoherence of the infalling mode. As a result, the entanglement of the Hawking pairs disappears and its state becomes separable.

black hole formed from gravitational collapse and describe how we calculate time evolution of the quantum state. The resolution to the firewall paradox is described in Sec. 5.3. We show that the quantum state of a Hawking pair, which is initially entangled state, would become a separable state due to environment-induced decoherence (a corresponding mechanism is discussed in Subsection 4.1.2, and for an excellent review of decoherence, see e.g. [162]). In Sec. 5.4 we confirm the consistency between our proposal, explaining how the Hawking pair evolves to a separable state from an initially entangled state, and the previous works that investigated how the purity of the Hawking radiation would be realized. Sec. 5.5 is dedicated to conclusions.

5.2 Formalism

The Unruh vacuum state [163] is the quantum state on an eternal black hole spacetime which models the late time properties of the *in vacuum* of a collapsing star, which is denoted by $|\text{in}\rangle$, that contains no Hawking particle at the past infinity. The Unruh vacuum is associated with the infalling modes and the outgoing modes that have positive frequency with respect to the Killing vector ∂_t and ∂_T respectively, where t is the Schwarzschild time and T is the Kruskal time. Introducing vacuum states $|0\rangle_c$ for the infalling modes and $|0\rangle_b$ for the outgoing modes,

the Unruh vacuum state can be expressed as $|U\rangle = |0\rangle_c |0\rangle_b$, and the relation between the in vacuum state $|\mathrm{in}\rangle$ and the Unruh vacuum state $|U\rangle$ has the form [164]

$$|\mathrm{in}\rangle \propto \frac{1}{\sqrt{Z_\omega}} \left(\sum_{n=0}^{\infty} e^{-\pi\omega n(\omega)/\kappa} (b_\omega^\dagger)^n (c_\omega^\dagger)^n / n! \right) |0\rangle_c |0\rangle_b \,, \tag{5.1}$$

where $b_\omega^\dagger$ and $c_\omega^\dagger$ are creation operators for the state $|0\rangle_b$ and $|0\rangle_c$, respectively, $n(\omega)$ is the number of particles with mode ω, $\kappa \equiv (4GM)^{-1}$ is the surface gravity, and $Z_\omega \equiv (1 - e^{-\pi\omega/\kappa})^{-1}$. In the following, we will use the Unruh vacuum state as a quantum state around a black hole although modeling the quantum state around the collapsing star with the (outgoing) Kruskal mode has not been fully successful and may demand us to take into account the technical issues, e.g., the backscattering effect in the definition of $|0\rangle_c$ and $|0\rangle_b$[†)].

The relation (5.1) implies that the infalling modes are fully entangled with the outgoing modes, which is the problematic entanglement and should be broken for the purity of the Hawking radiation as is pointed out by AMPS [31]. In the following, we will neglect multi-pair creations because the states of n-particles are suppressed by the exponential factor $e^{-\pi\omega n/\kappa}$ and their cumulative contribution to the entanglement entropy (EE) between the infalling and outgoing mode is negligibly small[‡)]. For simplicity and to grasp the essence, we here consider a generically entangled state

$$|\mathrm{in}\rangle \to \sqrt{1-p^2}\, |0\rangle_c |0\rangle_b + p\, |1\rangle_c |1\rangle_b \,, \tag{5.2}$$

$$|1\rangle_c = \int_0^\infty d\omega \varphi_c(\omega)\, |1,\omega\rangle_c \,, \tag{5.3}$$

$$|1\rangle_b = \int_0^\infty d\omega \varphi_b(\omega)\, |1,\omega\rangle_b \,, \tag{5.4}$$

where $|1,\omega\rangle_c \equiv c_\omega^\dagger |0\rangle_c$, $|1,\omega\rangle_b \equiv b_\omega^\dagger |0\rangle_b$, p is a real number satisfying $0 < |p| < 1/\sqrt{2}$, and $\varphi_c(\omega)$ ($\varphi_b(\omega)$) is a function satisfying $\int d\omega |\varphi_c(\omega)|^2 = 1$ ($\int d\omega |\varphi_b(\omega)|^2 = 1$), which ensures that $|1\rangle_c$ ($|1\rangle_b$) is a one-particle state of an infalling (outgoing) localized wave packet[§)]. In the latter part of this chapter, we will show that this entanglement is broken by the existence of the singularity,

[†)] See Ref. [165] for more details. They have discussed the definition of the standard quantum states around a black hole, including the Unruh vacuum state, focussing on the differences between fermionic and bosonic quantum field.

[‡)] The EE is given by $-\sum_{n=0}^{\infty} p_n \ln p_n$, where p_n is the probability for n-pair creation. Using Eq. (5.1) with the typical energy of a Hawking particle $\omega = \kappa$, we can find that the cumulative contribution of the multi-pair creations to the EE is less than 0.1%.

[§)] For example, taking the functions $\varphi_c(\omega)$ and $\varphi_b(\omega)$ to be $(\Delta E)^{-1/2}$ for $\omega_0 < \omega < \omega_0 + \Delta E$ and zero elsewhere, we can reproduce the wave packet introduced in Refs. [28,166], where ω_0 is the typical energy of a Hawking particle and ΔE gives the dispersion scale of the wave packet with $\sim 1/\Delta E$.

which is caused by the decoherence of an infalling mode. An infalling mode inside a black hole is redshifted as $\lambda = \lambda_0\sqrt{2GM/r-1}$, where λ_0 is the initial wavelength, and it diverges in the limit of $r \to 0$. Therefore, the infalling mode exits the particle horizon near the singularity and loses causal contact as a whole (Fig. 5.1), which is responsible for the squeezing (EPR-like correlation) of the infalling mode, that has the role to retain its coherent structure [156], and decoherence as is discussed in Section 5.3.

We consider a massless scalar field ϕ on the Schwarzschild spacetime with a mass M whose metric is given as $ds^2 = -f(r)dt^2 + f^{-1}(r)dr^2 + r^2 d\Omega_2^2$ with $f(r) \equiv 1 - 2GM/r$, where $d\Omega_2^2$ denotes the line element of a two-sphere $d\Omega_2^2 \equiv d\theta^2 + \sin^2\theta d\varphi^2$. Using the tortoise coordinate $r^* = r + 2GM\ln|1 - r/(2GM)|$, we can rewrite it as $ds^2 = g_{\mu\nu}dx^\mu dx^\nu \equiv f(r)\left[-dt^2 + dr^{*2}\right] + r^2 d\Omega_2^2$. In order to describe the infinite squeezing of an infalling mode, let us investigate the dynamics of the vacuum $|0\rangle_c$ inside the black hole $r < 2GM$. The action S is given as

$$\begin{aligned} S &= \int d^4x\mathcal{L} = -\frac{1}{2}\int d^4x\sqrt{-g}g^{\mu\nu}\partial_\mu\phi\partial_\nu\phi \\ &= \frac{1}{2}\int d^2x \sum_{l,m}\left[\chi'^2_{lm} - 2\chi_{lm}\chi'_{lm}\mathcal{G} + \mathcal{G}^2\chi^2_{lm} - \dot{\chi}^2_{lm} + f(r)\frac{l(l+1)}{r^2}\chi^2_{lm}\right], \end{aligned} \tag{5.5}$$

where we decompose the field ϕ into partial waves with an angular momentum l as $\phi \equiv \sum_{l,m}\chi_{lm}Y_{lm}/r$, a prime and a dot denote differentiation with respect to r^* and t respectively, and $\mathcal{G} \equiv r'/r$. From the action (5.5), the Euler-Lagrange equation can be derived as

$$\left[\frac{\partial^2}{\partial r^{*2}} - \frac{\partial^2}{\partial t^2} - f(r)\left(\frac{2GM}{r^3} + \frac{l(l+1)}{r^2}\right)\right]\chi_{lm} = 0. \tag{5.6}$$

We find that the mode functions satisfying (5.6) are almost independent of the angular momentum l in the vicinity of the singularity because $l(l+1)/r^2$ in (5.6) can be ignored for $r \ll 2GM$. We are interested in the behavior of an infalling mode near the singularity, and therefore, we set $l = 0$ and omit the suffixes (l, m) in the following. The time-like coordinate inside the black hole is r^*, therefore, the conjugate momentum π of the field χ is given as [167]

$$\pi \equiv \partial\mathcal{L}/\partial\chi' = \chi' - \mathcal{G}\chi \tag{5.7}$$

and then the Hamiltonian is

$$H = \int dt\frac{1}{2}\left[\pi^2 + \dot{\chi}^2 + 2\mathcal{G}\chi\pi\right]. \tag{5.8}$$

We can decompose the field χ and its conjugate momentum π as

$$\begin{aligned} \chi &\equiv \int_{-\infty}^{+\infty}\frac{d\omega}{\sqrt{2\pi}}\bar{\chi}_\omega(r^*)e^{-i\omega t} + (\text{O.M.}) \\ &\equiv \int_{-\infty}^{+\infty}\frac{d\omega}{\sqrt{2\pi}}\left[c_\omega\tilde{\chi}_\omega(r^*)e^{-i\omega t} + c^\dagger_\omega\tilde{\chi}^*_\omega(r^*)e^{+i\omega t}\right]\theta(\omega) + (\text{O.M.}), \end{aligned} \tag{5.9}$$

$$\begin{aligned}\pi &\equiv \int_{-\infty}^{+\infty} \frac{d\omega}{\sqrt{2\pi}} \bar{\pi}_\omega(r^*) e^{-i\omega t} + (\text{O.M.}) \\ &\equiv -i \int_{-\infty}^{+\infty} \frac{d\omega}{\sqrt{2\pi}} \left[c_\omega \tilde{\pi}_\omega(r^*) e^{-i\omega t} - c_\omega^\dagger \tilde{\pi}_\omega^*(r^*) e^{+i\omega t} \right] \theta(\omega) + (\text{O.M.}),\end{aligned} \tag{5.10}$$

where (O.M.) denotes the outgoing modes and $\theta(\omega)$ is a step function: $\theta(\omega) = 1$ for $\omega > 0$ and $\theta(\omega) = 0$ for $\omega < 0$. The canonical commutation relation is $[\bar{\chi}_\omega, \bar{\pi}^\dagger_{\omega'}] = i\delta(\omega - \omega')$. In the following, we will omit the suffix ω for simplicity. From (5.7) and the canonical commutation relation, we obtain the Wronskian condition as $(\tilde{\chi}'^* \tilde{\chi} - \tilde{\chi}' \tilde{\chi}^*) = i$.

The third term in (5.8) is responsible for the squeezing of infalling modes [141,155–158], which becomes stronger as $r^* \to 0$ as is shown later. To investigate the dynamics of the states $|0\rangle_c$ and $|1,\omega\rangle_c$, we first derive the wave functions for them, $\Psi_0[\bar{\chi}]$ and $\Psi_1[\bar{\chi}]$, that satisfy $c\,|0\rangle_c = 0$ and $|1,\omega\rangle_c = c^\dagger\,|0\rangle_c$ respectively. From (5.9) and (5.10), we can rewrite the former in the Schrödinger representation as $\left[\bar{\chi} + i\gamma^{-1}(r^*,\omega)\bar{\pi}\right]|0\rangle_c = 0$, where $\gamma(r^*,\omega) \equiv \tilde{\pi}^*/\tilde{\chi}^*$. Replacing the conjugate momentum $\bar{\pi}$ by $-i\partial/\partial\bar{\chi}^\dagger$, we obtain the wave function $\Psi_0[\bar{\chi}]$ of the state $|0\rangle_c$ as

$$\Psi_0[\bar{\chi}] = \sqrt{\frac{2\gamma_R}{\pi}} \exp\left[-\gamma(r^*,\omega)\bar{\chi}\bar{\chi}^\dagger\right], \tag{5.11}$$

where $\gamma_R \equiv \mathrm{Re}[\gamma(r^*,\omega)]$. On the other hand, $|1,\omega\rangle_c$ satisfies $|1,\omega\rangle_c = c^\dagger\,|0\rangle_c$, and hence we obtain $\Psi_1[\bar{\chi}] \propto \left(\bar{\chi} - \gamma^{*-1}(r^*)\partial/\partial\bar{\chi}^\dagger\right)\Psi_0[\bar{\chi}]$, which leads to

$$\Psi_1[\bar{\chi}] = \frac{2\gamma_R}{\sqrt{\pi}} \bar{\chi} \exp\left[-\gamma(r^*,\omega)\bar{\chi}\bar{\chi}^\dagger\right]. \tag{5.12}$$

The function γ can be calculated numerically from (5.6).

5.3 decoherence inside a black hole

In the following we show that the density matrix ρ_{co} of the quantum state (5.2) is reduced to a separable[¶)] density matrix ρ_{de} due to the decoherence once the infalling mode reaches the vicinity of the singularity, namely, $\rho_{co} \to \rho_{de}$ for $r^* \to 0$. To this end, we first show that the infalling mode becomes highly squeezed as the mode approaches the singularity, and secondly, that the squeezed state is highly sensitive to decoherence. The density matrix ρ_{co} can be written as

$$\begin{aligned}\rho_{co} \equiv{}& (1-p^2)\,|0\rangle_c\langle 0|_c \otimes |0\rangle_b\langle 0|_b + p^2\,|1\rangle_c\langle 1|_c \otimes |1\rangle_b\langle 1|_b \\ &+ p\sqrt{1-p^2}\left(|1\rangle_c\langle 0|_c \otimes |1\rangle_b\langle 0|_b + |0\rangle_c\langle 1|_c \otimes |0\rangle_b\langle 1|_b\right),\end{aligned} \tag{5.13}$$

[¶)] When a density matrix ρ can be rewritten as $\rho = \sum_k p_k \rho_k^{(c)} \otimes \rho_k^{(b)}$ with $\sum_k p_k = 1$, the density matrix ρ is said to be "separable", and this means that there is no entanglement.

and as is shown later, the separable density matrix ρ_{de} is

$$\rho_{de} = (1-p^2)\,|0\rangle_c\langle 0|_c \otimes |0\rangle_b\langle 0|_b + p^2\,|1\rangle_c\langle 1|_c \otimes |1\rangle_b\langle 1|_b\,. \tag{5.14}$$

Hence, we will show that the third and fourth terms in (5.13) disappear, that is, $\rho_{co} \to \rho_{de}$, as the infalling mode approaches the vicinity of the singularity.

Let us consider the time evolution of the off-diagonal terms of ρ_{co}. Using (5.3), $|0\rangle_c\langle 1|_c$ and $|1\rangle_c\langle 0|_c$ in the off-diagonal terms can be decomposed as

$$\begin{aligned} |0\rangle_c\langle 1|_c &= \int d\omega \varphi_c^*(\omega)\,|0\rangle_c\langle 1,\omega|_c\,, \\ |1\rangle_c\langle 0|_c &= \int d\omega \varphi_c(\omega)\,|1,\omega\rangle_c\langle 0|_c \end{aligned} \tag{5.15}$$

respectively, and we will show the decay of $|0\rangle_c\langle 1|_c$ and $|1\rangle_c\langle 0|_c$ by calculating the time evolution of $|0\rangle_c\langle 1,\omega|_c$ and $|1,\omega\rangle_c\langle 0|_c$. $|0\rangle_c\langle 1,\omega|_c$ and $|1,\omega\rangle_c\langle 0|_c$ component of the Wigner function of ρ_{co}, $W_{01}^{(c)}$ and $W_{10}^{(c)}$, are given as

$$\begin{aligned} W_{01}^{(c)} = W_{10}^{(c)*} &= \int\int \frac{dx_R dx_I}{(2\pi)^2} e^{-i(\bar{\pi}_R x_R + \bar{\pi}_I x_I)}\,\langle \bar{\chi} - \frac{x}{2}|\,|0\rangle_c\langle 1,\omega|_c\,|\bar{\chi}+\frac{x}{2}\rangle \\ &= \frac{1}{\pi^2}\left(\sqrt{2\gamma_R}\bar{\chi} - i\sqrt{\frac{2\gamma_I^2}{\gamma_R}}(\bar{\chi}+\frac{\bar{\pi}}{2\gamma_I})\right)\exp\left[-2\gamma_R|\bar{\chi}|^2\right]\exp\left[-\frac{2\gamma_I^2}{\gamma_R}\left|\bar{\chi}+\frac{\bar{\pi}}{2\gamma_I}\right|^2\right], \end{aligned} \tag{5.16}$$

where we used (5.11) and (5.12) and the suffixes R and I represent the real and imaginary part respectively. We numerically confirmed that they are infinitely squeezed in the limit of $r^* \to 0$ with $2GM\omega = 0.5$ (Fig.5.2 (a), (b), and (c)) and the ratio $\gamma_I/\gamma_R \propto \sinh 2s$ diverges in the vicinity of the singularity, $\gamma_I/\gamma_R \to -\infty$, where s is the squeezing parameter. This means that s also diverges, $|s| \to \infty$, as $r^* \to 0$ (see e.g., [155]).

Secondly, we will show that an infinitely squeezed state with an environment is highly fragile against decoherence, in which the environment plays an important role. For instance, let us consider a double-slit experiment with electrons in which they create an interference pattern (non-diagonal density matrix). If they are exposed to thermal noise (environment), the pattern will be coarse-grained and will disappear (decoherence). This is the intuitive interpretation for the role of environment in decoherence. We here take into account the environment as follows. The field χ can be separated into two parts, the long-wavelength part as the system (an infalling Hawking particle) and the short-wavelength part as the environment (vacuum fluctuations). We here regard only the modes with wavelengths much shorter than the gravitational curvature radius of black hole as the short-wavelength part, as in the stochastic inflation scheme [78, 160, 168]. Therefore, the environment can be regarded as a coherent state with a good approximation

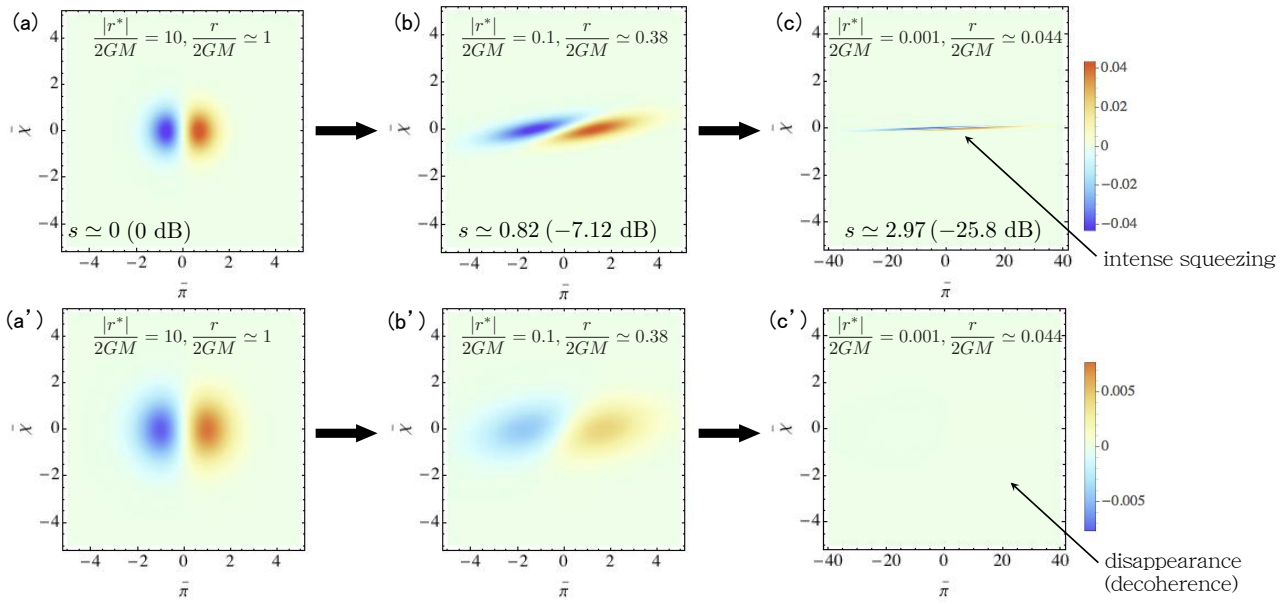

Figure 5.2: (a), (b), and (c) are the imaginary parts of the non-diagonal components $W_{01}^{(c)}$, and (a'), (b'), and (c') are the imaginary parts of the coarse-grained non-diagonal components $\mathcal{W}_{01}^{(c)}$, where we set $|r^*|/2GM = 10$ (for (a), (a')), $|r^*|/2GM = 0.1$ (for (b), (b')), $|r^*|/2GM = 0.001$ (for (c), (c')), and $2GM\omega = 0.5$. The non-diagonal term $W_{01}^{(c)} = W_{10}^{(c)*}$ has the form of $X\delta(X)$ in the limit of $r^* \to 0$, and therefore the coarse-grained distribution $\mathcal{W}_{01}^{(c)} = \mathcal{W}_{10}^{(c)*}$ disappears. This leads to the transition from the entangled Hawking pair to the separable Hawking pair in the vicinity of the singularity.

and we can consider the decoherence by tracing out the coherent environment. It is shown that the tracing out the coherent environment is corresponding to convolving (coarse-graining) the system's Wigner function (5.16) with that of a coherent state $W_{\rm E}$ [169],

$$W_{\rm E} \equiv \pi^{-2} \exp\left(-|\bar{\chi}|^2 - |\bar{\pi}|^2\right). \tag{5.17}$$

Taking the convolution of (5.16) and (5.17), the non-diagonal term of the coarse-grained Wigner function $\mathcal{W}_{01}^{(c)} = \mathcal{W}_{10}^{(c)*}$ is obtained as

$$\begin{aligned} &\mathcal{W}_{01}^{(c)} \equiv (W_{01}^{(c)} * W_E) \\ &= \frac{Q|Q|^2}{\pi^2}(\bar{\chi} - i\bar{\pi}) \exp\left[-|Q|^2\left\{(|\bar{\chi}|^2 + |\bar{\pi}|^2) + 2\gamma_R(|\bar{\chi}|^2 + |\bar{\pi}/(2\gamma_R) + (\gamma_I/\gamma_R)\bar{\chi}|^2)\right\}\right], \end{aligned} \tag{5.18}$$

where $Q \equiv \sqrt{2\gamma_R}/(1+2\gamma)$. In the limit of $r^* \to 0$, the real and imaginary parts of the function $\gamma(r^*, \omega)$ diverge and hence Q asymptotically approaches zero. Therefore, the non-diagonal term

$\mathcal{W}_{01}^{(c)}$ is decaying as approaching the singularity (Fig.5.2 (a'), (b'), and (c')), which means that the Hawking pair will experience decoherence as the infalling mode approaches the singularity since the effect of decoherence on a density matrix is essentially the decay of its off-diagonal terms, see e.g., [162]. Although GR and quantum field theory are, of course, no longer valid near the singularity at $r \lesssim r_{\rm Pl} = 2GM(M_{\rm Pl}/M)^{2/3}$[‖)], the decoherence is almost completed at $r \gg r_{\rm Pl}$ in the case of interest, namely a massive black hole $M \gg M_{\rm Pl}$ (remember postulate 2). That is, the above estimates suggest that the squeezing becomes so strong that the decoherence can take place well before the modes reach $r \sim r_{\rm Pl}$, and therefore using a (semi)classical spacetime picture of the mode evolution should still be reliable.

As is shown above, the intense squeezing leads to the decay of the off-diagonal terms. Therefore, the third and fourth terms in (5.13), containing the off-diagonal components $|1,\omega\rangle_c \langle 0|_c$ and $|0\rangle_c \langle 1,\omega|_c$ (see (5.15)), decay due to the decoherence and this leads to the transition of the state $\rho_{co} \to \rho_{de} = (1-p^2)\,|0\rangle_c \langle 0|_c \otimes |0\rangle_b \langle 0|_b + p^2\,|1\rangle_c \langle 1|_c \otimes |1\rangle_b \langle 1|_b$. This implies that the entanglement of Hawking pairs decays as the infalling mode approaches the singularity.

5.4 Microscopic picture of information recovery

We can apply the loss of the entanglement between a Hawking pair to the black hole information paradox. According to our proposal, the entanglement between B and C is broken when C approaches the singularity. Therefore, the time scale on which the entanglement is broken is of the order of the free fall time scale, $t_F \sim 2GM$, measured by a freely falling observer. In other words, we cannot avoid the entanglement between B and C only during the moment of the free fall $\sim t_F$. Therefore, we have to discuss how the scenario proposed here is consistent with the monogamy of entanglement and the previous works [170, 171], in which the time scale of information recovery is carefully discussed in the microscopic level.

In Ref. [170], the radiation around a gravitationally collapsing shell was analytically investigated and it was shown that the correlations between the Hawking particles (between A and B) are initially zero but grow on the time scale of t_F for an observer far from the black hole. Reference [171] also pointed out that the microscopic time scale of information recovery may be of the order of t_F by considering the interaction between a collapsing shell and the Hawking radiation. For these reasons, we can conclude that the entanglement between A and B would be initially zero and gradually appears on the time scale of t_F, and B can be allowed to be entangled with C only for the short time $\sim t_F$, which is quite consistent with our scenario. This implies that B would not be fully entangled with A and C simultaneously (Fig. 5.3), and therefore there

[‖)] The gravitational curvature is of the order of $M_{\rm Pl}^2$ at $r \sim r_{\rm Pl}$.

is no any violation of the monogamy of entanglement.

5.5 Summary

We have shown that a Hawking pair becomes a separable state from an entangled state by pointing out that the high squeezing and decoherence occur inside a black hole. The analysis was done with a simplified state (5.2) and the environment interacting with the infalling Hawking modes whose Wigner function is given by (5.17). The interaction with the environment can be effectively taken into account by smearing out the Wigner function of the infalling mode with that of the environment (5.18). As a result, we showed that the off-diagonal terms of the density matrix for the Hawking pair would decay quickly compared to the black hole evaporation time scale, which implies that the decoherence would be caused by the interior gravitational effect and that the entanglement between Hawking pairs will be broken. It should be emphasized that although GR and quantum field theory would break down near the singularity, our proposal is valid as long as the mass of black hole is much larger than the Planck mass, $M \gg M_{\rm Pl}$ [30, 31]. According to our proposal, we would no longer need firewalls. Therefore, cosmological horizons would be free from the firewall argument and the picture of the multiverse [35, 36] or eternal inflation [7, 37] do not suffer from it. We believe that our work can be important for the understanding of how the states of Hawking pairs of particles become separable, and how the black hole information paradox can be solved.

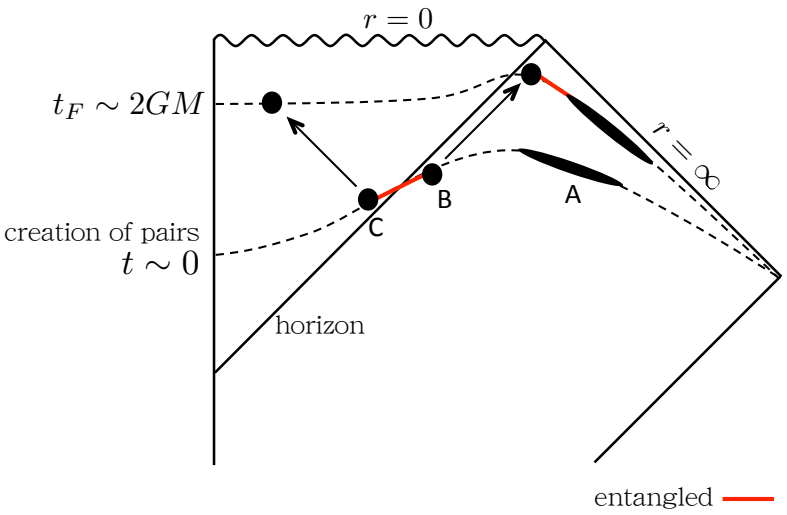

Figure 5.3: The schematic picture showing how the microscopic picture of information recovery [170, 171] is consistent with our proposal. B is initially entangled with C and its entanglement will decay on the time scale of t_F. On the other hand, the entanglement between A and B is initially zero and may grow on the time scale of t_F.

Chapter 6

Catalyzing effect for the Higgs metastability

6.1 Introduction

Compact objects are ubiquitous in high-energy physics as well as astrophysics and play significant roles in cosmological history of the Universe. To name a few, monopoles [39], Q-balls [40–49], oscillons [172–182], boson stars (including axion stars) [50–64], gravastars [183, 184], neutron stars, black hole remnants [82–85], and (primordial) black holes [185–195] are examples that have been studied extensively in the literature for several decades. Pursuing consistency of these objects in cosmology and astrophysics is important to construct a realistic particle physics model and is complementary to high-energy colliders to find a new physics beyond the SM.

It has been proposed that black holes may be objects catalyzing vacuum decays around them [118–120, 122, 123, 131, 196–200], which was pioneered by Hiscock [124]. The abundance of the catalyzing objects should be small enough to avoid the nucleation of AdS vacuum bubble within our observable Universe until present. Actually, this is particularly important in the standard model of particle physics [119,121,201], where the Higgs potential could develop an AdS vacuum at a high energy scale because of the running of quartic coupling [93–116]. According to their result, even a single black hole within our observable Universe leads to the bubble nucleation if its mass is small enough.

One may wonder what property of black holes contributes to the promotion of a vacuum decay around it. Gregory, Moss, and Withers found [118, 120] that the exponential factor of a vacuum decay rate around a black hole is determined by two factors, $\Gamma \propto e^{-B+\Delta S}$, where Γ is the vacuum decay rate, ΔS is the change of Bekenstein entropy of the black hole, and B is an on-shell Euclidean action depending on the Euclidean dynamics of a bubble wall. Then they

found that the decrement of B due to gravity of a black hole overwhelms the entropy decrement. Although they found an extremely large enhancement of bubble nucleation rate around a black hole, it has been discussed that the main effect comes from the thermal fluctuation due to the Hawking radiation [122]. This implies that the nucleation rate is overestimated because the same effect generates a thermal potential that tends to stabilize the Higgs at the symmetric phase [122, 123, 202] or because the thermal effect of Hawking radiation should be small for a large bubble. Thus, though the bubble nucleation rate is still enhanced around a Black hole because of the effect of gravity, it might not be so large as expected before. If gravity of a black hole mainly contributes to the promotion of a vacuum decay, it is meaningful to consider the catalyzing effect even around horizonless objects. The absence of horizons is equivalent to the absence of the suppression factor due to the change of Bekenstein entropy $e^{\Delta S}$, and therefore, horizonless compact objects may be more important candidates of catalyzing objects for vacuum decays. In this chapter, we discuss such a vacuum decay around a spherical horizonless object as a catalyzing one.

This Chapter is organized as follows. In Section 6.2.1, we explain the formalism to calculate the bubble nucleation rate around a generic compact object. We use a Gaussian density function for the object as an example to calculate the nucleation rate in Sec. 6.2.2. We will see that the efficient enhancement occurs if the radius of the compact object, its Schwarzschild radius, and the radius of the nucleated bubble are of the same order with each other. We then discuss a parameter region for a 't Hooft-Polyakov monopole that is excluded because of the nucleation of AdS vacuum in Sec. 6.2.3. In Section 6.3, we discuss differences from the bubble nucleation around a black hole. We will see that the nucleation rate is more enhanced around a horizonless compact object than around a black hole with the same total mass. The result is summarized in Section 6.4.

6.2 Bubble nucleation around a compact object

6.2.1 Formalism

We consider a nucleation of a thin wall vacuum bubble around a spherical object. If we assume that the system is static, the metric inside and outside of the bubble can be written as

$$ds^2 = -A_\pm(r_\pm)dt_\pm^2 + B_\pm(r_\pm)dr_\pm^2 + r_\pm^2 d\Omega_2^2, \tag{6.1}$$

where $A_\pm$ and $B_\pm$ are determined by the Einstein equation and will be specified later. The quantities associated with the outer and inner region are labeled by the suffix "+" and by "−", respectively.

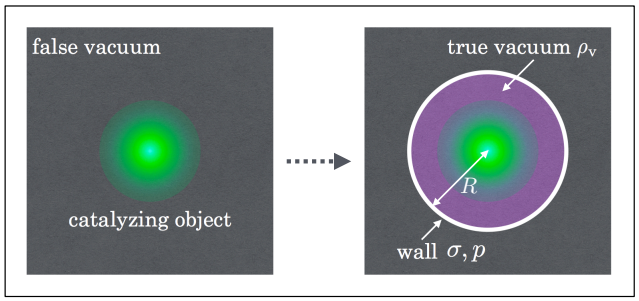

Figure 6.1: A schematic picture showing a vacuum decay catalyzed by a static and spherical object.

The thin wall vacuum bubble can be characterized by its energy density, σ, and pressure, p. The ratio of p to σ, $w \equiv p/\sigma$ (equation-of-state parameter), is assumed to be a constant. We here choose the scale of radial coordinates $r_\pm$ so that $r_+ = r_- \equiv R$ on the wall. A schematic picture showing the vacuum decay process we assume here is depicted in Fig. 6.1.

Introducing the extrinsic curvature on the outer (inner) surface of the wall, $K^{(+)}_{AB}$ ($K^{(-)}_{AB}$), the EMT of wall, S_{AB}, and the induced metric on the wall, h_{AB}, the dynamics of the thin wall with $\xi^A = (\tau, \theta, \phi)$ is described by the Israel junction conditions as

$$K^{(+)}_{AB} - K^{(-)}_{AB} = -8\pi G \left(S_{AB} - \frac{1}{2} h_{AB} S \right), \tag{6.2}$$

$$\sqrt{A_\pm B_\pm} K^{(\pm)}_{AB} = \mathrm{diag}\left(-\frac{d\beta_\pm}{dR}, \beta_\pm R, \beta_\pm R \sin^2\theta \right), \tag{6.3}$$

$$S^A{}_B \equiv \mathrm{diag}\left(-\sigma, p, p\right), h_{AB} \equiv \mathrm{diag}\left(-1, R^2, R^2 \sin^2\theta\right), \tag{6.4}$$

where

$$\beta_\pm \equiv \epsilon_\pm \sqrt{A_\pm + A_\pm B_\pm (dR/d\tau)^2}, \tag{6.5}$$

and τ is the proper time of the wall and $\epsilon_\pm$ is the sign of spatial components of extrinsic curvature. We here simply neglect the interaction between the horizonless object and the bubble except for their gravitational interaction. The case with such an interaction being taken into account will be discussed elsewhere (see also Refs. [203–205] in the context of Q-ball in supersymmetric models without taking gravity effects into account).

We are interested in the decay of Higgs vacuum, where the metastable vacuum has a negligibly small vacuum energy and the true vacuum has a negative vacuum energy $\rho_v < 0$. We also introduce a compact object at the origin of the spatial coordinate, which modifies the metric because of the nonzero mass density $\rho_c(r)$. For simplicity, we here assume the EMT of the object

which gives the following static solutions of the Einstein equation:

$$A_\pm = B_\pm^{-1} = f_\pm(r_\pm) \equiv 1 - 2GM(r_\pm)/r_\pm + H_\pm^2 r_\pm^2, \tag{6.6}$$

with

$$H_+ = 0,\ H_-^2 \equiv -\frac{8\pi G}{3}\rho_{\rm v}, \tag{6.7}$$

$$M(r_\pm) \equiv \int_0^{r_\pm} d\bar{r}_\pm 4\pi \bar{r}_\pm^2 \rho_{\rm c}(\bar{r}_\pm). \tag{6.8}$$

If we use an arbitrary mass density, $\rho_{\rm c}(r)$, the compact object does not satisfy the static Einstein equation unless an appropriate EMT for the chosen $\rho_{\rm c}(r)$ exists. Although in this case the metric (6.1) cannot be used, we expect that we can use it to capture a qualitative result. To be more rigorous, in the Appendix D, we calculate the vacuum decay rate around a gravastar-like object, which is constructed to be (approximately) static. We specify its interior EMT and use the metrics consistent with the specified EMT. Then one could find that the aforementioned assumption for the metrics, (6.1), does not qualitatively change our results and main conclusions.

Equation (6.2) now reduces to the following equations

$$\frac{d}{dR}\left(\beta_- - \beta_+\right) = -8\pi G\left(\sigma/2 + p\right), \tag{6.9}$$

$$\left(\beta_- - \beta_+\right) = 4\pi G\sigma(R)R. \tag{6.10}$$

One obtains $\sigma = m^{1-2w}R^{-2(1+w)}$ by solving (6.9), where m is the typical energy scale of the wall, and we can rewrite (6.10) as

$$\left(\frac{dz}{d\tau'}\right)^2 + V(z) = -1, \tag{6.11}$$

$$V(z) \equiv -\frac{a}{z} - \frac{z^2}{4}\left[\frac{z^{2(1+w)}\bar{m}^{2w-1}}{4\pi\bar{H}^{2w+1}} - \frac{4\pi\bar{H}^{2w+1}}{z^{2(1+w)}\bar{m}^{2w-1}}\right]^2 \leq 0, \tag{6.12}$$

where we re-defined the following non-dimensional variables and parameters:

$$\begin{aligned} &z \equiv H_- R,\ \tau' \equiv H_-\tau,\ a \equiv 2GMH_-, \\ &\bar{m} \equiv m/M_{\rm Pl},\ \bar{H} \equiv H_-/M_{\rm Pl}. \end{aligned} \tag{6.13}$$

The parameters $\bar{m}$ and $\bar{H}$ are the ones in the Planck units. The solution to Eq. (6.11) is the bounce solution that describes the bubble nucleation process.

The Euclidean action, $B_{\rm co}$, can be calculated from the bounce solution with the following integration [118]:

$$B_{\rm co} = \frac{1}{4G}\oint d\tau_{\rm E}(2R - 6GM + 2GM'R)\left(\frac{\beta_+}{f_+} - \frac{\beta_-}{f_-}\right), \tag{6.14}$$

where $\tau_{\rm E}$ is the Euclidean proper time of the wall. The transition rate, $\Gamma_{\rm D}$, can be estimated as

$$\Gamma_{\rm D} \sim R_{\rm CDL}^{-1} \sqrt{\frac{B_{\rm co}}{2\pi}} \exp(-B_{\rm co}), \tag{6.15}$$

where we estimate the prefactor by taking a factor of $\sqrt{B_{\rm co}/2\pi}$ for the zero mode associated with the time-translation of the instanton and we use the light crossing time of the bubble, $R_{\rm CDL}$, as a rough estimate of the determinant of fluctuations, which will be defined more precisely below.

6.2.2 Results for Gaussian mass distribution

As an example, we consider the case where the density distribution of the horizonless object is given by the Gaussian form:

$$\rho_{\rm c}(r) = \rho_0 e^{-r^2/\xi^2}, \tag{6.16}$$

where ρ_0 and ξ represent the typical mass density and the size of the compact object, respectively. Motivated by the Higgs vacuum decay, we take $\bar{H} = 10^{-6}$, $\bar{m} = 6\times10^{-4}$, and $w = -1$ throughout this chapter. Here, we implicitly assume that the Higgs potential is supplemented by a non-renormalizable ϕ^6 term as considered in Ref. [120] so that we can use the thin-wall approximation. We also take $\xi = 10^3 M_{\rm Pl}^{-1}$ as an example.

Effective potentials governing the wall position ($V(z)$) for the above parameters are plotted in Fig. 6.2-(a). The dashed line represents the case of CDL tunneling, where $M_{\rm tot}/M_{\rm Pl} = 0$ with $M_{\rm tot} \equiv \int_0^\infty dr' 4\pi r'^2 \rho_{\rm c}(r')$. In this case, a bubble is nucleated at the point P_0 i.e. with the radius $R \simeq \alpha H_-^{-1} \equiv R_{\rm CDL}$ for $\alpha \equiv 8\pi G m^3/H_- \ll 1$ [92, 118]. As we increase $M_{\rm tot}/M_{\rm Pl}$, the effective potential becomes lower. We plot the cases of $M_{\rm tot}/M_{\rm Pl} = 400$ (a black solid line), 872.6 (a black dashed-dotted line), and 952.1 (a blue solid line).

A nucleated vacuum bubble with $0 \leq M_{\rm tot}/M_{\rm Pl} \lesssim 872.6$ initially has its wall radius between P_1 and P_0 (black open circles in Fig. 6.2) and would expand soon after its nucleation. A nucleated bubble around the horizonless object with $872.6 \lesssim M_{\rm tot}/M_{\rm Pl} \lesssim 952.1$ would be trapped between P_2 and P_3, where the gravitational force and bubble tension are balanced, and then, it may eventually tunnel to a larger bubble, whose wall is in between P_4 and P_1. If the mass is larger than or equal to $952.1 M_{\rm Pl}$, one has $f_+ = 0$ (a black filled circle in Fig. 6.2-(b)), that is, a black hole forms.

One finds that the effective potential can be drastically distorted because of the gravitational effect of the horizonless object, which makes a bubble wall nucleated around a catalyzing object smaller compared to a CDL bubble (P_0 in Fig. 6.2-(a)). The distortion of the potential largely enhances the nucleation rate of vacuum bubble and the nucleation of bubbles could occur within the cosmological time as will be shown in the following.

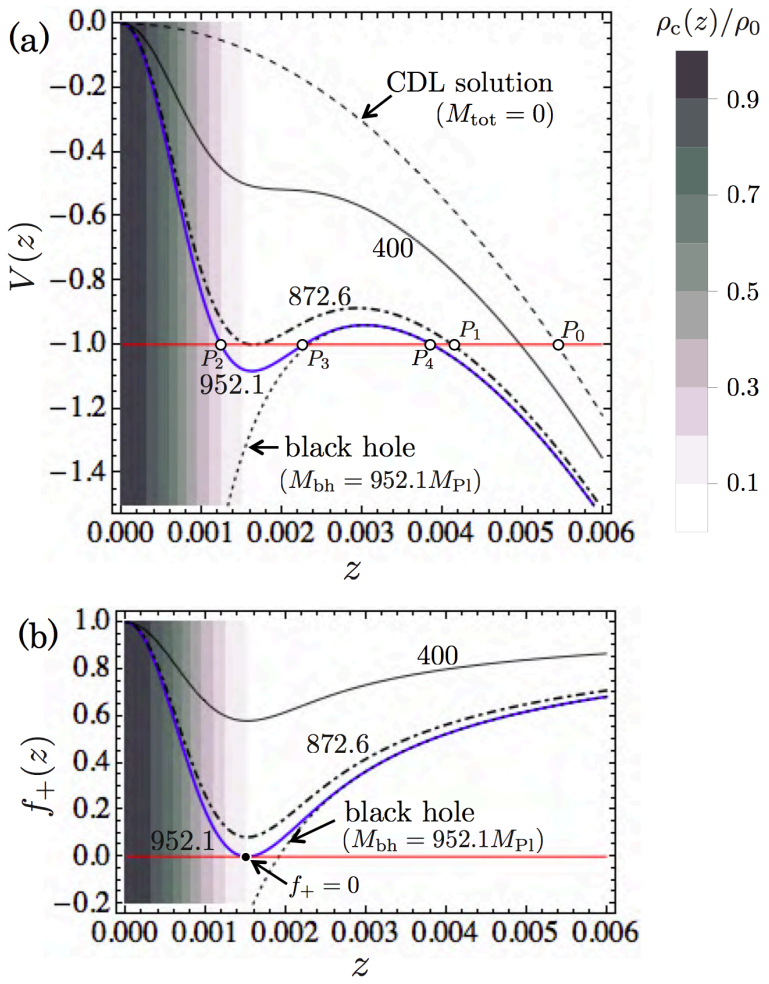

Figure 6.2: The effective potential (a) and f_+ (b) for the horizonless object with $M_{\rm tot}/M_{\rm Pl}=0$ (CDL solution), 400 (a black solid line), 872.6 (a black dashed-dotted line), and 952.1 (a blue solid line) and for a black hole with $M_{\rm tot}/M_{\rm Pl}=952.1$ (a black dotted line) are shown.

In Fig. 6.3, the ratio of the vacuum decay rate, $\Gamma_{\rm D}$, to the inverse of the cosmological time, $\Gamma_{\rm C}\equiv H_{\rm C}\simeq 10^{-61}M_{\rm Pl}$, is shown in the range of $1\leq M_{\rm tot}/M_{\rm Pl}\leq 15000$ and of $c\leq 5$, where we define the compactness parameter as

$$c\equiv \xi/(2GM_{\rm tot}). \tag{6.17}$$

In our setup, we find that the existence of even a single horizonless object with $M_{\rm tot}/M_{\rm Pl}$ and c within the region enclosed by the red line in the figure (i.e., $10^3\lesssim M_{\rm tot}/M_{\rm Pl}\lesssim 10^4$ and with $c\lesssim 2$) would be excluded since a bubble would be nucleated around it within the cosmological time.

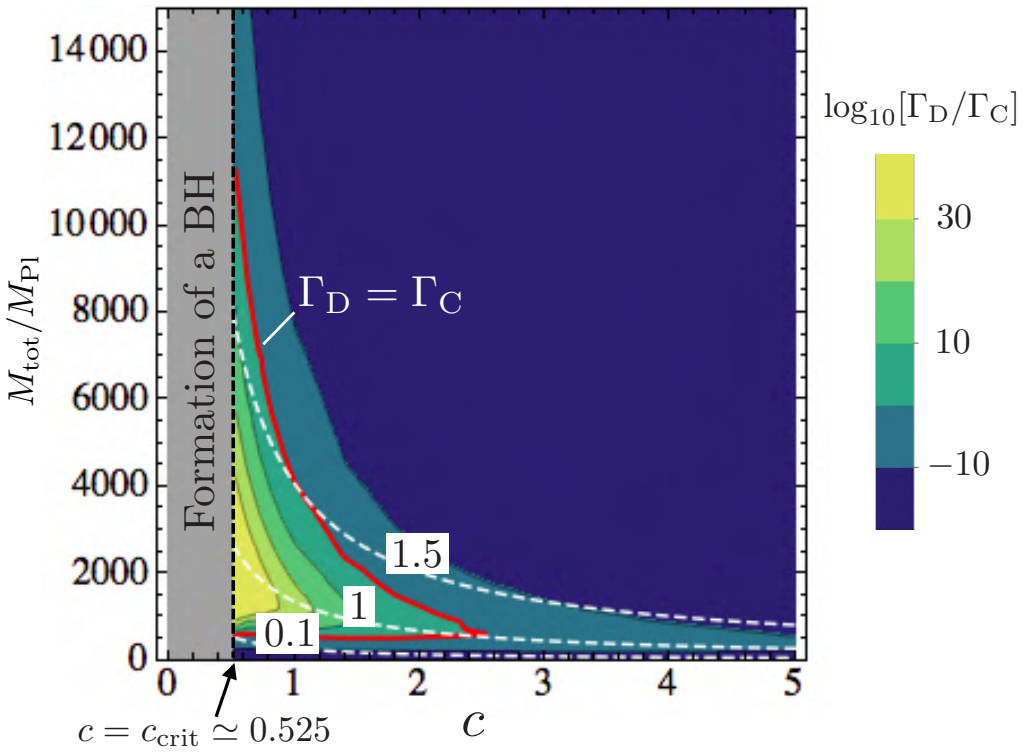

Figure 6.3: Plot of the ratio of the decay rate, $\Gamma_{\rm D}$, to the inverse of the cosmological time, $\Gamma_{\rm C}$, as a function of the mass and compactness of the horizonless object. The contour of $\Gamma_{\rm D}=\Gamma_{\rm C}$ (red solid line) and contours of $\xi/R_{\rm CDL}$ (white dashed lines) are marked for reference. In the case of $c\leq c_{\rm crit}\simeq 0.525$ (gray shaded region), the object inevitably collapses to a black hole since a function $f_+(r)$ has zero points there.

We show the contours of $\xi/R_{\rm CDL}$ as white dashed lines in Fig. 6.3. They indicate that an efficient enhancement occurs only when the radius of the nucleated bubble (which is of the same order with the CDL radius) is comparable to that of the compact object. An efficient enhancement also requires a small compactness so that the gravity effect is efficient around the dense compact object. Therefore, we conclude that the bubble nucleation rate is drastically enhanced around a compact object if the size of the horizonless object is comparable with the radius of CDL bubble and its compactness is of the order of unity.

6.2.3 Constraint on the abundance of compact objects

The nucleation of the AdS vacuum bubble, whose origin could be the Higgs instability, within the cosmological time obviously conflicts with the present Universe not filled by the negative

vacuum energy. It would expand with the light speed soon after its nucleation, which would lead to the Universe filled by the negative vacuum energy. Since a compact object could be a catalyst for the vacuum decay, we can put constraints on the abundance of horizonless objects in the Universe.

For instance, depending on the energy scale, magnetic monopoles could be ultra compact. Suppose that there is a (hidden) non-Abelian gauge field that is spontaneously broken by a (hidden) Higgs field. If the vacuum manifold has a non-trivial second homotopy group, monopoles arise at the spontaneously symmetry breaking. Introducing the vacuum expectation value of the hidden Higgs field, v, the mass and size of a 't Hooft-Polyakov monopole, denoted by $M_{\rm mono}$ and $R_{\rm mono}$, respectively, can be estimated as

$$M_{\rm mono} \sim v/\sqrt{\alpha_{\rm G}} \tag{6.18}$$

$$R_{\rm mono} \sim (\sqrt{\alpha_{\rm G}} v)^{-1}, \tag{6.19}$$

where $\alpha_{\rm G}$ is the running gauge coupling constant for the non-Abelian gauge interaction. Imposing the ultra compact condition, $c \simeq R_{\rm mono}/(2GM_{\rm mono}) \sim 1$, one obtains $v \sim M_{\rm Pl}$ and $R_{\rm mono} \sim \ell_{\rm Pl}/\sqrt{\alpha_{\rm G}}$. Therefore, as long as the Higgs potential accommodates a second lower minimum due to the Higgs instability, parameter regions which realize $v \sim M_{\rm Pl}$ and $R_{\rm CDL} \sim R_{\rm mono} \sim \ell_{\rm Pl}/\sqrt{\alpha_{\rm G}}$ should be excluded in order to be consistent with the present Universe not filled by the AdS vacuum. Since $R_{\rm CDL} = 8\pi G m^3/H_-^2 \simeq 5 \times 10^3$, $\alpha_{\rm G}$ should be as small as 3×10^{-8} to nucleate the Higgs vacuum bubble.

6.3 Comparison with the catalyzing effect of black holes

Now we compare our results with the case of bubble nucleation around a black hole, which has been extensively discussed in the literature. In Ref. [118], Gregory, Moss, and Withers pointed out that the Bekenstein entropy of a black hole with mass $M_{\rm tot}$ may contribute to the vacuum decay rates as

$$\Gamma_{\rm D} \sim R_{\rm CDL}^{-1} \sqrt{\frac{I_{\rm E}}{2\pi}} e^{-I_{\rm E}} = R_{\rm CDL}^{-1} \sqrt{\frac{I_{\rm E}}{2\pi}} e^{-B_{\rm bh} + \Delta S}, \tag{6.20}$$

$$B_{\rm bh} \equiv \frac{1}{4G} \oint d\tau_{\rm E} (2R - 6GM_{\rm tot}) \left(\frac{\beta_+}{f_+} - \frac{\beta_-}{f_-} \right), \tag{6.21}$$

where $I_{\rm E}$ is the total Euclidean action and $B_{\rm bh}$ is the bulk component of the on-shell Euclidean action depending on the Euclidean dynamics of a vacuum bubble. Contributions from the conical singularities on the Euclidean manifolds before and after the vacuum decay lead to a factor of ΔS, which is equivalent to the change of the Bekenstein entropy of a catalyzing black hole.

Note that even horizonless compact objects can emit Hawking radiation (see, e.g., Refs. [206–208]) because of the vacuum polarization in a strong gravitational field and its thermal effect on the Higgs potential may have to be taken into account. The details of the Higgs potential are characterized by the parameters (i.e. $\bar{H}$, $\bar{m}$, and w) in the thin-wall approximation, and therefore, those parameters could be affected by such a thermal effect in our setup. In addition, we here fix the mass of black hole singularity before and after the phase transition by simply assuming that matter fields forming the black hole singularity has no interaction with another matter field which eventually undergoes the phase transition.*)

When a black hole efficiently catalyzes the vacuum decay, the size of the black hole, $2GM_{\rm tot}$, is comparable with the CDL bubble radius, $R_{\rm CDL}$, and the prefactor in (6.20) can be rewritten as $(GM_{\rm tot})^{-1}\sqrt{I_{\rm E}/2\pi}$, which is consistent with the prefactor in Ref. [118]. The Bekenstein entropy decreases because of the vacuum decay since the decrease of the vacuum energy surrounding the black hole makes the area of its event horizon smaller. Although the gravitational effect is strong around a black hole, the vacuum decay rate would be suppressed by the change of Bekenstein entropy:

$$\Delta S = \pi \left[R_{\rm h,-}^2 - (2GM_{\rm tot})^2 \right] < 0, \tag{6.22}$$

where the horizon radius $R_{\rm h,-}$ after the bubble nucleation is defined by $f_-(R_{\rm h,-}) = 0$.

Horizonless compact objects have no Bekenstein entropy, so that they could more efficiently catalyze vacuum decays than black holes do. We here compare the vacuum decay rate around the horizonless compact object, whose mass is $M_{\rm tot}$ and compactness is fixed with $c = 1$, with that around a black hole whose mass is $M_{\rm tot}$. The result is shown in Fig. 6.4. Both the black hole and horizonless compact object efficiently catalyze the vacuum decay compared to the CDL solution shown as red points. If there were no contribution of Bekenstein entropy on the decay rate around the black hole, the exponential factor for the black hole would be larger than that for the horizonless object (blue dashed line in Fig. 6.4-(b)). However, the decay rate with the compact object (black solid line) is larger than that with the black hole (black dotted line) thanks to the absence of the decrement of Bekenstein entropy (red dashed-dotted line).

A bubble nucleated around a black hole with $M_{\rm tot} = M_{\rm crit} \simeq 1045 M_{\rm Pl}$ is static (black points in Fig. 6.4) because of the perfect balance between the gravity of the black hole and bubble's tension. On the other hand, there is no well-defined Euclidean solution for a black hole with $M_{\rm tot} \geq M_{\rm crit}$ [118].

*) Although it might be possible that the black hole mass changes due to the bubble nucleation [118–121], it was argued that it could be closely related to the thermal excitation of bubble due to the Hawking radiation [122,202].

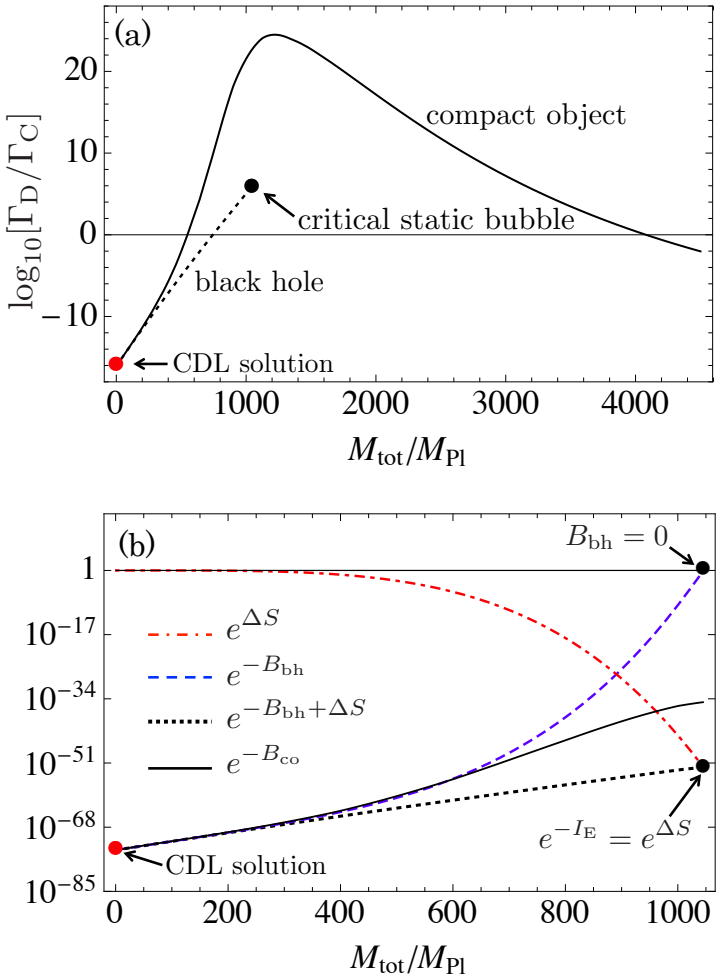

Figure 6.4: The vacuum decay rates around a black hole with mass $M_{\rm tot}$ (a dotted line) and that around a horizonless compact object, whose mass is $M_{\rm tot}$ and compactness is fixed with $\xi/2GM_{\rm tot} = 1$, (a solid line) are shown. Red and black points show the decay rate of the CDL solution and a critical static solution, respectively.

6.4 Summary

We have discussed a role of a horizonless compact object as a catalyst for a vacuum decay. As long as the interaction between a bubble and a catalyzing object is negligible, our results do not depend on the details of the object much and its gravity plays an essential role in the catalyzing process. The universality of our result is also discussed in the Appendix D. This suggests that one can put some constraints on the abundance of various kinds of horizonless compact objects, such as monopoles, Q-balls, Boson stars, gravastars, black hole remnants, and so on. In particular,

the Higgs vacuum may decay into an AdS vacuum if there exists even a single compact object whose radius is comparable to its Schwarzschild radius and the CDL bubble radius. For instance, depending on the energy scale, magnetic monopoles could be ultra compact. As long as the Higgs potential accommodates a second lower minimum causing its Higgs instability, parameter regions which realize the GUT symmetry breaking with $R_{\rm CDL} \sim R_{\rm mono}$ should be excluded in order to be consistent with the present Universe not filled by the AdS vacuum. More realistic cases may arise for Boson stars, oscillons, and Q-balls. In addition, in case that a single compact object is not enough to catalyze the Higgs vacuum to decay into the AdS one, multiple ones could do it, which leads to new constraints on the abundance of such a compact object.

It is also interesting to note that the catalyzing effect of horizonless objects is more efficient compared to that of black holes since there is no suppression of vacuum decay rate due to the decrement of Bekenstein entropy. Therefore, if there had been some ultra compact objects in the Universe, they could have played a critical role in the cosmological sense.

Finally, we comment on the case where the compact object has an interaction with the nucleated bubble, namely, the Higgs field. In this case, the mass of the compact object can change due to the bubble nucleation. Because of the conservation of energy, the nucleated bubble can use the mass difference of the compact object and the nucleation rate can be drastically enhanced. This is similar to the case of bubble nucleation in a finite temperature plasma, where a bubble can use the thermal energy to be excited with a finite energy. This is also similar to the case for a bubble nucleation around a black hole with the thermal effect of Hawking radiation, where the mass of black hole changes after the bubble nucleation. However, as the thermal effect stabilize the Higgs potential to the symmetric phase in these cases, the interaction between the compact object and the Higgs field may lead to an effective potential that stabilize the Higgs potential. Still, this results in a more efficient enhancement for the nucleation rate and is an interesting possibility for many particle physics models.

Chapter 7

Birth of an inflationary universe from a mini black hole

7.1 Background

Inflation in the early universe provides answers to a number of fundamental questions in cosmology such as why our Universe is big, old, full of structures, and devoid of unwanted relics predicted by particle physics models [209]. Furthermore, despite the great advancements in precision observations of CMB, there is no observational result that is in contradiction with inflationary cosmology so far [3, 4].

Inflationary cosmology has also revolutionized our view of the cosmos, namely, our Universe may not be the one and the only entity but there may be many universes. Indeed already in the context of the old inflation model [1, 2], Sato and his collaborators found possible production of child (and grand child...) universes [35, 71, 210].

Furthermore, if the observed dark energy consists of a cosmological constant Λ, our Universe will asymptotically approach the de Sitter space which may up-tunnel to another de Sitter universe with a larger vacuum energy density [32,34,211–213] to induce inflation again to repeat the entire evolution of another inflationary universe. In such a recycling universe scenario, the Universe we live in may not be of first generation, and we may not need the real beginning of the cosmos from the initial singularity [213].

In this context, so far only a phase transition between two pure de Sitter space has been considered. However, phase transitions which we encounter in daily life or laboratories are usually induced around some impurities which act as catalysts or boiling stones. In cosmological phase transitions, black holes may play such roles. In this chapter we discuss a cosmological phase transition around an evaporating black hole to show that a wormhole-like configuration

with an inflationary domain beyond the throat may be created after the transition.

The study of a phase transition around a black hole was pioneered by Hiscock [124]. More recently, Gregory, Moss and Withers revisited the problem [118]. They have observed that the black hole mass may change in the phase transition and calculated the Euclidean action taking conical deficits into account [118–120]. Moreover, a symmetry restoration activated by Hawking radiation [27, 28] near a microscopic black hole has been investigated by Moss [214].

7.2 Symmetry restoration around an evaporating black hole

We consider a high energy field theory of a scalar field ϕ whose potential allows a thin-wall bubble solution of a metastable local minimum at $\phi = 0$ with the energy density ϵ^4 surrounded by the true vacuum with a field value ϕ_0 where the mass square is given by m^2. In such a theory Moss [214] argues that the symmetry is restored in the vicinity of the black hole horizon inside a thin wall bubble as the Hawking temperature, $T_H = M_{Pl}^2/(8\pi M_+)$, reaches the mass scale of the theory. Here M_+ and M_{Pl} are the black hole mass and the Planck mass, respectively. In the presence of plausible couplings of the relevant fields, he shows that the medium inside the bubble, where fields coupled to ϕ are massless, is thermalized with a temperature T which is substantially smaller than $m \sim T_H$. Then the free energy of the bubble configuration is given by

$$F(r,T) = \frac{4}{3}\pi r^3\epsilon^4 + 4\pi r^2\sigma - \frac{\pi}{18}q\tilde{m}^2T^2r^3 \tag{7.1}$$

as a function of its radius r and T, where σ is the surface tension of the wall and $\tilde{m}^2$ denotes sum of the mass squared of species which receive a mass from ϕ outside the bubble. For simplicity we assume $\tilde{m}$ is of the same order of m and omit the tilde hereafter. Here q is related to the scattering parameter C defined by Moss [214] as $q \equiv (192\pi^2C)^{-2/3}$, which can take a value of order of unity or even larger.

The relation between the thermalized temperature T and the bubble radius r_w is obtained by solving the Boltzmann equations for the radiated beam particles and thermalized medium with the boundary condition that only particles with energy larger than m would escape the bubble wall, which reads

$$\frac{1}{216}q^{-3/2}T^3r^3 + 48mTr^2e^{-\beta m} = 1, \tag{7.2}$$

at $r = r_w$ with $\beta \equiv T^{-1}$.

The radius of the wall r_w is obtained by minimizing the free energy (7.1) under the condition (7.2). For example, when the inequality

$$mr_w \gg 10^4q^{2/3}(\beta m)^2e^{-\beta m} \tag{7.3}$$

is satisfied and the first term dominates the left hand side of (7.2), we find $T = 6\sqrt{q}/r_w$, so that the free energy is minimized at

$$r = r_w = \sqrt{\frac{3q}{2}}\frac{m}{\epsilon^2}. \tag{7.4}$$

For consistency of this solution with (7.3), ϵ and m must satisfy

$$\beta m = \frac{1}{6\sqrt{2}}\frac{m^2}{\epsilon^2} \gtrsim 10, \tag{7.5}$$

which we assume hereafter. Then the thin wall condition $mr_w = \sqrt{\frac{q}{2}}\frac{m^2}{\epsilon^2} \gg 1$ is naturally satisfied.

Under the condition (7.5) thermal energy inside the bubble is subdominant compared with ϵ^4, so the geometry inside the bubble can be described by the Schwarzschild de Sitter metric. Furthermore, as the radiation temperature increases in association with the increase of the Hawking temperature, more high energy particles, which escape from the bubble and do not contribute to support the wall, are created to lower the effect of the radiation pressure. Thus, contrary to naive expectation, thermal effects on the created bubble become less important as the temperature increases, which can be also understood from the inequality $dr_w/dT < 0$ derived from (7.2).

Thus the system can be approximated by a spherically symmetric thin wall with tension σ separating outside Schwarzschild geometry with mass parameter M_+ and inside Schwarzschild de Sitter geometry with vacuum energy density $\epsilon^4 \equiv 3M_{Pl}^2H^2/(8\pi)$ whose mass parameter we denote by M_-.

We use the equation of motion of the wall obtained by Israel junction condition to discuss quantum tunneling of the bubble to show that the final state is a wormhole-like configuration. Beyond the throat is a false vacuum state which inflates to create another big universe. Then one may regard that the final fate of an evaporating black hole is actually another universe. We do not take thermal effects to tunneling into account, as they would only enhance the tunneling rate.

We label the inner Schwarzschild de Sitter geometry with a suffix $-$ and outer Schwarzschild geometry with a suffix $+$. Then the outer and inner metrices are given by

$$\begin{aligned} ds^2 &= -f_\pm(r)dt^2 + \frac{dr^2}{f_\pm(r)} + r^2d\Omega^2, \\ f_+(r) &\equiv 1 - \frac{2GM_+}{r},\ f_-(r) \equiv 1 - \frac{2GM_-}{r} - H^2r^2. \end{aligned} \tag{7.6}$$

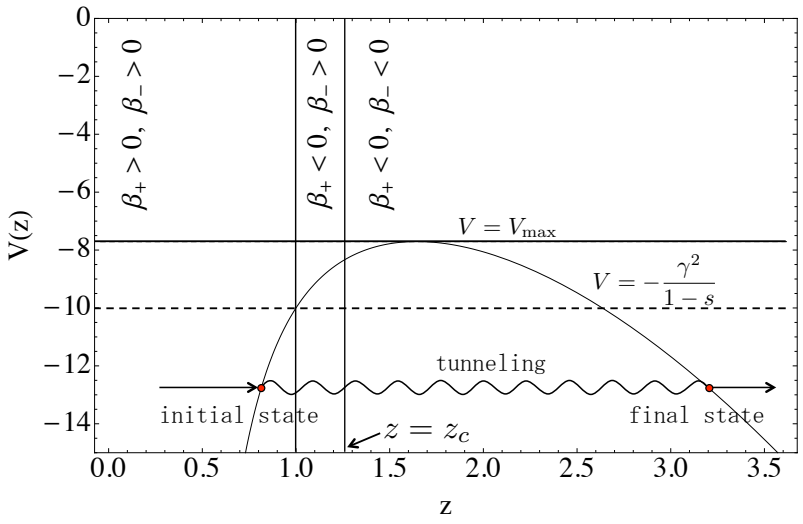

Figure 7.1: Shape of the potential $V(z)$ as a function of z with $s = 0.9$. We have taken $\gamma = 1$ for illustrative purpose, although we actually expect $\gamma \ll 1$ for $\phi_0 \ll M_{\rm Pl}$. β_+ changes its sign at $z = 1$, and β_- at $z = (1 - \gamma^2/2)^{-1/2} \equiv z_c$.

We describe the wall trajectory in terms of the local coordinates $(t_\pm(\tau), r_\pm(\tau), \theta, \varphi)$ on each side depending on the proper time τ of an observer on the wall. They satisfy

$$f_\pm(r_\pm)\dot{t}_\pm^2(\tau) - \frac{\dot{r}_\pm^2(\tau)}{f_\pm(r_\pm)} = 1, \tag{7.7}$$

where a dot denotes derivative with respect to τ. We take the radial coordinates so that the radius of the bubble is given by $R = r_+ = r_-$ in both outer and inner coordinates. The evolution of the bubble wall is described by the following equation [118, 130, 215] based on the Israel junction condition [125]

$$\beta_- - \beta_+ = 4\pi G\sigma R \equiv \Sigma R, \tag{7.8}$$

where $\beta_\pm \equiv f_\pm \dot{t}_\pm = \epsilon_\pm \sqrt{f_\pm + \dot{R}^2}$ with $\epsilon_\pm \equiv \mathrm{sign}[f_\pm \dot{t}_\pm]$. From (7.8) we find the wall radius satisfies the following equation similar to an energy conservation equation of a particle in a potential $V(z)$.

$$\left(\frac{dz}{d\tau'}\right)^2 + V(z) = E,\ V(z) \equiv -\frac{1}{1-s}\frac{\gamma^2}{z} - \left(\frac{1-z^3}{z^2}\right)^2, \tag{7.9}$$

$$E \equiv -\frac{\gamma^2}{[2GM_+\chi(1-s)]^{\frac{2}{3}}},\ \chi \equiv (H^2 + \Sigma^2)^{\frac{1}{2}}, \gamma \equiv \frac{2\Sigma}{\chi}. \tag{7.10}$$

Here dimensionless coordinate variables are defined by

$$\tau' \equiv \frac{\chi^2 \tau}{2\Sigma},\ z^3 \equiv \frac{\chi^2 R^3}{2GM_+(1-s)},\ \text{with } s \equiv \frac{M_-}{M_+}. \tag{7.11}$$

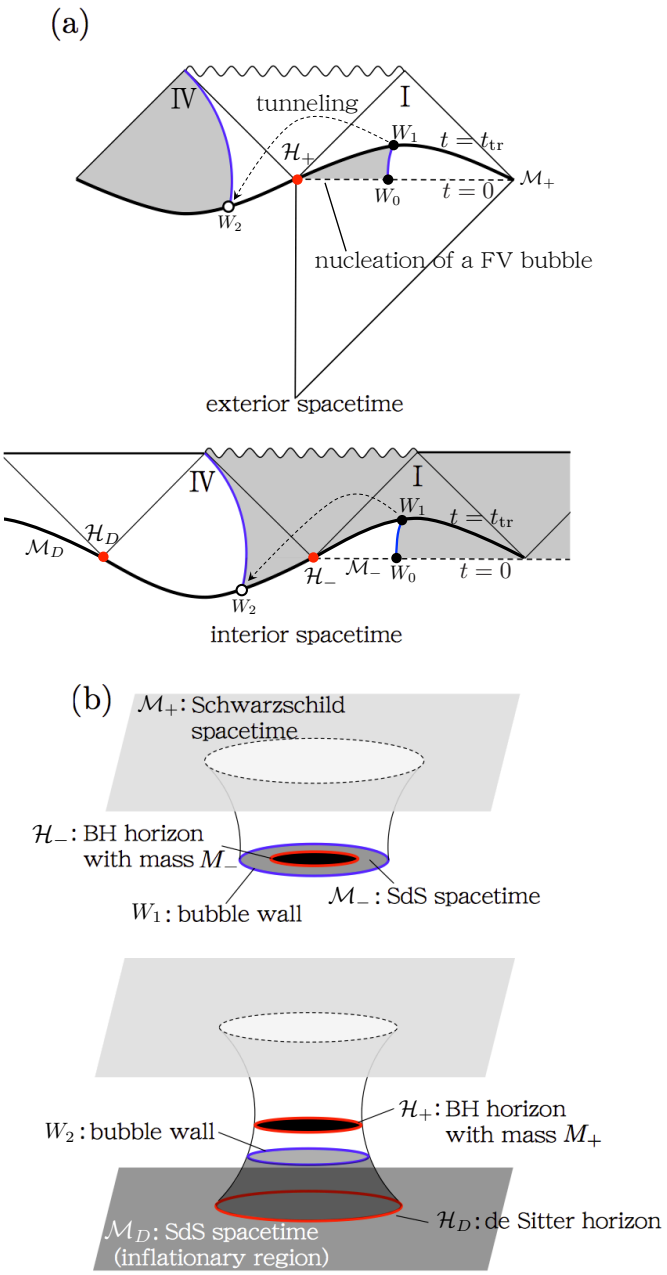

Figure 7.2: The trajectories of a bubble wall (blue line) on Penrose diagrams and a schematic figure of a wormhole-like configuration accommodating an inflationary region induced by a phase transition. The upper (lower) diagram in Figure (a) shows the spacetime outside (inside) the wall and a shaded region is to be replaced by the interior (exterior) spacetime. These diagrams depict the case a bubble wall is produced at the point W_0 at $t = t_w < 0$ through thermal effects of Hawking radiation, and the wall tunnels from W_1 to W_2 at $t = 0$ to create a wormhole-like configuration. Figures (b) depict the initial and final configurations schematically.

As is seen in Fig. 7.1, the potential $V(z)$ has a concave shape with the maximum $V(z_m) \equiv V_{\max}$ given by

$$V_{\max} = -3\frac{z_m^6 - 1}{z_m^4}, \tag{7.12}$$

with

$$z_m^3 = \left[2 + \left(\frac{1}{2} - \frac{\gamma^2}{4(1-s)}\right)^2\right]^{\frac{1}{2}} - \left(\frac{1}{2} - \frac{\gamma^2}{4(1-s)}\right), \tag{7.13}$$

for $s < 1$. From (7.8) we also find

$$M_+ = M_- + \frac{4\pi}{3}R^3\epsilon^4 + 4\pi R^2\sigma\frac{\beta_+ + \beta_-}{2}. \tag{7.14}$$

We may consider the evolution of the system taking the initial condition that the bubble is at rest at $R = r_w$ as the Hawking temperature has increased to above m so that thermal support on the wall has become less important as discussed above. For a thin wall bubble, (7.14) reads $M_+ \cong M_- + 4\pi r_w^3\epsilon^4/3$, and one can show that an inequality $E = V(z_w) < -\gamma^2/(1-s) = V(z=1)$ holds where $z_w \equiv \chi^{2/3} r_w [H^2 r_w^3 + \Sigma r_w^2(\beta_+ + \beta_-)]^{-1/3}$ is the value of z corresponding to $R = r_w$. Therefore $\beta_\pm$ are both positive initially as is shown in Fig. 7.1.

We can discuss quantum tunneling of the bubble wall from $R = r_w$ to a larger R, from which it expands in real time, by manipulating the Euclidean action. As one can see in Fig. 7.1, physically relevant expanding bubble nucleation is possible only for $\beta_+ < 0$ and $\beta_- < 0$. It has been shown in [130] that in this case the trajectory of the bubble wall after the transition exists in region IV on the Penrose diagram (Fig. 7.2-(a)), that is, a wormhole-like configuration is created [131, 216] and the false vacuum exists on the other side of the throat (Fig. 7.2-(b)).

Note that although β_+ and β_- change their signs at different radii, namely $z = 1$ and z_c, their physical separation

$$\Delta R_{c1} = \left[\frac{2GM_+(1-s)}{\chi^2}\right]^{1/3}\left(z_c^{1/3} - 1\right) \cong \frac{\gamma^2}{4}r_w \tag{7.15}$$

is actually smaller than the width of the wall $1/m$ for realistic values of parameters, so that we can regard that they change sign at the same radius in the thin wall approximation.

7.3 Quantum tunneling of the symmetry-restored region

Let us now calculate the transition rate to the wormhole-like configuration Γ by solving Euclidean equation of motion starting from the bubble radius $R = r_w$ at rest. Following Gregory, Moss, and Withers [118–120], the transition rate Γ has the form

$$\Gamma = me^{-I_{\mathcal{M}-\mathcal{B}}-I_{\mathcal{B}}} = me^{-B_{\rm tunnel}+\Delta S}, \tag{7.16}$$

where the prefactor m has been introduced on dimensional grounds. Here $I_{\mathcal{M}-\mathcal{B}}$ represents the action over the regular bulk Euclidean spacetime and $I_{\mathcal{B}}$ stands for the contribution of conical singularities. They are given by

$$\begin{aligned} I_{\mathcal{M}-\mathcal{B}} &= \int d\tau_E \left[(2R - 6GM_+)\dot{t}_{E+} \right. \\ &\qquad \left. - (2R - 6GM_-)\dot{t}_{E-} \right] \equiv B_{\rm tunnel}, \\ I_{\mathcal{B}} &= \frac{A_f}{4G} - \frac{A_i}{4G} \equiv \Delta S, \end{aligned} \tag{7.17}$$

respectively, where the suffix E indicates the Euclidean time and A_i (A_f) denotes the total horizon area in the initial (final) state. Obviously terms arising from conical singularities are identical to the difference of horizon (Bekenstein) entropies, ΔS, between initial and final states. These terms have been derived using another method of calculation, too [217–220].

It is well known that the Bekenstein entropy of horizon may be related to its number of microscopic states W although so far we do not know what the microscopic degrees of freedom are. In our case, the initial state before tunneling has a Schwarzschild de Sitter black hole horizon with its mass parameter M_-, whose area is denoted by A_-, and the final state has two gravitational horizons, namely, the black hole horizon with mass M_+ and the de Sitter horizon (Fig. 7.2-(b)), whose horizon areas are denoted by A_+ and A_D, respectively. Therefore, we have $A_i = A_-$ and $A_f = A_+ + A_D$ and the numbers of the initial and final microscopic degrees of freedom are given by $W_i = e^{A_i/4G}$ and $W_f = e^{A_f/4G}$, respectively [200].

From $e^{\Delta S} = W_f/W_i$ we can interpret the transition rate we have calculated, (7.16), as a transition from one microscopic initial state with a statistical weight $1/W_i$ to a final state with W_f microscopic degrees of freedom, and the transition rate from one microscopic state of the initial black hole to another microscopic state of the final wormhole configuration is given by

$$\Gamma_{\rm micro} = m e^{-B_{\rm tunnel}}, \tag{7.18}$$

up to the uncertainty of the prefactor.

Let us evaluate the transition rate by calculating $B_{\rm tunnel}$ and ΔS which are functions of q, the energy scales m and ϵ, and the tension of bubble wall σ. Here we can evaluate the tension as $\sigma \simeq \xi^4/m$, where ξ^4 is the potential energy density at the top of the potential barrier separating the false vacuum and true vacuum. We take M_+ at a reference value $M_+ = M_{Pl}^2/(8\pi m) \gg M_{\rm Pl}$ corresponding to $T_H = m$. Taking $m^2 = 120\sqrt{2}\epsilon^2$, $q = 1$, and $\xi^4/\epsilon^4 = 25$, as an example, one can satisfy the thin wall condition, $mr_w = 120 \gg 1/m$. $m\Delta R = m\gamma^2 r_w/4 \ll 1$ is also satisfied for $\epsilon \ll 10^{16}$ GeV.

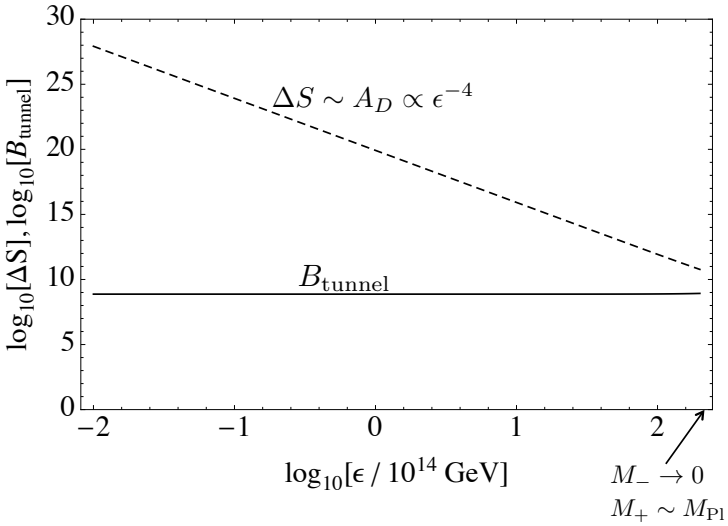

Figure 7.3: ΔS (dashed line) and $B_{\rm tunnel}$ (solid lines) as functions of ϵ for $m^2 = 120\sqrt{2}\epsilon^2$, $q = 1$ and $\xi^4/\epsilon^4 = 25$. The inner black hole mass, M_-, approaches to zero and M_+ becomes comparable to the Planck mass at $\epsilon \simeq 2 \times 10^{16}$ GeV, where $M_+ = 4 \times 10^2 M_{Pl}(\epsilon/10^{14}{\rm GeV})^{-1}$.

Fig. 7.3 depicts ΔS and $B_{\rm tunnel}$ as functions of ϵ. ΔS is proportional to ϵ^{-4} since the de Sitter horizon area, which is proportional to $H^{-2} \propto \epsilon^{-4}$, becomes dominant compared to the black hole horizon areas for $\epsilon \ll 10^{16}$ GeV. As is seen here, we always find $\Delta S \gg B_{\rm tunnel} \gg 1$. This means that even though the tunneling rate from one microscopic state to another is exponentially suppressed so that the semiclassical approximation is valid, due to the largeness of the number of microscopic degrees of freedom after the transition, the tunneling as a whole is unsuppressed and wormhole creation may take place with the relevant time scale $t \sim 1/T_H \sim 1/m$, once a bubble is thermally excited around an evaporating black hole with the proper conditions we discussed above. Similar enhancement of transition rate due to the large entropy in the final state has been observed by Mathur in a different problem [132].

7.4 Discussion

Then we can sketch the following scenario of cosmic evolution. Typical astrophysical black holes with mass $\sim 10M_\odot$ will evaporate in $\sim 10^{67}$ years from now. As its mass falls below a critical value so that the Hawking temperature become high enough for a false vacuum bubble to spontaneously nucleate around the black hole according to the process described by Moss [214]. Then the bubble wall will experience quantum tunneling rather efficiently to create a wormhole-like configuration with a de Sitter horizon, beyond which the false vacuum region is extended to

infinity. Thus the space on the other side of the throat will inflate which is causally disconnected from our patch of the universe. If inflation is appropriately terminated followed by reheating, another big bang universe will result there. For this purpose the old inflation model [1, 2] with thin wall bubble nucleation does not work, but we may make use of the results of open inflation models there [221–223] which can also realize an effectively flat universe.

Throughout these processes, the outer geometry remain Schwarzschild space with the mass parameter M_+, so those who live there do not realize a black hole in their universe has created a child universe. To this end alone, our model is similar to the scenario proposed by Frolov, Markov, and Mukhanov [224, 225]. However, there are two striking differences between our model and their scenario. One is that theirs is entirely dependent on the limiting curvature hypothesis and the assumption that in the regime of large curvature, the gravitational field equation would take the form in vacuum with a positive cosmological constant. They thereby find a Schwarzschild solution is continued to a deflating de Sitter space inside the black hole horizon which bounces to an inflating de Sitter universe. Our model, on the other hand, does not need such a speculative hypothesis near the singularity but creation of another inflationary universe is achieved by symmetry restoration due to the high Hawking temperature around an evaporating black hole which also induces a phase transition to produce a wormhole-like configuration in quantum field theory. Thus the entire processes can be described by known physics with appropriate values of the model parameters. Another difference lies in the causal structures as described in Fig. 7.2 of our paper and Figs. 3 and 6 of [224], that is, in our model the inflating domain is causally disconnected from the original universe unlike theirs.

In conclusion, our result may also suggest that our Universe may have been created from a black hole in the previous generation in the cosmos.

Chapter 8

Conclusions

In this thesis, we have investigated cosmological consequences of quantum effects in strong gravity throughout the history of the Universe. In particular, we focused on the initial singularity problem, problem of initial conditions for inflation, consistency between inflation and thermodynamics, firewall argument of black holes, and metastability of the Higgs vacuum. We restate here what we have achieved in this thesis.

In chapter 3, we discuss how the problem of initial conditions for inflation can be solved by taking into account the quantum tunneling effect. If the Universe at the pre-inflation epoch is dominated by radiation, its temperature gradually decreases due to cosmic expansion, and after the temperature falls below the critical temperature of a relevant theory, highly inhomogeneous space may be realized by the spontaneous symmetry breaking process. In this scenario, we investigated the quantum tunneling effect on the inhomogeneous space without homogeneous mode by modeling a part of the inhomogeneity as a false vacuum bubble including thermal radiation. We have found that the false vacuum bubble quantum tunnels to a larger inflationary domain. This implies that the initial inhomogeneity can be a seed of inflationary universes. Therefore, once taking into account the quantum tunneling effect, the problem of initial conditions for inflation that requires sufficiently homogeneous space beyond the Hubble horizon in the beginning would be no longer problematic. Furthermore, we found that the increment of Bekkenstein entropy enhances the tunneling process. This implies that the entropic nature of gravity may play an essential role in the origin of the Universe.

In chapter 4, we investigated the entropic nature of inflating space from the point of view of the GSL conjecture. In the first half of this chapter, we investigated the entropy production due to the cosmological decoherence and found that it can offset the decrement of the Bekenstein entropy during stochastic inflation. This means that the stochastic inflation formalism is well consistent with the GSL. Furthermore, this shows that the cosmological decoherence is

important to explain not only why our Universe looks classical but also how plausible the GSL is. In the second half of this chapter, we investigated the limitation of the GSL by taking into account the instantaneous quantum jump process of de Sitter universe, called the Hawking-Moss instanton. This process is very rare and its rate is exponentially suppressed. We have shown that the exponent of the rate is completely determined by the decrement of Bekenstein entropy. Since this tunneling process instantaneously occurs, the entropy production due to cosmological decoherence cannot offset this and the GSL is broken. Throughout this chapter, we found that the GSL conjecture is "statistically" valid in the inflating space thanks to cosmological decoherence.

In the present Universe, back holes are ubiquitous and they suffer from the black hole information loss paradox. In this context, the firewall conjecture was proposed to solve the problem of monogamy of entanglement in the black hole evaporation process. However, the firewall argument implies the breakdown of the equivalence principle of GR, and once we extend this argument to the cosmological horizons, drastic modifications to the picture of the multiverse and eternal inflation scenario would be required. In chapter 5, we proposed an alternative scenario to solve the tension between the firewall argument and GR. We investigated the disentanglement process of a Hawking pair created near the horizon, and found that since the infalling Hawking particle experiences gravitational decoherence, the quantum entanglement of the Hawking pair would be eventually lost, which may satisfy a necessary condition for the retrieval of information that has fallen into the back hole. This means that the firewall, leading to the inconsistency between the GR and quantum field theory, is no longer necessary to destroy the entanglement of the Hawking pair.

In the latter part of the thesis, we have discussed possible scenarios regarding the fate of the Universe. One interesting and possible scenario comes from the metastability of the Higgs vacuum. In the far future of the Universe, AdS vacuum bubble could be nucleated by the first order phase transition of Higgs vacuum and eventually fills the observable region of the Universe. In chapter 6, we especially investigated the catalyzing effect of compact objects that promotes a first order phase transition. We investigated the vacuum decay rate with some parameters characterizing compact objects, and found that they could more efficiently catalyze the vacuum decay than back holes would do and there exists a parameter region where the AdS vacuum bubble is nucleated within the age of the Universe. Since our Universe has not been filled by the negative vacuum energy, this leads to new constraints on the abundance of such a compact object.

Another interesting scenario in the future of the Universe is the creation of next-generation inflationary universes out of evaporating back holes. All black holes would be microscopic

in the future due to their evaporation process. In chapter 7, we investigated a possibility that such a microscopic black hole may lead to the birth of another inflationary universe by quantum tunneling process. Since the Hawking temperature is proportional to the inverse of black hole mass, a microscopic black hole is surrounded by highly energetic Hawking radiation. We consider a situation where the thermal radiation causes a symmetry restoration. Modeling this configuration by a thin wall false vacuum bubble surrounding the evaporating mini black hole, we found that the configuration quantum tunnels to a baby Universe accommodating an inflating domain. This implies that even our Universe may have been born out of a black hole in the previous generation of the Universe, and in this sense, the Universe can be eternal to past and the initial singularity is not necessary in our scenario.

We believe that quantum effects in strong gravity, such as the quantum tunneling processes, stochastic fluctuations of background, quantum entanglement, and gravitational decoherence, play essential roles throughout the history of the Universe, and we hope that our work has made some contribution towards solving several cosmological problems.

Appendix A

Calculation of Bogolubov coefficients in the gravitational collapse process

A.1 Analytic forms of the Bogolubov coefficients

In this Appendix, we provide the details of the derivation of (2.91). Substituting (2.78) and (2.88) into (2.90), we obtain

$$\beta_{\omega_{jn},\omega'} = \frac{-1}{2\pi\sqrt{\epsilon}} \int_{-\infty}^{v_H} dv \int_{j\epsilon}^{(j+1)\epsilon} d\omega e^{2\pi i\omega n/\epsilon} \sqrt{\frac{\omega'}{\omega}} \exp\left[-i\omega\left(v_H - 4GM\log\left(\frac{v_H - v}{4GM}\right)\right) - i\omega' v\right]. \tag{A.1}$$

Since w varies in a small interval, we can approximately perform the integration over frequencies and we obtain

$$\beta_{\omega_{jn},\omega'} = \frac{-e^{-i(\omega_{jn}+\omega')v_H}}{\pi\sqrt{\epsilon}} \sqrt{\frac{\omega'}{\omega_{jn}}} \int_0^{\infty} dx e^{i\omega' x} \frac{\sin\epsilon L_x/2}{L_x} e^{iL\omega_{jn}}, \tag{A.2}$$

where a new variable $x \equiv v_H - v$ is introduced and

$$L_x \equiv \frac{2\pi n}{\epsilon} + 4GM\frac{x}{4GM}. \tag{A.3}$$

In the similar way, we obtain the coefficients $\alpha_{\omega_{jn},\omega'}$

$$\alpha_{\omega_{jn},\omega'} = \frac{-e^{-i(\omega_{jn}-\omega')v_H}}{\pi\sqrt{\epsilon}} \sqrt{\frac{\omega'}{\omega_{jn}}} \int_0^{\infty} dx e^{-i\omega' x} \frac{\sin\epsilon L_x/2}{L_x} e^{iL\omega_{jn}}. \tag{A.4}$$

Let us investigate the relation between (A.2) and (A.4). In the following we denote the integration as

$$I(\omega') = \int_0^{+\infty} dx e^{-i\omega' x} \frac{\sin\epsilon L_x/2}{L_x} e^{iL\omega_{jn}}, \tag{A.5}$$

where $\omega' < 0$ for $\beta_{\omega_{jn},\omega'}$ and $\omega' > 0$ for $\alpha_{\omega_{jn},\omega'}$.

A.2 Relation between $\alpha_{\omega_{jn},\omega'}$ and $\beta_{\omega_{jn},\omega'}$

Performing the Wick rotation for x in (A.5), one can obtain the relation between the coefficients $\alpha_{\omega_{jn},\omega'}$ and $\beta_{\omega_{jn},\omega'}$. For $\omega' > 0$ we rotate the contour of integration to the negative imaginary axis so that the integration is convergent

$$I(\omega' > 0) = -i \int_0^{\inf} dy e^{-\omega' y} \frac{\sin \epsilon L_y/2}{L_y} e^{iL_y \omega_{jn}}, \tag{A.6}$$

where

$$L_y = \frac{2\pi n}{\epsilon} + 4GM \left(-\frac{i\pi}{2} + \log \frac{y}{4GM} \right). \tag{A.7}$$

Therefore, (A.6) reduces to

$$I(\omega' > 0) = -ie^{2GM\pi\omega_{jn}} e^{2\pi i n \omega_{jn}/\epsilon} \int_0^{+\infty} dy e^{-\omega' y} \frac{\sin \epsilon L_y/2}{L_y} e^{i4GM \log (y/4GM)\omega_{jn}}. \tag{A.8}$$

In the case of $\omega' < 0$, on the other hand, the contour should be rotated to the positive imaginary axis and we obtain

$$I(\omega' < 0) = i \int_0^{\infty} dz e^{\omega' z} \frac{\sin \epsilon L_z/2}{L_z} e^{iL_z \omega_{jn}}, \tag{A.9}$$

$$L_z = \frac{2\pi n}{\epsilon} + 4GM \left(\frac{i\pi}{2} + \log \frac{z}{4GM} \right). \tag{A.10}$$

Then the final expression for $I(\omega' < 0)$ is

$$I(\omega' < 0) = ie^{-2GM\pi\omega_{jn}} e^{2\pi i n \omega_{jn}/\epsilon} \int_0^{+\infty} dy e^{-\omega' y} \frac{\sin \epsilon L_y/2}{L_y} e^{i4GM \log (y/4GM)\omega_{jn}}. \tag{A.11}$$

From (A.2), (A.4), (A.8), and (A.11), we finally obtain the relation between $\alpha_{\omega_{jn},\omega'}$ and $\beta_{\omega_{jn},\omega'}$

$$\alpha_{\omega_{jn},\omega'} = -e^{4\pi GM\omega_{jn}} e^{2i\omega' v_H} \beta_{\omega_{jn},\omega'}. \tag{A.12}$$

This reduces to the relation (2.91).

Appendix B

Interior metric of the thermalized bubble

Here we derive the interior metric of a vacuum bubble including homogeneous radiation. We first derive the static form of the FLRW metric. The non-static form of the FLRW metric is

$$ds^2 = -dt^2 + a^2(t)\left(\frac{dr^2}{1-Kr^2} + r^2 d\Omega_2^2\right), \tag{B.1}$$

where r is the co-moving radial coordinate, t is the cosmic time, $a(t)$ is the scale factor, $d\Omega_2^2$ is the metric of a unit 2-sphere and $K = -1, 0, +1$. In the following we take $K = 0$. We define a new coordinate

$$\bar{r} = ra(t) \tag{B.2}$$

and this transformation puts (B.1) into the form

$$ds^2 = -\left(1 - H^2\bar{r}^2\right)dt^2 - 2H\bar{r}d\bar{r}dt + d\bar{r}^2 + \bar{r}^2 d\Omega_2^2, \tag{B.3}$$

where $H(t) \equiv (da(t)/dt)/a(t)$. Then the transformation

$$t = \bar{t} + Q(\bar{t}, \bar{r}), \tag{B.4}$$

$$Q(\bar{t}, \bar{r}) \equiv \frac{1}{2H(\bar{t})}\log\left(1 - H(\bar{t})^2\bar{r}^2\right) + q(\bar{t}), \tag{B.5}$$

yields the following form

$$ds^2 = -(1 + (\partial_{\bar{t}}Q)^2)\left(1 - H^2\bar{r}^2\right)d\bar{t}^2 + \frac{d\bar{r}^2}{1 - H^2\bar{r}^2} + \bar{r}^2 d\Omega_2^2, \tag{B.6}$$

where $q(\bar{t})$ is an arbitrary function of $\bar{t}$. Of course, this metric is not static since $H = H(\bar{t})$ is generically dynamical. However, when thermal radiation is completely trapped by the bubble

wall and the thermalized bubble is static, the corresponding metric should be a static FLRW metric. The Hamiltonian constraint in the FLRW background is given by

$$H^2 = \frac{8\pi G}{3}\rho, \tag{B.7}$$

where ρ is the energy density of a homogeneous medium. In our situation, the FLRW geometry has its boundary with radius R and the interior is filled by thermal radiation of energy density $\rho_{\rm rad} \equiv (\pi^2/30)T^4$ and a positive vacuum energy density of $\rho_{\rm vac}$, where T is the temperature of radiation. Since the radiation is trapped by the wall, the entropy of thermal radiation S is constant

$$S = \frac{8\pi^3}{135}T^3R^3. \tag{B.8}$$

From (B.6), (B.7), and (B.8), the interior metric of the vacuum bubble reduces to

$$ds^2 = -(1+(\partial_{\bar{t}}Q)^2)\left(1 - H_0^2\bar{r}^2 - \frac{(135S)^{4/3}}{180\pi}\frac{G\bar{r}^2}{R^4}\right)d\bar{t}^2 + \frac{d\bar{r}^2}{1 - H_0^2\bar{r}^2 - \frac{(135S)^{4/3}}{180\pi}\frac{G\bar{r}^2}{R^4}} + \bar{r}^2 d\Omega_2^2, \tag{B.9}$$

where $H_0^2 \equiv (8\pi G/3)\rho_{\rm vac}$. The time-development of $R = R(\bar{t})$ is determined by the Israel junction condition.

Let us calculate the (θ,θ)-component of the extrinsic curvature $K_{\theta\theta}$ for a dynamical spherical shell that is necessary to derive the equation of the Israel junction condition. Assuming the following metric

$$ds^2 = -A(t,r)dt^2 + B(t,r)dr^2 + r^2(d\theta^2 + \sin^2\theta d\varphi^2), \tag{B.10}$$

the trajectory of the wall u^μ is

$$u^\mu = (\dot{t}(\tau), \dot{R}(\tau), 0, 0), \tag{B.11}$$

and the normal vector on the wall n_μ is given by

$$n_\mu = \sqrt{|AB|}(-\dot{R}, \dot{t}, 0, 0), \tag{B.12}$$

where τ is the proper time on the wall and $R(\tau)$ is the wall radius. The extrinsic curvature $K_{\theta\theta}$ is given by

$$K_{\theta\theta} = e^\mu_\theta e^\mu_\theta \nabla_\mu n_\nu, \tag{B.13}$$

where e^μ_A with $(A = \tau, \theta, \varphi)$ is an orthonormal triad constructed on the wall with radius $r = R(\tau)$:

$$e^\mu_\tau = u^\mu,\ e^\mu_\theta = (0,0,1/R,0),\ \text{and}\ e^\mu_\varphi = (0,0,0,1/(R\sin\theta)). \tag{B.14}$$

Therefore, we have

$$K_{\theta\theta} = e^\mu_\theta e^\mu_\theta \nabla_\mu n_\nu = \frac{1}{R^2}(\partial_\theta n_\theta - \Gamma^\mu_{\theta\theta}|_{r=R} n_\mu) \tag{B.15}$$

$$= -\frac{1}{R^2}\Gamma^r_{\theta\theta}|_{r=R} n_r = \frac{\sqrt{|AB|}}{R}\frac{1}{B}\dot{t} = \frac{\epsilon}{R}\sqrt{\frac{1}{B(R)} + \dot{R}^2}, \tag{B.16}$$

where $\epsilon \equiv \text{sign}[\dot{t}/B]$ and we used $\Gamma^r_{\theta\theta} = -r/B$ and $A\dot{t}^2 - B\dot{R}^2 = 1$. One finds that $K_{\theta\theta}$ depends only on B and is independent of A. Finally, we obtain $K_{\theta\theta}$ in the FLRW background used in (3.15)

$$K_{\theta\theta} = \frac{\epsilon}{R}\sqrt{\left(1 - H_0^2 R^2 - \frac{(135S)^{4/3}}{180\pi}\frac{G}{R^2}\right) + \dot{R}^2}. \tag{B.17}$$

Appendix C

semi-classical description of a bubble wall

Here we will review the quantum tunneling of a bubble wall involving gravitational field.

C.1 Dynamics of a bubble wall

C.1.1 Setup

We first consider a situation that a spherical thin bubble wall of energy density σ separates two different spacetime whose metrics are given by

$$ds_{\pm}^2 = g_{\pm\mu\nu}dx^{\mu}dx^{\nu} = -f_{\pm}(r_{\pm})dt_{\pm}^2 + f_{\pm}^{-1}(r_{\pm})dr_{\pm}^2 + r_{\pm}^2(d\theta^2 + \sin^2\theta d\varphi^2) \tag{C.1}$$

where the indices $+$ and $-$ represent the exterior and interior coordinates, respectively. Denoting the manifold of the exterior and interior as $\mathcal{M}_+$ and $\mathcal{M}_-$, respectively, the total action of the system involving gravitational field $g_{\pm\mu\nu}$ and a matter field ϕ has the form

$$I = I_+ + I_- + I_W, \tag{C.2}$$

where I_W is the action of the thin wall

$$I_W = -4\pi R^2 \int d\lambda\sigma \tag{C.3}$$

and I_+ and I_- are the bulk actions with the Gibbons-Hawking-York boundary terms including the trace of the extrinsic curvature on the wall $K_{\pm}$

$$I_{\pm} = \frac{1}{16\pi G}\int_{\mathcal{M}_{\pm}} d^4x\sqrt{-g_{\pm}}\mathcal{R} + \int_{\mathcal{M}_{\pm}} d^4x\sqrt{-g_{\pm}}\mathcal{L}_m(g,\phi) \pm \frac{1}{8\pi G}\int_{\partial\mathcal{M}_{\pm}} K_{\pm}. \tag{C.4}$$

C.1.2 Israel junction condition

The trajectory of the bubble wall is

$$\xi^{\mu}_{\pm} = (t_{\pm}(\lambda), r_{\pm}(\lambda), \theta, \varphi), \tag{C.5}$$

where λ is the proper time on the wall. The induced metric on the dynamical wall is

$$ds^2 = h_{ab}dx^a dx^b = -d\lambda^2 T r^2_{\pm}(\lambda)\left[d\theta^2 + \sin^2\theta d\varphi^2\right]. \tag{C.6}$$

In the following we take $r_+(\lambda) = r_-(\lambda) \equiv R(\lambda)$ by which we can set the boundary separating the interior and exterior. We next construct normal vectors $n^{\mu}_{\pm}$ on each side of the wall. Requiring $\dot{\xi}^{\mu}_{\pm} n_{\pm\mu} = 0$, we have

$$n_{\pm\mu} = (-\dot{r}_{\pm}, \dot{t}_{\pm}, 0, 0), \tag{C.7}$$

where $n^{\mu}_{\pm}$ is normalized so that $n^{\mu}_{\pm} n_{\pm\mu} = 1$. Using the form of normal vectors, one can calculate the extrinsic curvatures on each side of the wall:

$$K_{\pm 00} \equiv K_{\pm\lambda\lambda} = \xi^{\mu}_{\pm,\lambda}\xi^{\nu}_{\pm,\lambda}\nabla_{\mu} n_{\pm\nu} = -\frac{d\beta_{\pm}}{dR}, \tag{C.8}$$

$$K_{\pm 11} \equiv e^{\mu}_{\theta} e^{\nu}_{\theta} \nabla_{\mu} n_{\pm\nu} = \frac{\beta_{\pm}}{R}, \tag{C.9}$$

$$K_{\pm 22} \equiv e^{\mu}_{\varphi} e^{\nu}_{\varphi} \nabla_{\mu} n_{\pm\nu} = \frac{\beta_{\pm}}{R}, \tag{C.10}$$

$$\text{with } \beta_{\pm} \equiv \epsilon_{\pm}\sqrt{f_{\pm}(R) + (dR/d\tau)^2}, \tag{C.11}$$

where e^{μ}_{A} is the vierbein on the wall defined as $\eta_{AB} \equiv e^{\mu}_{A} e^{\nu}_{B} g_{\pm\mu\nu}$ and $\epsilon_{\pm}$ is the sign of the spatial component of extrinsic curvature. The Israel junction condition, the jump of the extrinsic curvature should satisfy to be consistent with the Einstein equation, has the form

$$K_{+ab} - K_{-ab} = -8\pi G\left(S_{ab} - \frac{1}{2}h_{ab}\mathrm{Tr}(S_{ab})\right), \tag{C.12}$$

where S_{ab} is the energy momentum tensor of the bubble wall and here we assume $S_{ab} = -\sigma h_{ab}$. By solving the Israel junction condition, we can follow the dynamics of the wall.

C.1.3 Effective action of the wall

We will derive the effective action of the wall in this subsection. Let us first perform the ADM decomposition for the form of $I_{\pm}$ (C.4) as

$$I_{\pm} = \frac{1}{16\pi G}\int d\lambda \int_{\Sigma_\lambda} ({}^3\mathcal{R} + K^2 - K^2_{ab} + \mathcal{L}_m) \pm \frac{1}{8\pi G}\int d\lambda 4\pi R^2 n_{\pm\mu} u^{\nu}\nabla_{\nu} u^{\mu} \pm \frac{1}{8\pi G}\int d\lambda 4\pi R^2 K_{\pm}, \tag{C.13}$$

where u^μ is the normal vector on Σ_τ with $u^\mu u_\mu = -1$ and it has the form

$$u^\mu = (f_\pm^{-1/2}, 0, 0, 0). \tag{C.14}$$

Using (C.14), we can calculate $n_{\pm\mu}u^\nu\nabla_\nu u^\mu$ in (C.13)

$$\begin{aligned} &n_{\pm\mu}u^\nu\nabla_\nu u^\mu = n_{\pm\mu}u^0\nabla_0 u^\mu = n_{\pm\mu}f_\pm^{-1/2}\Gamma^\mu_{0\nu}u^\nu = n_{\pm\mu}f_\pm^{-1/2}\Gamma^\mu_{00}u^0 = n_{\pm 1}f_\pm^{-1}\Gamma^1_{00} \\ &= \dot{t}_\pm f_\pm^{-1}\frac{f_\pm f'_\pm}{2} = \dot{t}_\pm\frac{f'_\pm}{2}, \end{aligned} \tag{C.15}$$

where we used $\Gamma^\mu_{00} = (0, f_\pm f'_\pm/2, 0, 0)$. The first term in (C.13) vanishes due to the Hamiltonian constraint. From (C.3), (C.13), (C.15) Then we obtain the total action of the system

$$I = \frac{1}{16\pi G}\int_W \left[f^{-1}f'\beta\right]_-^+ + \frac{1}{8\pi G}\int_W [K]_-^+ - \int_W \sigma, \tag{C.16}$$

where $\int_W \equiv \int d\lambda 4\pi R^2$. Using the forms of extrinsic curvatures in (C.8), (C.9), and (C.10), the effective Lagrangian of the bubble wall is

$$I = \int d\lambda L, \tag{C.17}$$

$$L \equiv \frac{1}{2G}\left[\beta^{-1}R^2\ddot{R} + \frac{1}{2}R^2 f^{-1}f'\beta^{-1}\dot{R}^2 + 2\rho R\right]_-^+ - 4\pi R^2\sigma. \tag{C.18}$$

Since there is a degree of freedom N which corresponds to relabeling of the coordinate λ along the trajectory of the bubble wall as $d\lambda = Nd\lambda'$, one can obtain a first order constraint (Hamiltonian constraint) by taking variation of the action with respect to N. Then we find that the constrain reduces to

$$[\beta]_-^+ = -4\pi G\sigma R, \tag{C.19}$$

which is nothing but the spatial component of the Israel junction condition. After some calculations, this equation can be rewritten as

$$\mathcal{H} \equiv \frac{1}{2}\dot{R}^2 + U(R) = 0, \tag{C.20}$$

where $U(R)$ is a function of R. In the quantum mechanics, this Hamiltonian constraint $\mathcal{H}$ becomes an operator constraint $\hat{\mathcal{H}}\Psi = 0$, where Ψ is a wave function, and this is nothing but the Schrödinger equation.

C.2 Path integral method and semi-classical approximation

As a first example, let us consider a single particle in the framework of the one-dimensional quantum mechanics. Once specifying a path of the particle $x(t)$, the amplitude for the path is proportional to

$$\exp\left(iS[x(t)]\right), \tag{C.21}$$

where $S[x(t)]$ is the classical action of the particle. In particular, the amplitude that the particle is located at position x at time t while it initially exists at x' at time t' is given by

$$\psi(x,t;x',t') = N\int_{x(t)}^{x'(t')} \mathcal{D}\tilde{x}(\tilde{t}) \exp\left(iS[\tilde{x}(\tilde{t})]\right), \tag{C.22}$$

where N is a normalizing factor and the sum is over all paths which starts at $(x(t))$ and end at $x'(t')$. The integral is oscillatory due to the imaginary factor in the exponent but it can be well defined by rotating the time to imaginary values (Wick rotation) as $t \to -i\tau$:

$$\int_{x(t)}^{x'(t')} \mathcal{D}\tilde{x}(\tilde{t}) \exp\left(iS[\tilde{x}(\tilde{t})]\right) \to \int_{x(\tau)}^{x'(\tau')} \mathcal{D}\tilde{x}(\tilde{\tau}) \exp\left(-S_{\mathrm{E}}[\tilde{x}(\tilde{\tau})]\right). \tag{C.23}$$

This technique is useful when a path of interest is the lowest-energy path. For example, let us represent a Euclidean transition amplitude from an initial state $|q\rangle$ at time $-\beta/2$ to $|q'\rangle$ at $\beta/2$ by using the Hamiltonian operator $\hat{H}$:

$$\langle q|\, e^{-\beta\hat{H}}\, |q'\rangle = \sum_n \langle q|n\rangle \langle n|q'\rangle\, e^{-\beta E_n}, \tag{C.24}$$

where $|n\rangle_{n=1,2,\ldots,N}$ is energy eigenstates. If the transition time scale β is much longer than a relevant time scale determined by the energy gap between the ground energy and the next energy level $\beta \gg 1/(E_1 - E_0)$, the amplitude will be dominated by the ground state $|0\rangle$ and other excited states are exponentially suppressed. In the path integral method, since the most efficient path $\bar{x}(t)$ satisfies $\delta S_{\mathrm{E}} = 0$, the Euclidean amplitude can be approximated as

$$\psi(x,t;x',t') \sim \exp\left(-S_{\mathrm{E}}[\bar{x}(\tau)]\right), \tag{C.25}$$

and this approximation is known as the semi-classical approximation.

C.3 Tunneling rate of the bubble wall

It is found that only an on-shell Euclidean action $S_{\mathrm{E}}[\bar{x}[t]]$, where $\bar{x}[t]$ is the Euclidean classical solution, is necessary to evaluate a tunneling rate baed on the semi-classical approximation from the previous section. The on-shell Euclidean action of the original action (C.16) is obtained by plugging $[K]^+_- = 12\pi G\sigma$ into the original one:

$$I_{\mathrm{E}} = -\frac{1}{16\pi G}\int_W \left[f^{-1}f'\beta\right]^+_- - \frac{1}{2}\int_W \sigma, \tag{C.26}$$

which is the on-shell Euclidean action used in this dissertation and the transition rate is given by $e^{-I_{\mathrm{E}}}$. Using the relation $\beta/f = \dot{\tilde{\tau}}$, (C.26) is found to be equivalent to the second and third terms in (2.121).

Appendix D

Vacuum decay around a gravastar-like object

In Chapter 6 we assume that the compact object is static at least during the nucleation process and the metric is given by the static solution (6.1). This is (approximately) justified for most of the realistic situations, like neutron stars, boson stars, oscillons, monopoles, and Q-balls, and so on. However, the density function $\rho_{\rm c}(r)$ as well as the metric functions $A_\pm$ and $B_\pm$ should be carefully chosen so that it is a static solution to the Einstein equation. In this Appendix, we consider a gravastar-like object to show that the result in Fig. 6.3 does not change qualitatively as long as we choose those functions carefully to (approximately) satisfy the static equilibrium.

D.1 Gravastar model

We use the following EMT for the gravastar-like object:

$$T^\mu_\nu = \mathrm{diag}(-\rho(r), p(r), p(r), p(r)), \tag{D.1}$$

$$\rho(r) \equiv \rho_0 \frac{1-\tanh\left((r-\xi)/\delta\right)}{2} + \rho_{\rm v} = -p(r) \tag{D.2}$$

with $r < R$, where T^μ_ν is the bubble interior EMT and δ represents the thickness of the boundary of the gravastar-like object. When $\delta \ll \xi$, one can use the thin wall approximation and the bubble interior energy density, ρ, is written as

$$\rho(r) \simeq \begin{cases} \rho_0 + \rho_{\rm v} \equiv \rho_{\rm in} > 0 & \xi > r \\ \rho_{\rm v} < 0 & \xi < r < R, \end{cases} \tag{D.3}$$

where the energy density of the gravastar-like object ρ_0 is constant. Assuming the form of its pressure as $p = -\rho$, the inner metric of the gravastar-like object is given by

$$g_{\mu\nu}^{(\mathrm{in})} = \mathrm{diag}(-f_{\mathrm{in}}(r_{\mathrm{in}}), f_{\mathrm{in}}^{-1}(r_{\mathrm{in}}), r_{\mathrm{in}}^2, r_{\mathrm{in}}^2 \sin^2\theta), \tag{D.4}$$

$$f_{\mathrm{in}}(r) \equiv 1 - H_{\mathrm{in}}^2 r^2, \tag{D.5}$$

where $H_{\mathrm{in}}^2 \equiv (8\pi G/3)\rho_{\mathrm{in}}$ and r_{in} is the radial coordinate inside the object and we set its scale so that $r_{\mathrm{in}} = r_- = \xi$ on the boundary of gravastar-like object.

Although the bulk of gravastar-like object has its static metric, whether or not its boundary is also static should be determined by the Israel junction condition that is available only when the thickness of its boundary is smaller than its radius, $\delta \ll \xi$. In the thin wall approximation, the boundary can be characterized only by its energy density, σ_c, and pressure, p_c. Introducing the equation-of-state parameter, $w_c \equiv p_c/\sigma_c$, one has the Israel junction conditions:

$$\beta_{\mathrm{in}} - \beta_- = 4\pi G \sigma_c(\xi)\xi, \tag{D.6}$$

$$\frac{d}{d\xi}\left(\beta_{\mathrm{in}} - \beta_-\right) = -8\pi G \sigma_c(\xi)\left(1/2 + w_c\right), \tag{D.7}$$

where $\beta_{\mathrm{in}} \equiv \epsilon_{\mathrm{in}}\sqrt{f_{\mathrm{in}}(\xi) + (d\xi/d\tau_c)^2}$ and τ_c is the proper time on the boundary of the object. Solving (D.6) and (D.7), one has the form of $\sigma_c(\xi) \equiv m_c^{-1-2w_c}\xi^{-2(1+w_c)}$. Substituting $\sigma_c(\xi)$ into

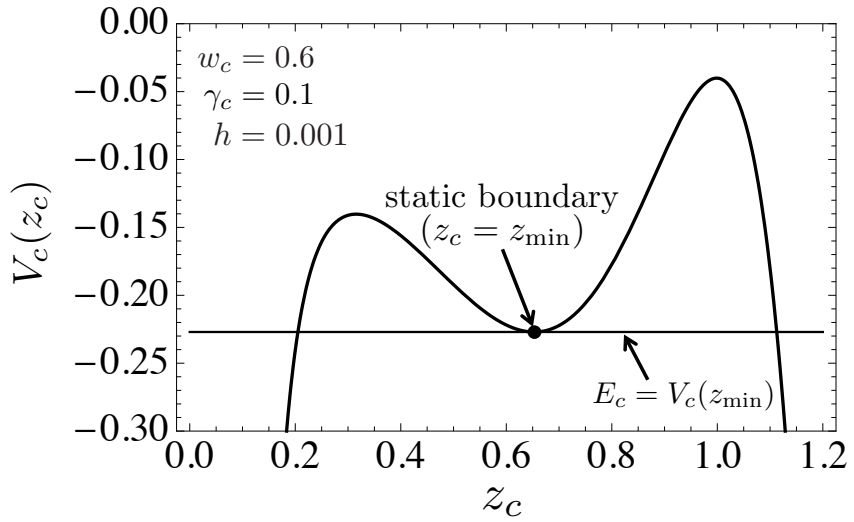

Figure D.1: A plot of the effective potential, $V_c(z_c)$, with $w_c = 0.6$, $\gamma_c = 0.1$, and $h = 10^{-3}$.

(D.6), one has

$$\left(\frac{dz_c}{d\tau_c'}\right)^2 + V_c(z_c) = E_c, \tag{D.8}$$

$$V_c(z_c) \equiv -\frac{4\gamma_c^2}{1+h^2} z_c^2 - z_c^{4w_c}\left(1 - z_c^3 + \frac{\gamma_c^2}{z_c^{1+4w_c}}\right)^2, \tag{D.9}$$

where we defined the following non-dimensional variables and parameters:

$$h \equiv H_-/H_{\rm in}, \tag{D.10}$$

$$z_c^3 \equiv \left(\frac{1+h^2}{2GM_{\rm tot}H_-}\right) H_-^3 \xi^3, \tag{D.11}$$

$$\tau_c' \equiv \frac{\sqrt{1+h^2}}{2\gamma_c} H_- \tau_c, \tag{D.12}$$

$$\gamma_c^2 \equiv H_-^{2(1+4w_c)/3} \frac{(4\pi G m^{-1-2w_c})^2}{2GM_{\rm tot}} \left(\frac{1+h^2}{2GM_{\rm tot}}\right)^{(1+4w_c)/3}, \tag{D.13}$$

$$E_c \equiv -\frac{4\gamma_c^2}{(2GM_{\rm tot}H_-)^{2/3}(1+h^2)^{1/3}}. \tag{D.14}$$

Now one obtains stable solutions by appropriately choosing the parameters. An effective potential, $V_c(z_c)$, governing the position of the boundary is plotted in Fig D.1. One finds a stable and static solution (a black filled circle in Fig. D.1), at which its radius is $z_c = z_{\rm min}$ and $E_c = V_c(z_{\rm min})$. An effective potential governing the dynamics of the boundary before the phase transition is obtained just by taking $h = 0$ in (D.9). Therefore, the effective potential, $V_c(z_c)$, is almost not affected by the phase transition as long as $h \ll 1$ is hold (see (D.9)). In this case, the gravastar-like object remains almost static even after the bubble nucleation and we can safely use the static metric (6.1) to calculate the bubble nucleation rate.

Fixing $h(\ll 1)$, γ_c, and w_c, one may obtain a static solution, $dV_c(z_c = z_{\rm min})/dz_c = 0$, and the total mass and size of the gravastar-like object are given by

$$M_{\rm tot} = \frac{8\gamma_c^3}{2GH_-(-V_c(z_c = z_{\rm min}))^{3/2}(1+h^2)^{1/2}}, \tag{D.15}$$

$$\xi = \frac{z_{\rm min}}{H_-}\left(\frac{2GM_{\rm tot}H_-}{1+h^2}\right)^{1/3}, \tag{D.16}$$

where we used (D.11) and (D.14).

D.2 Vacuum decay rate around the gravastar-like object

Here we calculate the on-shell Euclidean action as a function of $(M_{\rm tot}, c \equiv \xi/2GM_{\rm tot})$. Note that we do not take into account a parameter region where $h \geq 0.1$ to approximately keep the

gravastar-like object static before and after the phase transition. The mass function, $M(r)$, in (6.14) should have the form of

$$M(r) = \int_0^r dr' 4\pi r'^2 \rho_c(r') \simeq \begin{cases} (4\pi/3) r^3 \rho_0 & \xi > r \\ (4\pi/3)\xi^3 \rho_0 = M_{\rm tot} & \xi < r, \end{cases} \tag{D.17}$$

where $\delta \ll \xi$ is hold. This gives the metric on the inner and outer surface of the wall:

$$g_{\mu\nu}^{(\pm)} = \mathrm{diag}(-f_\pm(R), f_\pm^{-1}(R), R^2, R^2 \sin^2\theta), \tag{D.18}$$

with

$$f_+ \simeq \begin{cases} 1 - \dfrac{2GM_{\rm tot}}{R} & R > \xi \\ 1 - H_c^2 R^2 & R < \xi, \end{cases} \tag{D.19}$$

$$f_- \simeq \begin{cases} 1 - \dfrac{2GM_{\rm tot}}{R} + H_-^2 R^2 & R > \xi \\ 1 - H_{\rm in}^2 R^2 & R < \xi. \end{cases} \tag{D.20}$$

From (6.14), (6.15), (D.19), and (D.20), one can calculate the vacuum decay rate. Figure D.2 shows the result of $\Gamma_{\rm D}/\Gamma_{\rm C}$. One finds that the result shown in Fig. D.2 is qualitatively consistent with our conclusion based on the result in Fig. 6.3. However, the range of values of compactness, c, in which $\Gamma_{\rm D} > \Gamma_{\rm C}$ is satisfied, seems to be sensitive to the configuration of the boundary of a catalyzing object. The result in Fig. D.2 based on the more concrete set up would be a supporting evidence for the universality of our main proposal, that is, horizonless objects would catalyze vacuum decays when its size is comparable with the size of a CDL bubble and its compactness, $c \equiv \xi/2GM_{\rm tot}$, is of the order of unity, $c \sim \mathcal{O}(1)$.

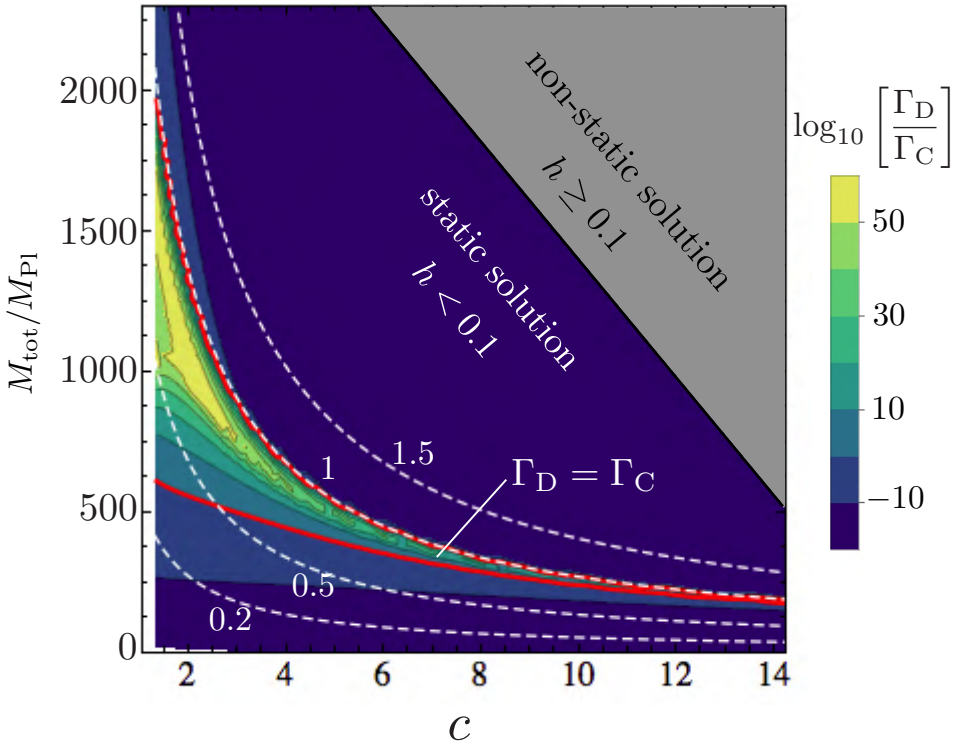

Figure D.2: A plot of the ratio Γ_D/Γ_C as a function of the mass and compactness of the gravastar-like object with $\bar{H} = 10^{-6}$, $\delta = 0.01\xi$, $\bar{m} = 6 \times 10^{-4}$, and $w = -1$. We here only take into account a parameter region corresponding to $h \leq 0.1$. The contours of ξ/R_{CDL} (white dashed lines) are marked for reference.

bibliography

[1] K. Sato. First Order Phase Transition of a Vacuum and Expansion of the Universe. *Mon. Not. Roy. Astron. Soc.*, 195:467–479, 1981.

[2] Alan H. Guth. The Inflationary Universe: A Possible Solution to the Horizon and Flatness Problems. *Phys. Rev.*, D23:347–356, 1981. [Adv. Ser. Astrophys. Cosmol.3,139(1987)].

[3] G. Hinshaw et al. Nine-Year Wilkinson Microwave Anisotropy Probe (WMAP) Observations: Cosmological Parameter Results. *Astrophys. J. Suppl.*, 208:19, 2013.

[4] Y. Akrami et al. Planck 2018 results. X. Constraints on inflation. 2018.

[5] Alexander Vilenkin. Creation of Universes from Nothing. *Phys. Lett.*, 117B:25–28, 1982.

[6] Alexander Vilenkin. Did the universe have a beginning? *Phys. Rev.*, D46:2355–2361, 1992.

[7] Arvind Borde and Alexander Vilenkin. Eternal inflation and the initial singularity. *Phys. Rev. Lett.*, 72:3305–3309, 1994.

[8] Arvind Borde and Alexander Vilenkin. Singularities in inflationary cosmology: A Review. *Int. J. Mod. Phys.*, D5:813–824, 1996.

[9] Arvind Borde, Alan H. Guth, and Alexander Vilenkin. Inflationary space-times are incompletein past directions. *Phys. Rev. Lett.*, 90:151301, 2003.

[10] Andreas Albrecht, Robert H. Brandenberger, and R. Matzner. Numerical Analysis of Inflation. *Phys. Rev.*, D32:1280, 1985.

[11] Andreas Albrecht, Robert H. Brandenberger, and Richard Matzner. Inflation With Generalized Initial Conditions. *Phys. Rev.*, D35:429, 1987.

[12] H. Kurki-Suonio, R. A. Matzner, J. Centrella, and J. R. Wilson. Inflation From Inhomogeneous Initial Data in a One-dimensional Back Reacting Cosmology. *Phys. Rev.*, D35:435–448, 1987.

[13] Robert H. Brandenberger and Hume A. Feldman. Effects of Gravitational Perturbations on the Evolution of Scalar Fields in the Early Universe. *Phys. Lett.*, B220:361–367, 1989.

[14] V. Muller, H. J. Schmidt, and Alexei A. Starobinsky. Power law inflation as an attractor solution for inhomogeneous cosmological models. *Class. Quant. Grav.*, 7:1163–1168, 1990.

[15] Hume A. Feldman and Robert H. Brandenberger. Chaotic Inflation With Metric and Matter Perturbations. *Phys. Lett.*, B227:359–366, 1989.

[16] Robert H. Brandenberger, Hume Feldman, and Jong Kung. Initial conditions for chaotic inflation. *Phys. Scripta*, T36:64–69, 1991.

[17] Dalia S. Goldwirth. On inhomogeneous initial conditions for inflation. *Phys. Rev.*, D43:3204–3213, 1991.

[18] Robert H. Brandenberger and J. H. Kung. Chaotic Inflation as an Attractor in Initial Condition Space. *Phys. Rev.*, D42:1008–1015, 1990.

[19] Dalia S. Goldwirth and Tsvi Piran. Initial conditions for inflation. *Phys. Rept.*, 214:223–291, 1992.

[20] P. Laguna, H. Kurki-Suonio, and R. A. Matzner. Inhomogeneous inflation: The Initial value problem. *Phys. Rev.*, D44:3077–3086, 1991.

[21] Hannu Kurki-Suonio, Pablo Laguna, and Richard A. Matzner. Inhomogeneous inflation: Numerical evolution. *Phys. Rev.*, D48:3611–3624, 1993.

[22] William E. East, Matthew Kleban, Andrei Linde, and Leonardo Senatore. Beginning inflation in an inhomogeneous universe. *JCAP*, 1609(09):010, 2016.

[23] J. D. Bekenstein. Black holes and the second law. *Lett. Nuovo Cim.*, 4:737–740, 1972.

[24] Jacob D. Bekenstein. Black holes and entropy. *Phys. Rev.*, D7:2333–2346, 1973.

[25] Jacob D. Bekenstein. Generalized second law of thermodynamics in black hole physics. *Phys. Rev.*, D9:3292–3300, 1974.

[26] G. W. Gibbons and S. W. Hawking. Cosmological Event Horizons, Thermodynamics, and Particle Creation. *Phys. Rev.*, D15:2738–2751, 1977.

[27] S. W. Hawking. Black hole explosions. *Nature*, 248:30–31, 1974.

[28] S. W. Hawking. Particle Creation by Black Holes. *Commun. Math. Phys.*, 43:199–220, 1975. [,167(1975)].

[29] S. W. Hawking. Breakdown of Predictability in Gravitational Collapse. *Phys. Rev.*, D14:2460–2473, 1976.

[30] Leonard Susskind, Larus Thorlacius, and John Uglum. The Stretched horizon and black hole complementarity. *Phys. Rev.*, D48:3743–3761, 1993.

[31] Ahmed Almheiri, Donald Marolf, Joseph Polchinski, and James Sully. Black Holes: Complementarity or Firewalls? *JHEP*, 02:062, 2013.

[32] S. W. Hawking and I. G. Moss. Supercooled Phase Transitions in the Very Early Universe. *Phys. Lett.*, 110B:35–38, 1982. [Adv. Ser. Astrophys. Cosmol.3,154(1987)].

[33] Naritaka Oshita. Generalized second law of thermodynamics and cosmological decoherence. *Phys. Rev.*, D97(2):023510, 2018.

[34] Naritaka Oshita and Jun'ichi Yokoyama. Entropic interpretation of the Hawking–Moss bounce. *PTEP*, 2016(5):053E02, 2016.

[35] Katsuhiko Sato, Hideo Kodama, Misao Sasaki, and Kei-ichi Maeda. Multiproduction of Universes by First Order Phase Transition of a Vacuum. *Phys. Lett.*, 108B:103–107, 1982.

[36] Bernard J. Carr, editor. *Universe or multiverse?* 2007.

[37] Andrei D. Linde. Eternally Existing Selfreproducing Chaotic Inflationary Universe. *Phys. Lett.*, B175:395–400, 1986.

[38] Naritaka Oshita. Resolution to the firewall paradox: The black hole information paradox and highly squeezed interior quantum fluctuations. *Class. Quant. Grav.*, 34(19):195002, 2017.

[39] A. Vilenkin and E. P. S. Shellard. *Cosmic Strings and Other Topological Defects*. Cambridge University Press, 2000.

[40] Sidney R. Coleman. Q Balls. *Nucl. Phys.*, B262:263, 1985. [Erratum: Nucl. Phys.B269,744(1986)].

[41] Alexander Kusenko and Mikhail E. Shaposhnikov. Supersymmetric Q balls as dark matter. *Phys. Lett.*, B418:46–54, 1998.

[42] Kari Enqvist and John McDonald. Q balls and baryogenesis in the MSSM. *Phys. Lett.*, B425:309–321, 1998.

[43] Kari Enqvist and John McDonald. B - ball baryogenesis and the baryon to dark matter ratio. *Nucl. Phys.*, B538:321–350, 1999.

[44] S. Kasuya and M. Kawasaki. Q ball formation through Affleck-Dine mechanism. *Phys. Rev.*, D61:041301, 2000.

[45] S. Kasuya and M. Kawasaki. Q Ball formation in the gravity mediated SUSY breaking scenario. *Phys. Rev.*, D62:023512, 2000.

[46] S. Kasuya and M. Kawasaki. Q ball formation: Obstacle to Affleck-Dine baryogenesis in the gauge mediated SUSY breaking? *Phys. Rev.*, D64:123515, 2001.

[47] Ki-Myeong Lee, Jaime A. Stein-Schabes, Richard Watkins, and Lawrence M. Widrow. Gauged q Balls. *Phys. Rev.*, D39:1665, 1989.

[48] Shinta Kasuya, Masahiro Kawasaki, and Tsutomu T. Yanagida. IceCube potential for detecting Q-ball dark matter in gauge mediation. *PTEP*, 2015(5):053B02, 2015.

[49] Jeong-Pyong Hong, Masahiro Kawasaki, and Masaki Yamada. Charged Q-balls in gauge mediated SUSY breaking models. *Phys. Rev.*, D92(6):063521, 2015.

[50] Remo Ruffini and Silvano Bonazzola. Systems of selfgravitating particles in general relativity and the concept of an equation of state. *Phys. Rev.*, 187:1767–1783, 1969.

[51] C. J. Hogan and M. J. Rees. AXION MINICLUSTERS. *Phys. Lett.*, B205:228–230, 1988.

[52] Edward W. Kolb and Igor I. Tkachev. Axion miniclusters and Bose stars. *Phys. Rev. Lett.*, 71:3051–3054, 1993.

[53] Edward Seidel and Wai-Mo Suen. Formation of solitonic stars through gravitational cooling. *Phys. Rev. Lett.*, 72:2516–2519, 1994.

[54] Wayne Hu, Rennan Barkana, and Andrei Gruzinov. Cold and fuzzy dark matter. *Phys. Rev. Lett.*, 85:1158–1161, 2000.

[55] F. Siddhartha Guzman and L. Arturo Urena-Lopez. Gravitational cooling of self-gravitating Bose-Condensates. *Astrophys. J.*, 645:814–819, 2006.

[56] P. Sikivie and Q. Yang. Bose-Einstein Condensation of Dark Matter Axions. *Phys. Rev. Lett.*, 103:111301, 2009.

[57] Alan H. Guth, Mark P. Hertzberg, and C. Prescod-Weinstein. Do Dark Matter Axions Form a Condensate with Long-Range Correlation? *Phys. Rev.*, D92(10):103513, 2015.

[58] Joshua Eby, Peter Suranyi, Cenalo Vaz, and L. C. R. Wijewardhana. Axion Stars in the Infrared Limit. *JHEP*, 03:080, 2015. [Erratum: JHEP11,134(2016)].

[59] Eric Braaten, Abhishek Mohapatra, and Hong Zhang. Dense Axion Stars. *Phys. Rev. Lett.*, 117(12):121801, 2016.

[60] Eric Braaten, Abhishek Mohapatra, and Hong Zhang. Nonrelativistic Effective Field Theory for Axions. *Phys. Rev.*, D94(7):076004, 2016.

[61] Lam Hui, Jeremiah P. Ostriker, Scott Tremaine, and Edward Witten. Ultralight scalars as cosmological dark matter. *Phys. Rev.*, D95(4):043541, 2017.

[62] Joshua Eby, Madelyn Leembruggen, Peter Suranyi, and L. C. R. Wijewardhana. Collapse of Axion Stars. *JHEP*, 12:066, 2016.

[63] Joshua Eby, Peter Suranyi, and L. C. R. Wijewardhana. Expansion in Higher Harmonics of Boson Stars using a Generalized Ruffini-Bonazzola Approach, Part 1: Bound States. *JCAP*, 1804(04):038, 2018.

[64] Joshua Eby, Kyohei Mukaida, Masahiro Takimoto, L. C. R. Wijewardhana, and Masaki Yamada. Classical Nonrelativistic Effective Field Theory and the Role of Gravitational Interactions. 2018.

[65] Naritaka Oshita, Masaki Yamada, and Masahide Yamaguchi. Compact objects as the catalysts for vacuum decays. arXiv: 1808.01382[gr-qc], 2018.

[66] Naritaka Oshita and Jun'ichi Yokoyama. Creation of an inflationary universe out of a black hole. *Phys. Lett.*, B785:197–200, 2018.

[67] Arvind Borde. Geodesic focusing, energy conditions and singularities. *Class. Quant. Grav.*, 4:343–356, 1987.

[68] Robert Brandenberger. Initial conditions for inflation — A short review. *Int. J. Mod. Phys.*, D26(01):1740002, 2016.

[69] Andrei D. Linde. A New Inflationary Universe Scenario: A Possible Solution of the Horizon, Flatness, Homogeneity, Isotropy and Primordial Monopole Problems. *Phys. Lett.*, 108B:389–393, 1982. [Adv. Ser. Astrophys. Cosmol.3,149(1987)].

[70] Andreas Albrecht and Paul J. Steinhardt. Cosmology for Grand Unified Theories with Radiatively Induced Symmetry Breaking. *Phys. Rev. Lett.*, 48:1220–1223, 1982. [Adv. Ser. Astrophys. Cosmol.3,158(1987)].

[71] Kei-ichi Maeda, Katsuhiko Sato, Misao Sasaki, and Hideo Kodama. Creation of De Sitter-schwarzschild Wormholes by a Cosmological First Order Phase Transition. *Phys. Lett.*, 108B:98–102, 1982.

[72] Mukunda Aryal and Alexander Vilenkin. The Fractal Dimension of Inflationary Universe. *Phys. Lett.*, B199:351–357, 1987.

[73] Tanmay Vachaspati and Mark Trodden. Causality and cosmic inflation. *Phys. Rev.*, D61:023502, 1999.

[74] Lasha Berezhiani and Mark Trodden. How Likely are Constituent Quanta to Initiate Inflation? *Phys. Lett.*, B749:425–430, 2015.

[75] S. W. Hawking and R. Penrose. The Singularities of gravitational collapse and cosmology. *Proc. Roy. Soc. Lond.*, A314:529–548, 1970.

[76] P. C. W. Davies. Cosmological Horizons and the Generalized Second Law of Thermodynamics. *Class. Quant. Grav.*, 4:L225, 1987.

[77] S. W. Hawking. Black holes in general relativity. *Commun. Math. Phys.*, 25:152–166, 1972.

[78] Alexei A. Starobinsky and Jun'ichi Yokoyama. Equilibrium state of a selfinteracting scalar field in the De Sitter background. *Phys. Rev.*, D50:6357–6368, 1994.

[79] Erick J. Weinberg. Hawking-Moss bounces and vacuum decay rates. *Phys. Rev. Lett.*, 98:251303, 2007.

[80] Alexander Vilenkin. The Birth of Inflationary Universes. *Phys. Rev.*, D27:2848, 1983.

[81] A. Fabbri and J. Navarro-Salas. *Modeling black hole evaporation.* 2005.

[82] Y. Aharonov, A. Casher, and S. Nussinov. The Unitarity Puzzle and Planck Mass Stable Particles. *Phys. Lett.*, B191:51, 1987.

[83] Tom Banks, M. O'Loughlin, and Andrew Strominger. Black hole remnants and the information puzzle. *Phys. Rev.*, D47:4476–4482, 1993.

[84] Steven B. Giddings. Quantum mechanics of black holes. In *Proceedings, Summer School in High-energy physics and cosmology: Trieste, Italy, June 13-July 29, 1994*, pages 0530–574, 1994.

[85] Ronald J. Adler, Pisin Chen, and David I. Santiago. The Generalized uncertainty principle and black hole remnants. *Gen. Rel. Grav.*, 33:2101–2108, 2001.

[86] Leonard Susskind and Larus Thorlacius. Gedanken experiments involving black holes. *Phys. Rev.*, D49:966–974, 1994.

[87] Don N. Page. Average entropy of a subsystem. *Phys. Rev. Lett.*, 71:1291–1294, 1993.

[88] Don N. Page. Information in black hole radiation. *Phys. Rev. Lett.*, 71:3743–3746, 1993.

[89] Don N. Page. Time Dependence of Hawking Radiation Entropy. *JCAP*, 1309:028, 2013.

[90] Sidney R. Coleman. The Fate of the False Vacuum. 1. Semiclassical Theory. *Phys. Rev.*, D15:2929–2936, 1977. [Erratum: Phys. Rev.D16,1248(1977)].

[91] Curtis G. Callan, Jr. and Sidney R. Coleman. The Fate of the False Vacuum. 2. First Quantum Corrections. *Phys. Rev.*, D16:1762–1768, 1977.

[92] Sidney R. Coleman and Frank De Luccia. Gravitational Effects on and of Vacuum Decay. *Phys. Rev.*, D21:3305, 1980.

[93] Peter Brockway Arnold. Can the Electroweak Vacuum Be Unstable? *Phys. Rev.*, D40:613, 1989.

[94] Guido Altarelli and G. Isidori. Lower limit on the Higgs mass in the standard model: An Update. *Phys. Lett.*, B337:141–144, 1994.

[95] J. R. Espinosa and M. Quiros. Improved metastability bounds on the standard model Higgs mass. *Phys. Lett.*, B353:257–266, 1995.

[96] J. A. Casas, J. R. Espinosa, and M. Quiros. Standard model stability bounds for new physics within LHC reach. *Phys. Lett.*, B382:374–382, 1996.

[97] Thomas Hambye and Kurt Riesselmann. Matching conditions and Higgs mass upper bounds revisited. *Phys. Rev.*, D55:7255–7262, 1997.

[98] Dario Buttazzo, Giuseppe Degrassi, Pier Paolo Giardino, Gian F. Giudice, Filippo Sala, Alberto Salvio, and Alessandro Strumia. Investigating the near-criticality of the Higgs boson. *JHEP*, 12:089, 2013.

[99] A. Gorsky, A. Mironov, A. Morozov, and T. N. Tomaras. Is the Standard Model saved asymptotically by conformal symmetry? *J. Exp. Theor. Phys.*, 120(3):344–353, 2015. [Zh. Eksp. Teor. Fiz.147,399(2015)].

[100] Fedor Bezrukov and Mikhail Shaposhnikov. Why should we care about the top quark Yukawa coupling? *J. Exp. Theor. Phys.*, 120:335–343, 2015. [Zh. Eksp. Teor. Fiz.147,389(2015)].

[101] John Ellis. Discrete Glimpses of the Physics Landscape after the Higgs Discovery. *J. Phys. Conf. Ser.*, 631(1):012001, 2015.

[102] Kfir Blum, Raffaele Tito D'Agnolo, and JiJi Fan. Vacuum stability bounds on Higgs coupling deviations in the absence of new bosons. *JHEP*, 03:166, 2015.

[103] Gino Isidori, Giovanni Ridolfi, and Alessandro Strumia. On the metastability of the standard model vacuum. *Nucl. Phys.*, B609:387–409, 2001.

[104] Manfred Lindner, Marc Sher, and Helmut W. Zaglauer. Probing Vacuum Stability Bounds at the Fermilab Collider. *Phys. Lett.*, B228:139–143, 1989.

[105] Marc Sher. Electroweak Higgs Potentials and Vacuum Stability. *Phys. Rept.*, 179:273–418, 1989.

[106] N. Cabibbo, L. Maiani, G. Parisi, and R. Petronzio. Bounds on the Fermions and Higgs Boson Masses in Grand Unified Theories. *Nucl. Phys.*, B158:295–305, 1979.

[107] J. R. Espinosa, G. F. Giudice, and A. Riotto. Cosmological implications of the Higgs mass measurement. *JCAP*, 0805:002, 2008.

[108] Gino Isidori, Vyacheslav S. Rychkov, Alessandro Strumia, and Nikolaos Tetradis. Gravitational corrections to standard model vacuum decay. *Phys. Rev.*, D77:025034, 2008.

[109] J. Ellis, J. R. Espinosa, G. F. Giudice, A. Hoecker, and A. Riotto. The Probable Fate of the Standard Model. *Phys. Lett.*, B679:369–375, 2009.

[110] Joan Elias-Miro, Jose R. Espinosa, Gian F. Giudice, Gino Isidori, Antonio Riotto, and Alessandro Strumia. Higgs mass implications on the stability of the electroweak vacuum. *Phys. Lett.*, B709:222–228, 2012.

[111] Georges Aad et al. Combined search for the Standard Model Higgs boson using up to 4.9 fb^{-1} of pp collision data at $\sqrt{s} = 7$ TeV with the ATLAS detector at the LHC. *Phys. Lett.*, B710:49–66, 2012.

[112] Serguei Chatrchyan et al. Combined results of searches for the standard model Higgs boson in pp collisions at $\sqrt{s} = 7$ TeV. *Phys. Lett.*, B710:26–48, 2012.

[113] A. V. Bednyakov, B. A. Kniehl, A. F. Pikelner, and O. L. Veretin. Stability of the Electroweak Vacuum: Gauge Independence and Advanced Precision. *Phys. Rev. Lett.*, 115(20):201802, 2015.

[114] Giuseppe Degrassi, Stefano Di Vita, Joan Elias-Miro, Jose R. Espinosa, Gian F. Giudice, Gino Isidori, and Alessandro Strumia. Higgs mass and vacuum stability in the Standard Model at NNLO. *JHEP*, 08:098, 2012.

[115] K. G. Chetyrkin and M. F. Zoller. Three-loop beta-functions for top-Yukawa and the Higgs self-interaction in the Standard Model. *JHEP*, 06:033, 2012.

[116] F. Bezrukov, M. Y. Kalmykov, B. A. Kniehl, and M. Shaposhnikov. Higgs boson mass and new physics. *Journal of High Energy Physics*, 10:140, October 2012.

[117] C. Ford, D. R. T. Jones, P. W. Stephenson, and M. B. Einhorn. The Effective potential and the renormalization group. *Nucl. Phys.*, B395:17–34, 1993.

[118] Ruth Gregory, Ian G. Moss, and Benjamin Withers. Black holes as bubble nucleation sites. *JHEP*, 03:081, 2014.

[119] Philipp Burda, Ruth Gregory, and Ian Moss. Gravity and the stability of the Higgs vacuum. *Phys. Rev. Lett.*, 115:071303, 2015.

[120] Philipp Burda, Ruth Gregory, and Ian Moss. Vacuum metastability with black holes. *JHEP*, 08:114, 2015.

[121] Philipp Burda, Ruth Gregory, and Ian Moss. The fate of the Higgs vacuum. *JHEP*, 06:025, 2016.

[122] Kyohei Mukaida and Masaki Yamada. False Vacuum Decay Catalyzed by Black Holes. *Phys. Rev.*, D96(10):103514, 2017.

[123] Kazunori Kohri and Hiroki Matsui. Electroweak Vacuum Stability and Gravitational Vacuum Polarization in Schwarzschild Black-hole Background. 2017.

[124] W. A. Hiscock. CAN BLACK HOLES NUCLEATE VACUUM PHASE TRANSITIONS? *Phys. Rev.*, D35:1161–1170, 1987.

[125] W. Israel. Singular hypersurfaces and thin shells in general relativity. *Nuovo Cim.*, B44S10:1, 1966. [Nuovo Cim.B44,1(1966)].

[126] G. W. Gibbons and S. W. Hawking. Action Integrals and Partition Functions in Quantum Gravity. *Phys. Rev.*, D15:2752–2756, 1977.

[127] Peter Brockway Arnold. A Review of the Instability of Hot Electroweak Theory and its Bounds on m_h and m_t. In *7th International Seminar on High-energy Physics (Quarks 92) Zvenigorod, Russia, May 11-17, 1992*, pages 403–412, 1992.

[128] Nobuyuki Sakai and Kei-ichi Maeda. Junction conditions of Friedmann-Robertson-Walker space-times. *Phys. Rev.*, D50:5425–5428, 1994.

[129] J. R. Morris. Stability of a class of neutral vacuum bubbles. *Phys. Rev.*, D87(8):085022, 2013.

[130] Steven K. Blau, E. I. Guendelman, and Alan H. Guth. The Dynamics of False Vacuum Bubbles. *Phys. Rev.*, D35:1747, 1987.

[131] V. A. Berezin, V. A. Kuzmin, and I. I. Tkachev. O(3) Invariant Tunneling in General Relativity. *Phys. Lett.*, B207:397–403, 1988.

[132] Samir D. Mathur. Tunneling into fuzzball states. *Gen. Rel. Grav.*, 42:113–118, 2010.

[133] S. W. Hawking and I. G. Moss. Fluctuations in the Inflationary Universe. *Nucl. Phys.*, B224:180, 1983.

[134] Andrei D. Linde. Hard art of the universe creation (stochastic approach to tunneling and baby universe formation). *Nucl. Phys.*, B372:421–442, 1992.

[135] Leonard Susskind. The Anthropic landscape of string theory. pages 247–266, 2003.

[136] Andrei D. Linde. Scalar Field Fluctuations in Expanding Universe and the New Inflationary Universe Scenario. *Phys. Lett.*, 116B:335–339, 1982.

[137] Alexei A. Starobinsky. Dynamics of Phase Transition in the New Inflationary Universe Scenario and Generation of Perturbations. *Phys. Lett.*, 117B:175–178, 1982.

[138] P. C. W. Davies. Cosmological Horizons and Entropy. *Class. Quant. Grav.*, 5:1349, 1988.

[139] Claus Kiefer, David Polarski, and Alexei A. Starobinsky. Entropy of gravitons produced in the early universe. *Phys. Rev.*, D62:043518, 2000.

[140] David Campo and Renaud Parentani. Inflationary spectra and partially decohered distributions. *Phys. Rev.*, D72:045015, 2005.

[141] Claus Kiefer and David Polarski. Why do cosmological perturbations look classical to us? *Adv. Sci. Lett.*, 2:164–173, 2009.

[142] T. J. Hollowood and J. I. McDonald. Decoherence, discord and the quantum master equation for cosmological perturbations. *Phys. Rev.*, D95(10):103521, 2017.

[143] Robert H. Brandenberger, Viatcheslav F. Mukhanov, and T. Prokopec. Entropy of a classical stochastic field and cosmological perturbations. *Phys. Rev. Lett.*, 69:3606–3609, 1992.

[144] Robert H. Brandenberger, T. Prokopec, and Viatcheslav F. Mukhanov. The Entropy of the gravitational field. *Phys. Rev.*, D48:2443–2455, 1993.

[145] D. Boyanovsky. Effective field theory during inflation. II. Stochastic dynamics and power spectrum suppression. *Phys. Rev.*, D93:043501, 2016.

[146] Vincent Vennin and Alexei A. Starobinsky. Correlation Functions in Stochastic Inflation. *Eur. Phys. J.*, C75:413, 2015.

[147] Arjun Berera. Warm inflation. *Phys. Rev. Lett.*, 75:3218–3221, 1995.

[148] Arjun Berera, Ian G. Moss, and Rudnei O. Ramos. Warm Inflation and its Microphysical Basis. *Rept. Prog. Phys.*, 72:026901, 2009.

[149] Sam Bartrum, Mar Bastero-Gil, Arjun Berera, Rafael Cerezo, Rudnei O. Ramos, and Joao G. Rosa. The importance of being warm (during inflation). *Phys. Lett.*, B732:116–121, 2014.

[150] Mar Bastero-Gil, Arjun Berera, Rudnei O. Ramos, and Joao G. Rosa. Warm Little Inflaton. *Phys. Rev. Lett.*, 117(15):151301, 2016.

[151] C. Jarzynski. Nonequilibrium Equality for Free Energy Differences. *Phys. Rev. Lett.*, 78(14):2690–2693, 1997.

[152] Denis J. Evans, E. G. D. Cohen, and G. P. Morriss. Probability of second law violations in shearing steady states. *Phys. Rev. Lett.*, 71:2401–2404, Oct 1993.

[153] G. Gallavotti and E. G. D. Cohen. Dynamical ensembles in nonequilibrium statistical mechanics. *Phys. Rev. Lett.*, 74:2694–2697, Apr 1995.

[154] Richard L. Arnowitt, Stanley Deser, and Charles W. Misner. Dynamical Structure and Definition of Energy in General Relativity. *Phys. Rev.*, 116:1322–1330, 1959.

[155] David Polarski and Alexei A. Starobinsky. Semiclassicality and decoherence of cosmological perturbations. *Class. Quant. Grav.*, 13:377–392, 1996.

[156] Claus Kiefer, Ingo Lohmar, David Polarski, and Alexei A. Starobinsky. Pointer states for primordial fluctuations in inflationary cosmology. *Class. Quant. Grav.*, 24:1699–1718, 2007.

[157] J. Lesgourgues, David Polarski, and Alexei A. Starobinsky. Quantum to classical transition of cosmological perturbations for nonvacuum initial states. *Nucl. Phys.*, B497:479–510, 1997.

[158] Claus Kiefer, David Polarski, and Alexei A. Starobinsky. Quantum to classical transition for fluctuations in the early universe. *Int. J. Mod. Phys.*, D7:455–462, 1998.

[159] David H. Lyth and David Seery. Classicality of the primordial perturbations. *Phys. Lett.*, B662:309–313, 2008.

[160] Cliff P. Burgess, R. Holman, and D. Hoover. Decoherence of inflationary primordial fluctuations. *Phys. Rev.*, D77:063534, 2008.

[161] Claus Kiefer and David Polarski. Emergence of classicality for primordial fluctuations: Concepts and analogies. *Annalen Phys.*, 7:137–158, 1998.

[162] D. Giulini, C. Kiefer, E. Joos, J. Kupsch, I. O. Stamatescu, and H. D. Zeh. *Decoherence and the appearance of a classical world in quantum theory.* 1996.

[163] W. G. Unruh. Notes on black hole evaporation. *Phys. Rev.*, D14:870, 1976.

[164] R. Brout, S. Massar, R. Parentani, and Ph. Spindel. A Primer for black hole quantum physics. *Phys. Rept.*, 260:329–454, 1995.

[165] Marc Casals, Sam R. Dolan, Brien C. Nolan, Adrian C. Ottewill, and Elizabeth Winstanley. Quantization of fermions on Kerr space-time. *Phys. Rev.*, D87(6):064027, 2013.

[166] Jurgen Audretsch and Rainer Muller. Amplification of the black hole Hawking radiation by stimulated emission. *Phys. Rev.*, D45:513–519, 1992.

[167] U. A. Yajnik and K. Narayan. CPT invariance and canonical quantization inside the Schwarzschild black hole. *Class. Quant. Grav.*, 15:1315–1321, 1998.

[168] Esteban A. Calzetta and Bei-Lok B. Hu. *Nonequilibrium Quantum Field Theory.* Cambridge Monographs on Mathematical Physics. Cambridge University Press, 2008.

[169] Yoshiko Kanada-En'yo. Quantum decoherence in the entanglement entropy of a composite particle and its relationship to coarse graining in the Husimi function. *PTEP*, 2015(5):051D01, 2015.

[170] Anshul Saini and Dejan Stojkovic. Radiation from a collapsing object is manifestly unitary. *Phys. Rev. Lett.*, 114(11):111301, 2015.

[171] Hikaru Kawai and Yuki Yokokura. Interior of Black Holes and Information Recovery. *Phys. Rev.*, D93(4):044011, 2016.

[172] I. L. Bogolyubsky and V. G. Makhankov. On the Pulsed Soliton Lifetime in Two Classical Relativistic Theory Models. *JETP Lett.*, 24:12, 1976.

[173] H. Segur and M. D. Kruskal. Nonexistence of Small Amplitude Breather Solutions in ϕ^4 Theory. *Phys. Rev. Lett.*, 58:747–750, 1987.

[174] Marcelo Gleiser. Pseudostable bubbles. *Phys. Rev.*, D49:2978–2981, 1994.

[175] Edmund J. Copeland, M. Gleiser, and H. R. Muller. Oscillons: Resonant configurations during bubble collapse. *Phys. Rev.*, D52:1920–1933, 1995.

[176] Marcelo Gleiser and Andrew Sornborger. Longlived localized field configurations in small lattices: Application to oscillons. *Phys. Rev.*, E62:1368–1374, 2000.

[177] S. Kasuya, M. Kawasaki, and Fuminobu Takahashi. I-balls. *Phys. Lett.*, B559:99–106, 2003.

[178] Marcelo Gleiser. d-dimensional oscillating scalar field lumps and the dimensionality of space. *Phys. Lett.*, B600:126–132, 2004.

[179] Gyula Fodor, Peter Forgacs, Philippe Grandclement, and Istvan Racz. Oscillons and Quasi-breathers in the phi**4 Klein-Gordon model. *Phys. Rev.*, D74:124003, 2006.

[180] Mark Hindmarsh and Petja Salmi. Numerical investigations of oscillons in 2 dimensions. *Phys. Rev.*, D74:105005, 2006.

[181] Mustafa A. Amin, Richard Easther, Hal Finkel, Raphael Flauger, and Mark P. Hertzberg. Oscillons After Inflation. *Phys. Rev. Lett.*, 108:241302, 2012.

[182] Kyohei Mukaida, Masahiro Takimoto, and Masaki Yamada. On Longevity of I-ball/Oscillon. *JHEP*, 03:122, 2017.

[183] Pawel O. Mazur and Emil Mottola. Gravitational condensate stars: An alternative to black holes. 2001.

[184] Pawel O. Mazur and Emil Mottola. Gravitational vacuum condensate stars. *Proc. Nat. Acad. Sci.*, 101:9545–9550, 2004.

[185] Stephen Hawking. Gravitationally collapsed objects of very low mass. *Mon. Not. Roy. Astron. Soc.*, 152:75, 1971.

[186] Bernard J. Carr and S. W. Hawking. Black holes in the early Universe. *Mon. Not. Roy. Astron. Soc.*, 168:399–415, 1974.

[187] Bernard J. Carr. The Primordial black hole mass spectrum. *Astrophys. J.*, 201:1–19, 1975.

[188] P. Ivanov, P. Naselsky, and I. Novikov. Inflation and primordial black holes as dark matter. *Phys. Rev.*, D50:7173–7178, 1994.

[189] Juan Garcia-Bellido, Andrei D. Linde, and David Wands. Density perturbations and black hole formation in hybrid inflation. *Phys. Rev.*, D54:6040–6058, 1996.

[190] M. Kawasaki, N. Sugiyama, and T. Yanagida. Primordial black hole formation in a double inflation model in supergravity. *Phys. Rev.*, D57:6050–6056, 1998.

[191] Jun'ichi Yokoyama. Chaotic new inflation and formation of primordial black holes. *Phys. Rev.*, D58:083510, 1998.

[192] Jaume Garriga, Alexander Vilenkin, and Jun Zhang. Black holes and the multiverse. *JCAP*, 1602(02):064, 2016.

[193] Juan Garcia-Bellido and Ester Ruiz Morales. Primordial black holes from single field models of inflation. *Phys. Dark Univ.*, 18:47–54, 2017.

[194] Heling Deng and Alexander Vilenkin. Primordial black hole formation by vacuum bubbles. *JCAP*, 1712(12):044, 2017.

[195] Mark P. Hertzberg and Masaki Yamada. Primordial Black Holes from Polynomial Potentials in Single Field Inflation. *Phys. Rev.*, D97(8):083509, 2018.

[196] Peter Brockway Arnold. GRAVITY AND FALSE VACUUM DECAY RATES: O(3) SOLUTIONS. *Nucl. Phys.*, B346:160–192, 1990.

[197] V. A. Berezin, V. A. Kuzmin, and I. I. Tkachev. Black holes initiate false vacuum decay. *Phys. Rev.*, D43:3112–3116, 1991.

[198] A. Gomberoff, M. Henneaux, C. Teitelboim, and F. Wilczek. Thermal decay of the cosmological constant into black holes. *Phys. Rev. D*, 69(8):083520, April 2004.

[199] J. Garriga and A. Megevand. Decay of de Sitter Vacua by Thermal Activation. *International Journal of Theoretical Physics*, 43:883–904, March 2004.

[200] Pisin Chen, Guillem Domenech, Misao Sasaki, and Dong-han Yeom. Thermal activation of thin-shells in anti-de Sitter black hole spacetime. *JHEP*, 07:134, 2017.

[201] Philippa S. Cole and Christian T. Byrnes. Extreme scenarios: the tightest possible constraints on the power spectrum due to primordial black holes. *JCAP*, 1802(02):019, 2018.

[202] Dmitry Gorbunov, Dmitry Levkov, and Alexander Panin. Fatal youth of the Universe: black hole threat for the electroweak vacuum during preheating. *JCAP*, 1710(10):016, 2017.

[203] Alexander Kusenko. Phase transitions precipitated by solitosynthesis. *Phys. Lett.*, B406:26–33, 1997.

[204] D. Metaxas. Nontopological solitons as nucleation sites for cosmological phase transitions. *Phys. Rev.*, D63:083507, 2001.

[205] Lauren Pearce. Solitosynthesis induced phase transitions. *Phys. Rev.*, D85:125022, 2012.

[206] H. Kawai, Y. Matsuo, and Y. Yokokura. a Self-Consistent Model of the Black Hole Evaporation. *International Journal of Modern Physics A*, 28:1350050, June 2013.

[207] H. Kawai and Y. Yokokura. Phenomenological description of the interior of the Schwarzschild black hole. *International Journal of Modern Physics A*, 30:1550091, May 2015.

[208] H. Kawai and Y. Yokokura. A Model of Black Hole Evaporation and 4D Weyl Anomaly. *Universe*, 3:51, June 2017.

[209] Katsuhiko Sato and Jun'ichi Yokoyama. Inflationary cosmology: First 30+ years. *Int. J. Mod. Phys.*, D24(11):1530025, 2015.

[210] Katsuhiko Sato, Misao Sasaki, Hideo Kodama, and Kei-ichi Maeda. Creation of Wormholes by First Order Phase Transition of a Vacuum in the Early Universe. *Prog. Theor. Phys.*, 65:1443, 1981.

[211] Ki-Myeong Lee and Erick J. Weinberg. Decay of the True Vacuum in Curved Space-time. *Phys. Rev.*, D36:1088, 1987.

[212] Puneet Batra and Matthew Kleban. Transitions Between de Sitter Minima. *Phys. Rev.*, D76:103510, 2007.

[213] Jaume Garriga and Alexander Vilenkin. Recycling universe. *Phys. Rev.*, D57:2230–2244, 1998.

[214] I. G. Moss. BLACK HOLE BUBBLES. *Phys. Rev.*, D32:1333, 1985.

[215] Anthony Aguirre and Matthew C. Johnson. Two tunnels to inflation. *Phys. Rev.*, D73:123529, 2006.

[216] S. Ansoldi and T. Tanaka. Tunnelling with wormhole creation. *J. Exp. Theor. Phys.*, 120(3):460–469, 2015.

[217] Edward Farhi, Alan H. Guth, and Jemal Guven. Is It Possible to Create a Universe in the Laboratory by Quantum Tunneling? *Nucl. Phys.*, B339:417–490, 1990.

[218] Willy Fischler, Daniel Morgan, and Joseph Polchinski. Quantum Nucleation of False Vacuum Bubbles. *Phys. Rev.*, D41:2638, 1990.

[219] W. Fischler, D. Morgan, and J. Polchinski. Quantization of False Vacuum Bubbles: A Hamiltonian Treatment of Gravitational Tunneling. *Phys. Rev.*, D42:4042–4055, 1990.

[220] Pisin Chen, Yao-Chieh Hu, and Dong-han Yeom. Two interpretations of thin-shell instantons. *Phys. Rev.*, D94:024044, 2016.

[221] Misao Sasaki, Takahiro Tanaka, Kazuhiro Yamamoto, and Jun'ichi Yokoyama. Quantum state inside a vacuum bubble and creation of an open universe. *Phys. Lett.*, B317:510–516, 1993.

[222] Kazuhiro Yamamoto, Misao Sasaki, and Takahiro Tanaka. Large angle CMB anisotropy in an open universe in the one bubble inflationary scenario. *Astrophys. J.*, 455:412–418, 1995.

[223] Martin Bucher, Alfred S. Goldhaber, and Neil Turok. An open universe from inflation. *Phys. Rev.*, D52:3314–3337, 1995.

[224] Valeri P. Frolov, M. A. Markov, and Viatcheslav F. Mukhanov. Black Holes as Possible Sources of Closed and Semiclosed Worlds. *Phys. Rev.*, D41:383, 1990.

[225] Valeri P. Frolov, M. A. Markov, and Viatcheslav F. Mukhanov. THROUGH A BLACK HOLE INTO A NEW UNIVERSE? *Phys. Lett.*, B216:272–276, 1989. [,52(1990)].